

## 附錄：WHOI 學者提供之參考文獻

# Correcting acoustic measurements of scatterer density for extinction

Kenneth G. Foote

Institute of Marine Research, 5024 Bergen, Norway

(Received 8 March 1990; accepted for publication 31 May 1990)

Extinction is sometimes a major problem in acoustic surveys of fish stocks, as it often occurs when the fish are concentrated and easiest to survey. The same may be true of certain macrozooplankton, such as krill in swarms. This study aims to describe how to correct single-ping measurements of the vertical distribution of scatterer density for extinction. The general case is considered in which the aggregation density is variable and the mean backscattering and extinction cross sections vary with depth. By dividing the water column into a finite number of layers, with constant properties within each, a closed-form mean-field solution is derived. Methods of applying this to single-ping echo records and the quality of the solution are both examined. Extinction is discussed vis-à-vis multiple scattering. Application of the technique in other areas, e.g., in remote probing of the atmosphere by lidar, is mentioned.

PACS numbers: 43.30.Xm, 43.20.Fn, 43.60.Pt

## INTRODUCTION

In the last several fishing seasons, the all-important 1983 year class of Norwegian spring-spawning herring (*Clupea harengus*), on which the future of the stock depends,<sup>1,2</sup> has been decimated by disastrously large catches that have literally burst nets. Such lost catches are not counted in the present quota system, and hence represent a pure, if inadvertent, overexploitation of the stock. Awareness of the need for caution in catching operations explains the following radio conversation, overheard between two fishing vessels in a northern Norwegian fjord in December 1989. First fisherman: "Is it safe to fish here?" Second fisherman: "Yes; we can see the bottom."

That is, the second fisherman has concluded from the appearance of the echogram that the likely catch size will be manageable. Because the bottom echo signal could be "seen," or discerned, the column density of fish was not considered excessive for purse seining. Evidently, it is the fisherman's experience that fishing on an aggregation of herring that blocks or extinguishes the bottom echo signal is risky!

The phenomenon of extinction by fish aggregations is also of practical importance to researchers who must estimate fish abundance by acoustic means.<sup>3</sup> This has been recognized in a number of experimental studies,<sup>4-11</sup> which have sought to measure the effect of extinction or the extinction cross section. It has also been considered in several theoretical studies.<sup>3,12-14</sup>

Extinction may also be of interest in scattering by plankton. While this is undoubtedly negligible for phytoplankton, such as the unicellular green algae *Scenedesmus* and diatom *Nitzschia closterium f. minutissima*,<sup>15</sup> whether singly or in colonies, and some zooplankton, it may be quite important for macrozooplankton. Examples include Antarctic krill (*Euphausia superba*), observed by underwater divers in swarms with densities estimated to be of the order of 20 000–60 000 animals/m<sup>3</sup> (Ref. 16), and the krill *Meganyctiphanes norvegica*, which was recently observed acoustically in layers over 50 m thick and with an average density of 800 animals/m<sup>3</sup> (Ref. 17). Even at these densities the effect may not be

large, and second-order scattering effects may be significant.<sup>18</sup> Whether dense and extended aggregations of soft-bodied scatterers, such as jellyfish or salps, extinguish sound measurably, or produce significant echoes for that matter, is unknown.<sup>19</sup>

The effect of extinction has been described in several places for constant-density scattering layers.<sup>3,13,14</sup> It may be thought that the generalization to variable-density layers is straightforward. However, there seems to be some confusion about this, at least in fisheries acoustics. In addition, for studies of structure in scatterer aggregations, such as fish schools, it is desired to describe the vertical distribution of density as sensed by single pings.

It is the present aim to extend the theory for constant density to variable density, and show how to correct single-ping measurements of the vertical distribution of scatterer density for extinction.

## I. THEORY

Several different quantities are suitable for describing acoustic measures of scatterer density. In Ref. 13, echo energy is used. The area or column backscattering coefficient<sup>20</sup> or strength<sup>21</sup> is the most widely used today. Since the present object is correction of density estimates for extinction in a variable-density layer, the derivative of the area backscattering coefficient with respect to depth is most convenient. This is just the volume backscattering coefficient.<sup>22</sup> For a scatterer aggregation of constant number density  $\rho$  and mean backscattering cross section  $\sigma_b$ , the volume backscattering coefficient in the neglect of extinction is

$$s_v = \rho(\sigma_b/4\pi). \quad (1)$$

That is, the measured quantity  $s_v$  is directly proportional to the scatterer density. This equation applies strictly only in the mean of a large number of independent observations on the same aggregation or, to a good approximation, to a single observation when the number of observed scatterers in the beam is sufficiently large. Assumptions of stationarity and sufficient numbers of scatterers are thus implicit in the use of

Eq. (1) in this study. The theory consequently belongs to the category called "mean-field."

For a scattering layer of constant density  $\rho$  and constant  $\sigma_b$  over the depth range  $[z_1, z_2]$ ,  $s_v$  is generally less than that indicated in Eq. (1). The degree of reduction is determined by integrating the steadily decreasing mean echo intensity, after the usual "20 log  $r + 2\alpha r$ " type of range compensation for a scattering layer,<sup>2,23</sup> over the interval  $[z_1, z_2]$ . If there are no scatterers in the interval  $[0, z_1]$ ,  $s_v$  for the scattering layer is thus modified by the single multiplicative factor

$$\int_{z_1}^{z_2} \exp[-2\rho\sigma_e(\xi - z_1)] d\xi / (z_2 - z_1),$$

where  $\sigma_e$  is the mean extinction cross section. Here and elsewhere in this study, beam spreading is ignored. The incurred approximation is excellent for echo sounders using ordinary narrow beams, typically of the order of 8 deg or less as measured between opposite -3-dB levels. Integrating, then,

$$s_v = \rho \frac{\sigma_b}{4\pi} \frac{1 - \exp[-2\rho\sigma_e(z_2 - z_1)]}{2\rho\sigma_e(z_2 - z_1)}. \quad (2)$$

This result is consistent with the various formulas given in the cited theoretical studies. It also agrees with the analogous expression used in studies of backscattering of light by aerosols.<sup>24</sup>

In general, scatterer density does vary with depth in an aggregation. The mean quantities  $\sigma_b$  and  $\sigma_e$  may also vary with depth. To lessen the chances of confusion in addressing the general case, extinction is treated in elementary fashion.

The intensity of a plane acoustic wave incident on a scattering aggregation diminishes, in the mean, with depth of penetration into the aggregation. To first order, the relative change in intensity  $\Delta I/I$  over the depth range from  $z$  to  $z + \Delta z$  is linearly proportional to the scatterer density  $\rho$  and mean extinction cross section  $\sigma_e$  characterizing the depth interval, and the interval thickness  $\Delta z$ :

$$\Delta I/I = -\rho\sigma_e \Delta z. \quad (3)$$

Since this applies for the arbitrary interval, at any  $z$ , it can be integrated over  $[0, z]$ :

$$I(z) = I(0) \exp\left(-\int_0^z \rho(\xi)\sigma_e(\xi)d\xi\right), \quad (4)$$

where  $I(0)$  is the effective incident intensity at the reference depth  $z = 0$ , and the general depth dependences of the several factors in Eq. (3) are shown explicitly.

The volume backscattering coefficient at  $z$ , shown in Eq. (1), is thus diminished, in the mean, by the square of the exponential factor in Eq. (4), hence

$$s_v(z) = \exp\left(-2 \int_0^z \rho(\xi)\sigma_e(\xi)d\xi\right) \rho(z) \frac{\sigma_b(z)}{4\pi}. \quad (5)$$

The represented function is continuous. In practice,  $s_v$  is sampled at discrete depths  $\{z_j\}$  and either represented as such or, more often, averaged over subsets of the points, spanning small or large intervals. For this second case of averaging over a finite interval, say from  $z_1$  to  $z_2$ ,  $s_v(z)$  in Eq. (5) should be replaced by the expression

$$\begin{aligned} s_v(z_1, z_2) &= \exp\left(-2 \int_0^{z_1} \rho(\xi)\sigma_e(\xi)d\xi\right) \\ &\times \int_{z_1}^{z_2} \rho(z) \frac{\sigma_b(z)}{4\pi} \\ &\times \exp[-2\rho(z)\sigma_e(z)(z - z_1)] dz / (z_2 - z_1), \end{aligned} \quad (6)$$

where the applicable interval of integration is indicated explicitly in the arguments of  $s_v$ . For the special case of a single scattering layer confined to the depth interval  $[z_1, z_2]$ , in which  $\rho$ ,  $\sigma_b$ , and  $\sigma_e$  are constant, Eq. (6) reduces to Eq. (2).

To compare Eqs. (5) or (6) with Eq. (34) in Ref. 3, the observational quantity  $s_v$  here may be replaced by the product of an apparent density and  $\sigma_b/4\pi$ , according to Eq. (1), and  $\sigma_b(z)$  and  $\sigma_e(z)$  may be replaced by constants. Neither of the resulting equations is equivalent to the expression in Ref. 3, although purporting to describe the same, unknown density.

## II. SOLUTION

The echo integration method aims to relate an acoustic measurement, such as that of the volume backscattering coefficient, to the causative scatterer density, given knowledge of the scatterer type. In the case of negligible extinction,  $s_v$  and  $\rho$  are proportional, and solution of Eq. (1) for  $\rho$  is immediate. In the presence of extinction, and with ordinary discrete sampling, Eq. (6) must be solved. Several approaches are possible. The one presented here is the more heuristic.

The scatterer aggregation is assumed, for generality in analysis, to be divided into  $N$  layers between the depths  $z_1$  and  $z_{N+1}$ , which may represent the surface and bottom, respectively. The depth limits of the  $j$ th layer are  $z_j$  and  $z_{j+1} = z_j + \Delta z_j$ , where  $\Delta z_j$  is the thickness of the  $j$ th layer. Each layer thickness is chosen to be sufficiently small so that  $\rho$ ,  $\sigma_b$ , and  $\sigma_e$  may be assumed to be constant in the particular layer, with mean values  $\rho_j$ ,  $\sigma_{b,j}$ , and  $\sigma_{e,j}$ . The volume backscattering coefficient is similarly distinguished by the depth of sampling, viz.  $s_{v,j}$ .

Equation (6) is evaluated for the  $n$ th layer, with limits  $z_n$  and  $z_{n+1}$ . The first integral, after redefinition of its limits as  $z_1$  and  $z_n$ , can be written as

$$\exp\left(-2 \sum_{j=1}^{n-1} \rho_j \sigma_{e,j} \Delta z_j\right),$$

with the implicit value of unity understood for  $n = 1$ . By assumption of constant values  $\rho_n$ ,  $\sigma_{b,n}$ , and  $\sigma_{e,n}$  for the  $n$ th layer, the second integral is just

$$(1/8\pi)(\sigma_{b,n}/\sigma_{e,n})[1 - \exp(-2\rho_n\sigma_{e,n}\Delta z_n)].$$

Combining the several results,

$$\begin{aligned} s_{v,n} &= (1/8\pi\Delta z_n)(\sigma_{b,n}/\sigma_{e,n})[1 - \exp(-2\rho_n\sigma_{e,n}\Delta z_n)] \\ &\times \exp\left(-2 \sum_{j=1}^{n-1} \rho_j \sigma_{e,j} \Delta z_j\right). \end{aligned} \quad (7)$$

The solution for  $\rho_n$  is immediate. Defining

$$\hat{s}_{v,n} = s_{v,n} \exp\left(2 \sum_{j=1}^{n-1} \rho_j \sigma_{e,j} \Delta z_j\right). \quad (8a)$$

$$\rho_n = -\frac{I}{2\sigma_{e,n}\Delta z_n} \ln \left( 1 - \frac{8\pi\delta_{e,n}\Delta z_n\sigma_{e,n}}{\sigma_{b,n}} \right). \quad (8b)$$

With the aforementioned understanding that the exponential term in Eq. (8a) is unity for  $n = 1$ ,  $\rho_n$  is evaluated in successive order from  $n = 1$  to  $n = N$ .

The solution given in Eq. (8) is generally well-behaved. In the limit that  $\Delta z_n$  or  $\sigma_{e,n}$  vanishes,  $\rho_n = 4\pi\delta_{e,n}/\sigma_{b,n}$ , which is better interpreted as the result for an acoustically thin layer, by analogy with optics. For an empty layer, with  $s_{e,n} = 0$ ,  $\rho_n = 0$ . Layers with few scatterers are subject to larger fluctuations in  $s_{e,n}$  than those with many scatterers, but the influence of fluctuations in the first  $n - 1$  layers on  $\rho_n$  is damped by the manner of combination of the  $n - 1$  density estimates in Eq. (8a).

### III. DISCUSSION

#### A. Applying the solution

Measurements of scatterer density may be corrected for extinction according to Eq. (8). This may be done for a series of layers of arbitrary thickness, as long as  $\rho$ ,  $\sigma_b$ , and  $\sigma_e$  remain essentially constant in each. A practicable scheme for ensuring this in ordinary survey work entails choosing layers of equal thickness  $\Delta z = 1$  m. This is also a very common unit of resolution in digital representations of  $s_e$ .

Application of the formula in real time, based on prior assumption of the kind of scatterer, hence  $\sigma_b$  and  $\sigma_e$ , is also possible. Such adaptive processing would, however, make excessive demands on even the latest-generation scientific echo sounding and integration system,<sup>25</sup> and is moreover unnecessary because of the ease and speed of postprocessing by means of workstation-level computers.<sup>26,27</sup>

A particular advantage of the formula is that it can be executed without further operator assistance once the scatterer is classified. This initial operator-determined process consists of specification of scatterer identity, namely species and size distribution, hence mean backscattering and extinction cross sections, with or without specified depth dependences, in the case of a single-species aggregation. In the case of a mixed aggregation or multiple scattering layers, the species content, several size distributions, and respective depth ranges must also be specified. Notwithstanding the apparent magnitude and difficulty of this assignment, it is nothing more than is done every time that an echogram is interpreted for the purpose of estimating fish density along an acoustic survey track. The single new element in the formula is the mean extinction cross section, but this is known for some species,<sup>7,8,12</sup> and is being<sup>11</sup> or will be specified for others. As noted by MacLennan *et al.*,<sup>11</sup>  $\sigma_e$  will undoubtedly vary with fish behavior and physiological condition, but then so does  $\sigma_b$ , and to a greater degree too, since the extent of the averaging implicit in  $\sigma_e$  exceeds that in  $\sigma_b$ .

A second advantage of the formula is that it subsumes arbitrary density variations or fluctuations. A scattering layer need not be stratified vertically, but may vary in any or all directions.

#### B. Quality of the solution

The numerical error incurred in evaluating Eq. (8a) is readily defined by a simple analysis. If the formula is effected on a digital computer with a single-precision floating-point word size that allots  $m$  bits to the mantissa, exclusive of the sign bit, then the numerical error  $\epsilon_i$  in the density estimate  $\rho_i$  will lie in the range  $[-0.5, 0.5]$  of the last or  $m$ th bit. A more complete representation of a single component of the exponential factor in Eq. (8a) is  $\exp[x_j(1 + \epsilon_i/\rho_i)]$  or  $\exp(x_j + \delta_j)$ , where  $\delta_j = x_j\epsilon_i/\rho_i = 2\epsilon_i\sigma_{e,j}\Delta z_j$ . Since  $\delta_j$  is generally quite small, the following Maclaurin expansion is appropriate:

$$\exp(\delta_j) = 1 + \delta_j + (\delta_j^2/2) + \dots,$$

hence, the relative cumulative error in, say,  $\rho_{n+1}$  due to the exponential factor in Eq. (8a) is

$$\begin{aligned} \exp\left(\sum_{j=1}^n \delta_j\right) - 1 &= \sum_{j=1}^n \delta_j + \frac{1}{2} \sum_{j=1}^n \delta_j^2 \\ &\quad + \sum_{j \neq k} \sum_{k=1}^n \delta_j \delta_k + O(\delta_j \delta_k \delta_l). \end{aligned}$$

If there are  $N$  contributing terms in the summation, then the worst-case error is  $N|\delta_j|_{\max} = N \cdot 2|\epsilon_i\sigma_{e,j}\Delta z_j|_{\max} = N(\sigma_{e,j}\Delta z_j)_{\max}/2^m$ . A more realistic analysis assumes that the errors are independent and uniformly distributed on the interval  $[-0.5, 0.5]$  of the  $m$ th bit, with variance  $1/12$ . By the central limit theorem, their sum over a sufficiently large number of samples will be normally distributed. Thus the relative cumulative error will be less than  $2.88(N/12)^{1/2}(\sigma_{e,j}\Delta z_j)_{\text{rms}}/2^m$  with 99.9% probability.

To judge the magnitude of the several errors described here, the case that  $N = 500$  and  $m = 23$  is considered. This corresponds to, for example, a 500-m depth range with depth resolution  $\Delta z = 1$  m in  $s_e$ , and processing by the SUN-4 workstation series of digital computers, among other machines, with a 32-bit single-precision word size. If  $(\sigma_{e,j}\Delta z_j)_{\max}$  were to equal unity in SI units, which is a gross overestimate, the worst-case relative cumulative error is of the order of  $3 \times 10^{-5}$ .

Clearly, the purely numerical error that can arise in effecting the formula will be negligible, at least for digital processing with ordinary 32-bit word sizes. Errors due to uncertainty in  $\sigma_b$ ,  $\sigma_e$ , and their several depth dependences are more serious.

Fluctuations in the acoustic field from the assumed mean-field will also contribute to the overall error. Extinction by an ensemble of scatterers is a stochastic process, and the solution derived here is therefore applicable in a statistical sense, namely in the mean of a large number of observations or approximately in the presence of a large number of scatterers. Likely magnitudes of errors resulting from failure of the mean-field assumption can be investigated by simulation, although involving formidable numerical computations.

What is theoretically most hazardous is attempting to correct measurements of scatterer density when the effect of extinction is very large. In this case, which is fortunately expected to be very rare, evaluation of the formula must be

halted well before the noise level is reached. As the noise level is approached, the uncertainty in density estimates, hence also in the extinction-adjusted estimates  $\hat{s}_{v,n}$ , must be very large. The damaging effect of an error in  $\hat{s}_{v,n}$  on  $\rho_n$  is apparent from Eq. (8b). Thus in the presumed case of very high extinction, an impasse will be met. Advances must then be sought in alternate instrumentation, e.g., a lower-frequency transducer.

### C. Multiple scattering

The overall objective in correcting scatterer density estimates for extinction is to derive the best possible estimates. Thus multiple scattering also deserves to be considered. This was done by Stanton for second-order scattering by a random distribution of isotropic scatterers, yielding upper bounds for the effect.<sup>18</sup> One conclusion of this study was that extinction would be the dominant effect if the degree of extinction were significant. Another conclusion was that the effect of second-order scattering is less for narrower transducer beams.

With respect to the envisaged particular application to dense and thick aggregations of herring, the degree of extinction is particularly large. Sometimes the bottom echo signal does disappear on the echogram, i.e., becomes indistinguishable from noise. Considering the geometric extent of typical fish aggregations, transducer beamwidths of survey use are very or extremely narrow by Stanton's criterion. Since nominal acoustic wavelengths, 1–4 cm, are also much smaller than typical fish lengths, 30–35 cm, and smaller than corresponding swimbladder lengths, approximately 10–12 cm, the scattering is directional, or anisotropic, and second-order scattering effects are indeed expected to be quite small.

Interestingly, application of the extinction-correction algorithm to macrozooplankton may require careful attention to second- or even higher-order scattering. The reason is that the animals are smaller and their densities higher, and they are often surveyed at shorter ranges, hence with effectively wider-beam scattering geometries, according to Stanton.<sup>18</sup> The literature review performed by this author, in 1982,<sup>28</sup> supports Stanton's more detailed conclusions here.

### D. Other applications

While the present work is aimed at acoustic scattering in the ocean, it also has applicability to other ranging systems and media. A particular example of this is provided by monostatic lidar,<sup>29</sup> or light detection and ranging, which is being used, inter alia, to characterize the atmospheric surface layer over the sea.<sup>30,31</sup> In studies of cloud reflectance, for example, the optical analog to Eq. (2) has been recognized.<sup>24</sup>

### ACKNOWLEDGMENT

Dr. D. E. Weston is thanked for his review of the manuscript.

<sup>1</sup>I. Røttingen, "Distribution and migration of the 1983 year class of Norwegian spring spawning herring in the period July 1987–August 1988," Counc. Meet. Int. Counc. Explor. Sea 1988/H: 41, Copenhagen, Denmark.

- <sup>2</sup>I. Røttingen, "Reappearance of Norwegian spring spawning herring on spawning grounds south of 60°N," Counc. Meet. Int. Counc. Explor. Sea 1989/H: 22, Copenhagen, Denmark.
- <sup>3</sup>D. N. MacLennan, "Acoustical measurement of fish abundance," J. Acoust. Soc. Am. **87**, 1–15 (1990).
- <sup>4</sup>D. E. Weston, "Sound propagation in the presence of bladder fish," in *Underwater Acoustics*, edited by V. M. Albers (Plenum, New York, 1967), Vol. 2, pp. 55–88.
- <sup>5</sup>I. E. Davies, "Attenuation of sound by schooled anchovies," J. Acoust. Soc. Am. **54**, 213–217 (1973).
- <sup>6</sup>I. Røttingen, "On the relation between echo intensity and fish density," Fiskeridir. Skr. Ser. Havunders. **16**, 301–314 (1976).
- <sup>7</sup>M. G. Ertugrul and B. V. Smith, "Multiple scattering effects in fish abundance estimation," Dept. of Electronic and Electrical Engineering Mem. 492 (University of Birmingham, Birmingham, England, 1982).
- <sup>8</sup>M. Furusawa, K. Ishii, Y. Miyanohana, and Y. Maniwa, "Experimental investigation of an acoustic method to estimate fish abundance using culture nets," Jpn. J. Appl. Phys. **23** (S23-1), 101–103 (1984).
- <sup>9</sup>K. Olsen, "Sound attenuation within schools of herring," Counc. Meet. Int. Counc. Explor. Sea 1986/B: 44, Copenhagen, Denmark.
- <sup>10</sup>F. Armstrong, E. J. Simmonds, and D. N. MacLennan, "Sound losses through aggregations of fish," Proc. IOA **11** (3), 35–43.
- <sup>11</sup>D. N. MacLennan, F. Armstrong, and E. J. Simmonds, "Further observations on the attenuation of sound by aggregations of fish," Proc. IOA **12** (1), 99–106 (1990).
- <sup>12</sup>K. G. Foote, "Analysis of empirical observations on the scattering of sound by encaged aggregations of fish," Fiskeridir. Skr. Ser. Havunders. **16**, 423–456 (1978).
- <sup>13</sup>K. G. Foote, "Linearity of fisheries acoustics, with addition theorems," J. Acoust. Soc. Am. **73**, 1932–1940 (1983).
- <sup>14</sup>D. W. Lytle and D. R. Maxwell, "Hydroacoustic assessment in high density fish schools," FAO Fish. Rep. **300**, 157–171 (1983).
- <sup>15</sup>J. D. Watson and R. Meister, "Ultrasonic absorption in water containing plankton in suspension," J. Acoust. Soc. Am. **35**, 1584–1589 (1963).
- <sup>16</sup>W. M. Hamner, P. P. Hamner, S. W. Strand, and R. W. Gilmer, "Behaviour of Antarctic krill, *Euphausia superba*: chemoreception, feeding, schooling, and molting," Nature **220**, 433–435 (1983).
- <sup>17</sup>C. H. Greene, P. H. Wiebe, J. Burczynski, and M. J. Youngbluth, "Acoustical detection of high-density krill demersal layers in the submarine canyons off Georges Bank," Science **241**, 359–361 (1988).
- <sup>18</sup>T. K. Stanton, "Multiple scattering with applications to fish-echo processing," J. Acoust. Soc. Am. **73**, 1164–1169 (1983).
- <sup>19</sup>T. K. Stanton, R. D. M. Nash, R. L. Eastwood, and R. W. Nero, "A field examination of acoustical scattering from marine organisms at 70 kHz," IEEE J. Ocean Eng. **12**, 339–348 (1987).
- <sup>20</sup>C. S. Clay and H. Medwin, *Acoustical Oceanography: Principles and Applications* (Wiley, New York, 1977).
- <sup>21</sup>R. J. Urick, *Principles of Underwater Sound* (McGraw-Hill, New York, 1983), 3rd ed.
- <sup>22</sup>J. B. Hersey and R. H. Backus, "Sound scattering by marine organisms," in *The Sea*, edited by M. N. Hill (Wiley, New York, 1962), Chap. 13, pp. 498–539.
- <sup>23</sup>R. B. Mitson, *Fisheries Sonar* (Fishing News Books, Farnham, England, 1983).
- <sup>24</sup>R. C. Anderson and E. V. Browell, "First- and second-order backscattering from clouds illuminated by finite beams," Appl. Opt. **11**, 1345–1351 (1972).
- <sup>25</sup>H. Bodholt, H. Nes, and H. Solli, "A new echo-sounder system," Proc. IOA **11** (3), 123–130 (1989).
- <sup>26</sup>H. P. Knudsen, "Bergen echo integrator: an introduction," J. Cons. Int. Explor. Mer (in press).
- <sup>27</sup>K. G. Foote, H. P. Knudsen, R. J. Kornelussen, P. E. Nordbø, and K. Røang, "Postprocessing system for echo sounder data," J. Acoust. Soc. Am. (to be published).
- <sup>28</sup>K. G. Foote, "On multiple scattering in fisheries acoustics," Counc. Meet. Int. Counc. Explor. Sea 1982/B: 38, Copenhagen, Denmark.
- <sup>29</sup>C. F. Bohren and D. R. Huffman, *Absorption and Scattering of Light by Small Particles* (Wiley, New York, 1983).
- <sup>30</sup>G. de Leeuw, "Modeling of extinction and backscatter profiles in the marine mixed layer," Appl. Opt. **28**, 1356–1359 (1989).
- <sup>31</sup>G. de Leeuw, "Profiling of aerosol concentrations, particle size distributions and relative humidity in the atmospheric surface layer over the North Sea," Tellus **42** B (4) (1990) (in press).



*Reprinted from*

# THE JOURNAL of the Acoustical Society of America

---

Vol. 91, No. 4, Pt. 1, April 1992

## Determining the extinction cross section of aggregating fish

Kenneth G. Foote, Egil Ona, and Reidar Toresen

*Institute of Marine Research, 5024 Bergen, Norway*

pp. 1983-1989

measured coefficient by compensating for the unknown effect of extinction, which is being determined. Even if this can be done iteratively, as stated by the authors of Ref. 11, the algorithm they give is erroneous.

In this paper, a simpler and more general theory is presented. This enables the extinction cross section of scatterers in an aggregation to be determined from their echo together with the echo from a reference target under the aggregation. This is applied to a series of measurements on large and dense aggregations of herring hibernating in a fjord with flat bottom areas.

## I. THEORY

Measurement of fish and flat bottom is assumed to be made by a downward-looking, narrow-beam transducer. Transmission and reception is controlled by a calibrated echo sounder. Range compensation is effected according to the ordinary function used in echo integration, namely  $20 \log r + 2\alpha r$ , where  $r$  is the range and  $\alpha$  is the absorption coefficient. In terms of the elapsed time  $t$  from signal transmission,  $r = ct/2$ , where  $c$  is the speed of sound.

The range-compensated signal is integrated in piecewise fashion over a succession of range intervals  $\{(r_i, r_{i+1})\}$ . The range is assumed to be equivalent to the depth  $z_i = r_i$  by assumption of a narrow, downward-looking transducer beam. The result of integration is a series of area or column backscattering coefficients  $s_a(z_i, z_{i+1})$ .<sup>17</sup> These may be alternatively expressed through the mean volume backscattering coefficient  $s_v(z_i, z_{i+1})$  in each interval, which is the mean cumulative backscattering cross section of scatterers per unit sampled volume per ping.<sup>18</sup> For sampling by a narrow-beam transducer,  $s_v = s_a(z_i, z_{i+1}) / (z_{i+1} - z_i)$ .

A layer of aggregating fish is imagined to be confined to the depth interval  $[z_1, z_2]$ , if only occupying a portion of this. No other significant scatterers are present between the transducer and fish layer or between the fish layer and seabed, or bottom. The bottom is assumed, moreover, to be flat and acoustically uniform in the region beneath the fish layer. If the vertical extent of the fish layer within  $[z_1, z_2]$  is  $\Delta z$  and the fish density  $\rho$  is constant, then

$$s_v = \rho \frac{\sigma_b}{4\pi} \frac{1 - \exp(-2\rho\sigma_e \Delta z)}{2\rho\sigma_e \Delta z}, \quad (1)$$

where  $\sigma_b$  is the average backscattering cross section, and  $\sigma_e$  is the average extinction cross section. This expression is also well known from lidar applications in the atmosphere.<sup>19</sup>

The extinction cross section  $\sigma_e$  in Eq. (1) is the arithmetic mean of the average extinction cross sections in both downward and upward directions. For fish that are oriented with respect to the horizontal plane, these two directions correspond, respectively, to the dorsal and ventral aspects. The extinction cross section defined here is the appropriate quantity for application in echo integration surveys, as in the extinction correction algorithm presented in Ref. 15, although not elaborated there. For applications in which the transmitted waveform is monitored, as in fish pens,<sup>6</sup> a one-way average extinction cross section is required.

The vertical extent  $\Delta z$  of the fish layer is used in Eq. (1). This could be replaced by a larger quantity if embracing  $\Delta z$ . Equation (1) would still apply, but  $s_v$  would be reduced in inverse proportion to the assumed vertical extent. The density would be similarly reduced, while the product  $\rho\Delta z$  remains unchanged.

The result of integrating  $s_v$  over the assumed depth interval, or indeed over an arbitrary interval if including the fish layer and excluding the bottom, is independent of the assumed vertical extent. This result is just the area backscattering coefficient associated with the fish layer,

$$s_{a,F} = (\sigma_b/8\pi\sigma_e) [1 - \exp(-2\rho\sigma_e \Delta z)]. \quad (2)$$

Integration of the bottom echo over its full extent in time yields a corresponding area backscattering coefficient  $s_{a,B}$ . If fish are present in the described layer, then the average intensity of the pressure wave is diminished by the factor  $\exp(-\rho\sigma_{v,d} \Delta z)$  compared to that incident on the bottom in the absence of the layer. Here,  $\sigma_{v,d}$  indicates the dorsal-aspect part of  $\sigma_v$ . The bottom echo itself is diminished in its upward passage through the fish layer by a similar factor,  $\exp(-\rho\sigma_{v,v} \Delta z)$ , where  $\sigma_{v,v}$  denotes the ventral aspect part of  $\sigma_v$ . Thus, in terms of the area backscattering coefficient of the bottom in the absence of fish,  $s_{a,B_0}$ ,

$$s_{a,B} = s_{a,B_0} \exp(-2\rho\sigma_e \Delta z), \quad (3)$$

where  $\sigma_e$  is the aforementioned arithmetic mean of dorsal- and ventral-aspect average extinction cross sections.

Simultaneous solution of Eqs. (2) and (3) yields the result

$$s_{a,B} = s_{a,B_0} [1 - (8\pi\sigma_e/\sigma_b)s_{a,F}]. \quad (4)$$

This form emphasizes the dependence of  $s_{a,B}$  on extinction due to the fish layer.

Equation (4) also suggests how the problem of determining  $\sigma_e$  can be addressed. Specifically,  $s_{a,F}$  and  $s_{a,B}$  can usually be measured pairwise over a range of values of  $s_{a,F}$ , if only because of variations in optical thickness  $\rho\sigma_e \Delta z$  with observation point. Linear regression of  $s_{a,B}$  on  $s_{a,F}$  estimates the regression coefficients  $\alpha$  and  $\beta$  in

$$s_{a,B} = \alpha + \beta s_{a,F}. \quad (5)$$

The extinction cross section is conveniently expressed through its ratio with the backscattering cross section,

$$\sigma_e/\sigma_b = -\hat{\beta}/(8\pi\hat{\alpha}), \quad (6)$$

where  $\hat{\alpha}$  and  $\hat{\beta}$  are the estimated regression coefficients.

In practice, almost any fish layer will span a range of optical thicknesses, hence, values of  $s_{a,F}$ . By choosing sufficiently short intervals of sailed distance or sufficiently small numbers of successive pings to be combined in computing  $s_{a,F}$  and  $s_{a,B}$ , at least a partial range of values of  $s_{a,F}$  may be measured. In the very special case of an essentially uniform fish aggregation of constant optical thickness, the range in values of  $s_{a,F}$  will be negligible or quite small, rendering regression analysis futile. Indeed, it is important that the observations span a range of optical thicknesses, since the quality of the result is generally directly related to the range of values spanned by the independent variable,  $s_{a,F}$  here; being better for wider ranges.

# Determining the extinction cross section of aggregating fish

Kenneth G. Foote, Egil Ona, and Reidar Toresen  
Institute of Marine Research, 5024 Bergen, Norway

(Received 23 September 1991; accepted for publication 6 December 1991)

When fish are aggregated over a flat bottom, and fish and bottom echoes can be distinguished, it is possible to determine the fish extinction cross section by a simple application of the echo integration method. The theory for this is developed. Measurements at 38 kHz are presented for aggregations of the same 1983-year class of herring over flat-bottomed fjord areas in 1988, 1990, and 1991. The ratio of extinction and backscattering cross sections is found to lie in the approximate range from 1.2–2.3, depending on fish size and time of day.

PACS numbers: 43.30.Xm, 43.30.Pc, 43.30.Ft, 43.30.Gv

## INTRODUCTION

Interest in extinction of underwater sound by biological scatterers has had several sources. One has recognized the need to account for biological effects in other kinds of acoustic measurements,<sup>1</sup> for example, to understand fluctuations in long-range transmissions. Another has attempted to exploit the attenuation part of short-range fluctuations to measure fish density in fish-farming pens.<sup>2</sup> A third source has aimed to correct measurements of fish density in dense or extended aggregations of fish.<sup>3</sup> In most cases, swimbladder-bearing fish have been the targeted scatterer type.

The three sources of interest have spawned a variety of measurements, which have yielded or might yield values for the extinction cross section of fish. Davies has measured attenuation of sound due to the northern anchovy (*Engraulis mordax*) confined in a Plexiglas sphere over the frequency range 1–20 kHz.<sup>4</sup>

A number of Japanese researchers has measured the extinction of sound due to fish aggregations by means of hydrophone observations of the transmitted waveform before and after passage through penned aggregations of fish. Measured fish species have included Japanese anchovy (*Engraulis japonicus*) at 50 kHz by Hashimoto in 1955 and Maniwa in 1962, cited by Ishii *et al.* in 1983,<sup>5</sup> sea bream (*Chrysophrys major*) and yellowtail (*Seriola quinqueradiata*) at 50 kHz,<sup>2</sup> and recently sea bream (*Pagrus major*), spotted mackerel (*Scomber australasicus*), and yellowtail at 25, 50, 100, and 200 kHz.<sup>6</sup>

Röttingen has measured the echo energy from encaged aggregations of sprat (*Sprattus sprattus*), saithe (*Pollachius virens*), and mackerel (*Scomber scombrus*) at 38 and 120 kHz.<sup>7</sup> An underwater acoustics research group in Norway has made simultaneous observations of the echo intensity from an aggregation of herring (*Clupea harengus*) and from the underlying flat, sandy seabed at 38 kHz, which were analyzed at the University of Birmingham.<sup>8</sup> More recently, Toresen has made similar measurements, but with integration of the echo intensity over the entire ranges of the respective fish aggregation and bottom echoes.<sup>9</sup> A Scottish research group has employed this reference-target technique in several variants on encaged aggregations of herring at 38 kHz,<sup>10</sup> and on encaged aggregations of cod (*Gadus morhua*)

at 38 and 120 kHz and on a dense aggregation of hibernating herring *in situ* at 38 kHz.<sup>11</sup>

The various measurements have been aided by theoretical analyses. Weston derived an expression for the extinction cross section in terms of fundamental physical properties of a swimbladdered fish, modeled as an ellipsoidal air bubble,<sup>1</sup> which extended Andreeva's basic spherical air-bubble model.<sup>12</sup> Analysis of Röttingen's purely backscattered data has allowed determination of the extinction cross section through a parameter-fitting exercise.<sup>13</sup> Measurements of the herring aggregation and underlying flat bottom described in Ref. 8 might have yielded a value for the extinction cross section, but the authors, Ertugrul and Smith, were more interested in examining the phenomenon of multiple scattering. However, for measurements of fish at ultrasonic frequencies, multiple scattering effects are entirely negligible.<sup>14,15</sup> Toresen has proved severe shadowing effects in dense herring schools, while using these quantitatively to derive an empirical factor for correcting the apparent measurements of fish density.<sup>9</sup> The extinction cross section was not separated from this factor. Both Refs. 8 and 9 show a recognition of the usefulness of simultaneous observations of fish aggregation and bottom echoes. A similar recognition has been made by Hay for measuring the attenuating effect of suspended matter near the seabed.<sup>16</sup>

The usefulness of combined echo measurements of fish aggregations and bottom has also been clearly recognized in the cited Scottish work.<sup>10,11</sup> This has employed spherical targets suspended beneath the fish aggregations in addition to the bottom echo in order to determine the extinction cross section. The work does suffer, however, from two limitations. One is a bias incurred whenever the data include cases of substantial extinction, when the reference target echo is relatively weak. Because of the use of the logarithmic measure of reference-target echo energy in the analysis, weak reference-target echoes are disproportionately weighted. In the limit of total extinction, the weight is negative infinity. The second problem is evident from the way in which the extinction cross section is determined, by regressing the logarithm of reference-target echo energy on the product of number density and mean backscattering cross section of the scatterer. In the absence of extinction, this product is just the area backscattering coefficient. In the presence of extinction,

The range of values of  $s_{a,F}$  may be further extended by observing the bottom echo in the absence of a covering fish layer. This would be crucial in the rare case of an essentially uniform fish aggregation. However, to use bottom-only data, for which  $s_{a,F} = 0$  and  $s_{a,B} = s_{a,B_0}$ , the bottom state must be the same as beneath the fish layer. Specifically, the bottom flatness and acoustic uniformity that apply beneath the fish layer must also apply in the absence of the fish.

The present formulation is nominally concerned only with extinction by a layer of aggregating fish over a flat bottom. It applies equally well to other scatterers in a layer and to other reference targets than a flat bottom. Thus a standard spherical target suspended beneath, or behind, a layer could also serve as the reference necessary for deducing the extinguishing effect of scatterers in the layer.

## II. MEASUREMENTS

The primary measurement object is the 1983-year class of herring (*Clupea harengus*). This has been measured in Ofotfjord in northern Norway, Fig. 1, over a period of years.

In particular, it has been measured in the hibernating state in the winters of 1988, 1990, and 1991. It often forms a quite dense and distinct layer in mid-water, sometimes also extending over flat-bottomed areas of the fjord, indicated by the thick lines in Fig. 1. In 1988, the herring was measured over the shorter, inner-fjord track, with bottom depth of 350 m. In 1990 and 1991, the herring was measured over the longer, outer-fjord track, with bottom depth of 540 m.<sup>9</sup> Based on the appearance of the echograms, the conditions for applying the measurement method described in Sec. I were fulfilled.

The precise unit of measurement is the area backscattering coefficient  $s_A$ , as defined by Knudsen.<sup>20</sup> This refers the mean cumulative backscattering cross section in square meters to one square nautical mile (NM), hence,  $s_A = 4\pi 1852^2 s_a$ .

An exemplary echogram is shown in Fig. 2. The data were collected on 14 January 1990 under night-time conditions along the outer-fjord track indicated in Fig. 1. The displayed depth range is 100–600 m. Echo integration was performed under very similar conditions over a 5-NM interval of sailed distance, which included the current, roughly 2-NM interval shown in Fig. 2. Average values of the area backscattering coefficient for the herring layer and bottom, applicable over the entire 5-NM interval, are, respectively,  $106\,000 \text{ m}^2/\text{NM}^2$  and  $961\,000 \text{ m}^2/\text{NM}^2$ . The area backscattering coefficient due to other fish and plankton is less than  $100 \text{ m}^2/\text{NM}^2$ .

Two different acoustic systems operating at 38 kHz were used in the course of the measurements. In 1988, the SIMRAD EK400 echo sounder<sup>21</sup> was used on board R/V ELDJARN together with the Institute's digital echo integrator based on the Norsk Data ND-10 computer. The receiving sensitivity of the echo sounder was reduced, relative to normal operation, by means of an attenuator in order to avoid saturation due to echoes from either the herring layer or bottom. In 1990 and 1991, the SIMRAD EK500 echo sounding system<sup>22</sup> was used on board R/V MICHAEL SARS. Because of the large dynamic range of this second system, nominally 160 dB, there was no danger of receiver saturation, and the instrument operation was normal in all respects.

Both systems were operated with hull-mounted transducers resonant at 38 kHz. The nominal beamwidth between opposite – 3-dB levels is 8.0 deg for the EK400 transducer used in 1988 and 7.0 deg for the EK500 transducer used in 1990 and 1991. The acoustic systems were calibrated according to the standard-target method recommended by the International Council for the Exploration of the Sea.<sup>23</sup> The particular calibration target was a 60-mm-diam solid copper sphere, with nominal target strength of –33.6 dB at 38 kHz.

Vessel speeds of 3, 6, and 10 kn were used during the measurements in 1988, without apparent difference in echo data. The nominal vessel speed during the measurements in 1990 and 1991 was 10 kn. Since the integration interval was typically one cable length, or 0.1 NM, estimates of the mean area backscattering coefficient were based on at least 36 pings. These were derived in pairwise fashion from echoes

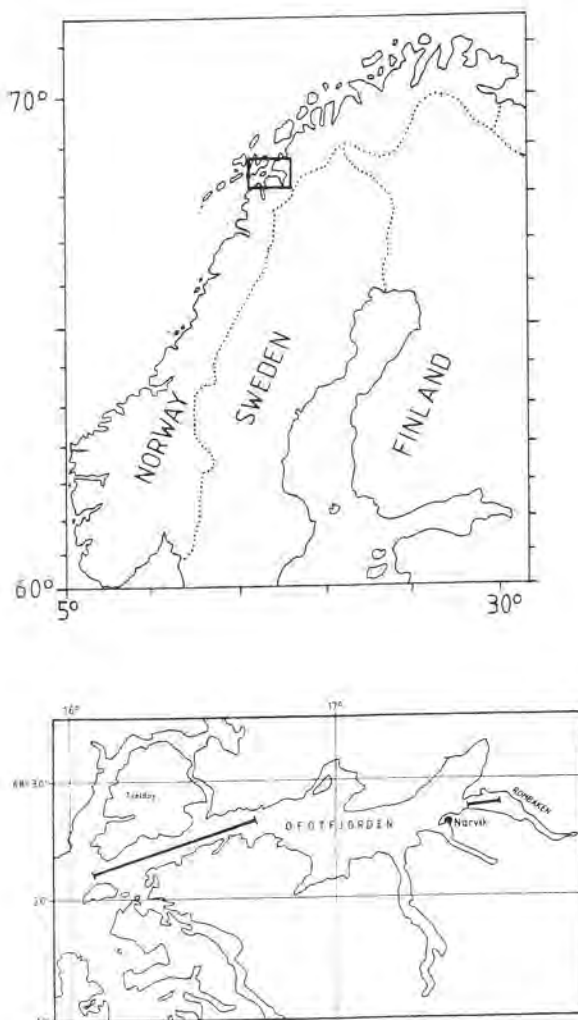


FIG. 1. Sites of data collection.

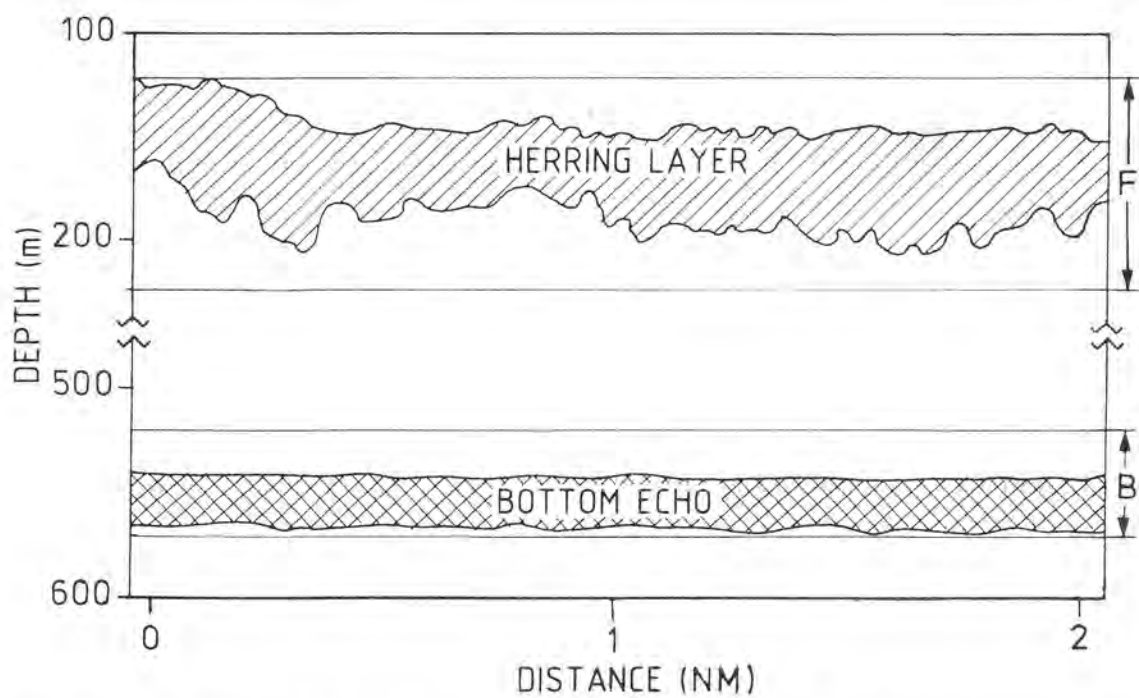
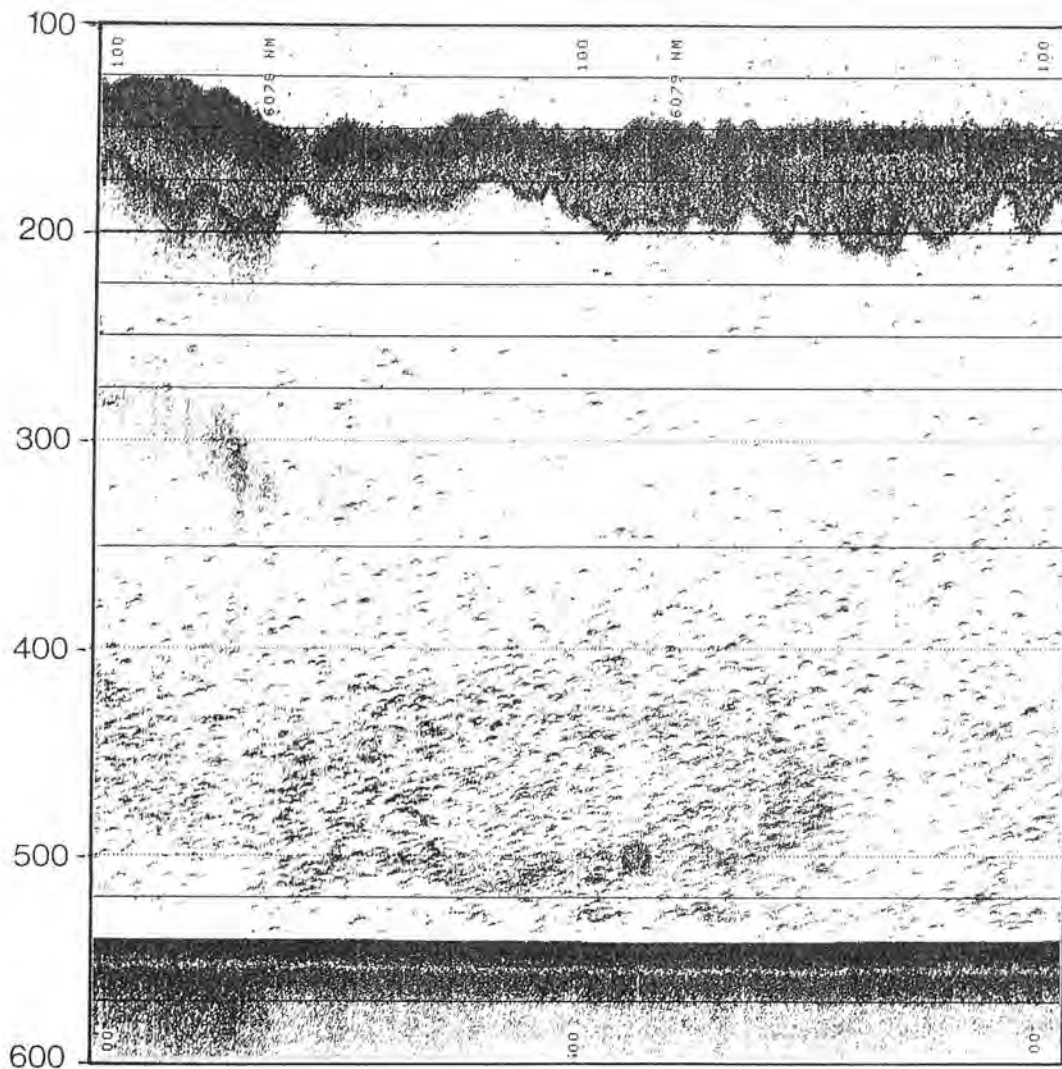


FIG. 2. Exemplary echogram with illustrative sketch showing a herring layer in outer Ofotfjord, under night-time conditions on 14 January 1990. The symbols "F" and "B" in the right margin of the sketch indicate the integration limits for fish and bottom echoes.

from both the fish layer and bottom for each ping.

Measurements were made in early January in each of the three years. The sun does not rise at this time, but a period of twilight extends over the hours 1000–1400. Night conditions prevail otherwise, barring possible periods with strong moonlight.

Data on fish size have been gathered by trawling with the standard pelagic "Harstad" trawl, which is otherwise known as a capelin trawl, with  $16 \times 16$  fathoms opening. The sampled fish aggregations were composed entirely of herring, mainly of the 1983-year class, but with admixture of other year classes according to the data in Table I. Included in this table is the mean fish length.

### III. DATA ANALYSIS

Sets of data for each year were separated into daytime and night-time subsets. A total of six subsets of data were thus available for statistical analysis. Two of these were rejected for covering only a narrow range of low fish densities, with maximum  $s_{A,F}$  of about  $10^5 \text{ m}^2/\text{NM}^2$ . Data with vanishing, or zero, values of  $s_{A,F}$  were purged from the sets in order to relate the bottom echo data as much as possible to the extinction-causing fish layer. The resulting four sets of data are shown through the scatter diagrams of Fig. 3. Included with each is the least-mean-squares regression curve and its 95% confidence interval.

The linear regression analysis indicated in Eq. (5) is performed in terms of  $s_A$  instead of  $s_a$ ; i.e.,

$$s_{A,B} = \alpha' + \beta' s_{A,F}. \quad (7a)$$

Thus

$$\sigma_e / \sigma_b = -1852^2 \hat{\beta}' / (2\hat{\alpha}'). \quad (7b)$$

Confidence intervals were attached to this estimate by observing that the ratio  $-\hat{\alpha}' / \hat{\beta}'$  describes the value of  $s_{A,F}$  for which  $s_{A,B} = 0$ , i.e., for which extinction is total. This maximum value is itself uncertain insofar as the data do not lie exactly on a straight line. The confidence interval for the value of  $(s_{A,F})_{\max}$  may be derived by inverse prediction using Eq. (7a) with  $s_{A,B} = 0$ .<sup>24</sup> Bounds on  $(s_{A,F})_{\max}$  can be computed for the mean of a large number of estimates of  $(s_{A,F})_{\max}$ . The bounds are used in Eq. (7b) to assign limits to the ratio  $\sigma_e / \sigma_b$ . This has been done according to simple linear regression analysis.

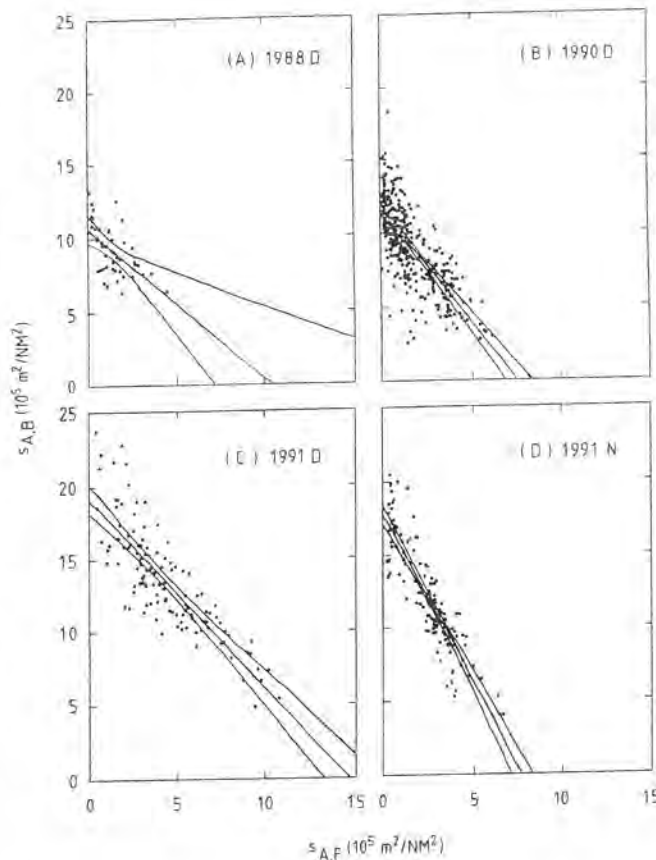


FIG. 3. Scatter diagrams of the data pair  $(s_{A,F}, s_{A,B})_r$  for fish and bottom echoes, respectively, for each of the four data sets, distinguished by year or time of day (D = day or N = night). The least-mean-squares regression of  $s_{A,B}$  on  $s_{A,F}$  is shown together with its 95% confidence interval.

### IV. RESULTS AND DISCUSSION

Some details of the linear regression analyses are presented in Table II. These are the estimated coefficients  $\hat{\alpha}$  and  $\hat{\beta}$  and the standard error SE of the regression. The estimate of the ratio  $\sigma_e / \sigma_b$  is shown together with its 95% confidence limits  $(\sigma_e / \sigma_b)_-$  and  $(\sigma_e / \sigma_b)_+$ .

The mean values of  $\sigma_b$  and  $\sigma_e$  are also shown in Table II. These assume that the mean backscattering cross section is given by the following equation for the target strength:<sup>25</sup>

$$TS = 20 \log l - 71.9 = 10 \log (\sigma_b / 4\pi). \quad (8)$$

where  $l$  is the mean fish length in units of centimeters, given in Table I, and  $\sigma_b$  is expressed in units of square meters. This equation is currently used in stock assessment work to specify  $\sigma_b$  for Atlanto-Scandinavian herring.

The mean estimates for  $\sigma_e / \sigma_b$  for 1990D and 1991N are essentially the same. The mean estimate for 1991D is significantly lower, but with similar 95% confidence interval of about  $\pm 10\%$  of the mean. The mean estimate for 1988D is intermediate, but its confidence interval overlaps those of the other estimates. This is understandable, for the number of data pairs in the 1988D set is only 45.

TABLE I. Percentage composition of the herring 1983-year class, mean length  $l$ , associated standard error SE, and mean mass  $m$ , based on  $n$  samples, arranged by year of observation.

Year	Percentage composition	$l$ (cm)	SE (cm)	$m$ (g)	$n$
1988	96.8	30.9	0.12	200	100
1990	91.3	32.9	0.10	309	123
1991	82.9	34.3	0.13	326	300

TABLE II. Results of the linear regression analysis of  $s_{\text{ext}}$  on  $s_{\text{bottom}}$  according to Eq. (7a), including estimated value for the ratio  $\sigma_e/\sigma_b$ , with 95% confidence limits, assumed value for  $\sigma_b$ , and computed value for  $\sigma_e$ . The units of  $\sigma_b$  and  $\sigma_e$  are square centimeters.

Year	D/N	$\hat{\alpha}$	$\hat{\beta}$	SE	$n$	$\sigma_e/\sigma_b$	$(\sigma_e/\sigma_b)$	$(\sigma_e/\sigma_b)$	$\sigma_b$	$\sigma_e$
1988	D	1059	-1.012	144	45	1.64	0.97	2.24	7.7	12.7
1990	D	1162	-1.548	191	324	2.28	2.10	2.46	8.8	20.0
1991	D	1916	-1.304	204	120	1.17	1.06	1.26	9.5	11.2
1991	N	1778	-2.320	169	140	2.24	2.10	2.37	9.5	21.4

The reasons for the close agreement of the 1990D and 1991N values and for their significant difference with the 1991D value are unknown, as is the reason for the particular magnitudes. It is not, however, difficult to understand why the values might be different. A primary cause may be that of behavior. Studies on the relationship of mean backscattering cross section  $\sigma_b$  to the fish orientation distribution shows that  $\sigma_b$  does vary systematically with changes in orientation distribution.<sup>26,27</sup> The extinction cross section  $\sigma_e$  is expected to be less sensitive, for it consists principally of the total scattering cross section, with greater degree of implicit averaging than that in  $\sigma_b$ . Unfortunately, too little is known about the orientation distribution of fish *in situ* to speculate further on the present data, although it is conceivable that a theoretical study might permit inference of the orientation distribution, as in Ref. 28.

There are other sources of variability in the data that should be acknowledged, although the authors do not believe that these are responsible for the basic differences in estimates of  $\sigma_e/\sigma_b$ . (1) The four data sets were collected over a three-year period, during which the predominant 1983-year class matured. In addition to increasing in length, as documented in Table I, other acoustically significant properties of the animal may have changed. (2) Variations in the bottom, both in local flatness, local slope, and acoustic properties, may explain some of the dispersion of the data in Fig. 3, without, however, significantly affecting the mean regression estimate. The bottom appeared to be quite uniform according to the echogram, but the major region of bottom ensonification is quite large. For an 8-deg beam at 350 m, for instance, this area is about 1800 m<sup>2</sup>, which suggests the coarseness of the echogram. (3) The density of herring in the aggregation did vary with depth, but in the worst observed instance, only by a factor of about 2.8 between minimum and peak density values in an 80-m-thick layer divided into eight sublayers.<sup>9</sup> The minimum was observed at an edge, and the other measured density values were more uniform, with approximate range of variation of  $\pm 10\%$ . Correction of these for extinction would increase the range of variation significantly, perhaps to  $\pm 15\%$ , but, it is believed, without significant violation of the hypothesis of a uniform layer. In any case, the extinction cross section of fish in an aggregation may simply be defined according to Eq. (1), without regard to the constancy of or degree of variation in density with depth.

Vessel-specific differences might be discounted from consideration, for the value  $\sigma_e/\sigma_b$  from R/V ELDJARN, a

fishing vessel converted to research use, is intermediate to the values from R/V MICHAEL SARS, which was built specifically for acoustic sampling. Vessel speed may also be discounted as an influencing factor, because of the negative results obtained during the experiments performed on R/V ELDJARN at 3, 6, and 10 kn in 1988. The herring indeed appear to be in a quiescent state at this time of year, and insensitive to vessel passage.

It is interesting to compare the present results with other measurements on herring at 38 kHz. Armstrong *et al.* measured caged herring of 26-cm length, with result for  $\sigma_e/\sigma_b$  of  $3.3 \pm 1.3$ .<sup>10</sup> MacLennan *et al.* report a value for *in situ* herring of 33-cm length of  $1.4 \pm 0.3$ ,<sup>11</sup> although the quality of this result is unknown, for reasons given in the Introduction. The *in situ* measurements were made from R/V MICHAEL SARS at night in December 1989, in a fjord north of Ofotfjord, but containing the same 1983-year class that was observed again, under daylight conditions, in January 1990. From Table II, the 1990D measurements are seen to be significantly higher, namely  $2.3 \pm 0.2$ . The fact that the day-night difference is exactly reversed in 1991 highlights the state of ignorance about  $\sigma_e/\sigma_b$ .

The new series of measurements reported here will be continued in the future, but with collection of additional data. These may involve ping-by-ping recording of the depth dependence of the mean volume backscattering coefficient, use of a focusing sphere<sup>29</sup> suspended beneath the fish layer to serve as a more stable reference target, and closer attention to light levels. The fat content of the fish may also be measured, in order to assess the state of the swimbladder.<sup>30</sup> Given better understanding of the nature of  $\sigma_e$ , acoustic estimates of density may be corrected according to the algorithm described in Ref. 15.

## V. SUMMARY

A simple and robust theory for determining the extinction cross section of aggregating fish has been developed. The principal requirement for applying this is that the fish be confined to a layer that is clear of a more or less flat and acoustically uniform seabed, or bottom. Given this condition, the procedure for determining the extinction cross section consists of the following steps: (1) measurement of the area backscattering coefficients of fish layer and bottom in pairwise fashion and with sufficient resolution along the survey track to differentiate regions of varying degrees of extinction; (2) linear regression of the bottom coefficient on

the fish layer coefficient to minimize the mean-square error; (3) computation of  $\sigma_e$  from Eq. (6) or (7b) or like, depending on the units used for the area backscattering coefficient, assuming a value for  $\sigma_b$ ; and (4) estimation of associated confidence limits of  $\sigma_e/\sigma_h$  or  $\sigma_e$  according to inverse prediction, observing that  $\sigma_e/\sigma_h$  is inversely proportional to the extrapolated value for the fish layer coefficient when the bottom coefficient vanishes.

The same theory applies to other scatterers and to other reference targets, discrete as well as extended. Thus, anticipated measurement of the lateral-aspect extinction cross section of schooling fish with a directional sonar beam, by means of a standard target suspended behind the school, also falls within the scope of the present theory.

The theory has been applied to acoustic measurements on dense aggregations of hibernating herring in a Norwegian fjord. Results for  $\sigma_e/\sigma_h$  have been in the approximate range from 1.2–2.3. Significant day and night differences have been observed, but without showing a consistent pattern or suggesting particular reasons for the differences.

Further research on the extinction cross section is planned. The goal is sufficient knowledge about  $\sigma_e$  so that values can be assigned in an algorithm to remove the biasing effect of extinction from conventional echo integration measurements of fish density.

- <sup>1</sup>D. E. Weston, "Sound propagation in the presence of bladder fish," in *Underwater Acoustics*, edited by V. M. Albers (Plenum, New York, 1967), Vol. 2, pp. 55–88.
- <sup>2</sup>M. Furusawa, K. Ishii, Y. Miyahana, and Y. Maniwa, "Experimental investigation of an acoustic method to estimate fish abundance using culture nets," *Jpn. J. Appl. Phys.* **23** (S23-1), 101–103 (1984).
- <sup>3</sup>I. Røttingen, "On the relation between echo intensity and fish density," *Fiskeridir. Skr. Ser. Havunders.* **16**, 301–314 (1976).
- <sup>4</sup>I. E. Davies, "Attenuation of sound by schooled anchovies," *J. Acoust. Soc. Am.* **54**, 213–217 (1973).
- <sup>5</sup>K. Ishii, M. Furusawa, and Y. Miyahana, "Measurements of attenuation of sound by schooling fish," *Tech. Rep. Natl. Res. Inst. Fisheries Eng. Fishing Boat Instrum.* **4**, 73–94 (1983).
- <sup>6</sup>M. Furusawa, K. Ishii, and Y. Miyahana, "Attenuation of sound by schooling fish," *J. Acoust. Soc. Am.* submitted (1992).
- <sup>7</sup>I. Røttingen, "Relasjoner mellom integrerte ekkointensiteter og fiskefattetheter," Cand. real. dissertation, University of Bergen, Bergen, Norway (1975).
- <sup>8</sup>M. G. Ertugrul and B. V. Smith, "Multiple scattering effects in fish abundance estimation," Department of Electronic and Electrical Engineering Memo. 492, University of Birmingham, Birmingham, England (1982).

- <sup>9</sup>R. Tøresen, "Absorption of acoustic energy in dense herring schools studied by the attenuation in the bottom echo signal," *Fish. Res.* **10**, 317–327 (1991).
- <sup>10</sup>F. Armstrong, E. J. Simmonds, and D. N. MacLennan, "Sound losses through aggregations of fish," *Proc. IOA* **11**(3), 35–43 (1989).
- <sup>11</sup>D. N. MacLennan, F. Armstrong, and E. J. Simmonds, "Further observations on the attenuation of sound by aggregations of fish," *Proc. IOA* **12**(1), 99–106 (1990).
- <sup>12</sup>I. B. Andreeva, "Scattering of sound by air bladders of fish in deep sound-scattering ocean layers," *Sov. Phys. Acoust.* **10**, 17–20 (1964).
- <sup>13</sup>K. G. Foote, "Analysis of empirical observations on the scattering of sound by encaged aggregations of fish," *Fiskeridir. Skr. Ser. Havunders.* **16**, 423–456 (1978).
- <sup>14</sup>T. K. Stanton, "Multiple scattering with applications to fish-echo processing," *J. Acoust. Soc. Am.* **73**, 1164–1169 (1983).
- <sup>15</sup>K. G. Foote, "Correcting acoustic measurements of scatterer density for extinction," *J. Acoust. Soc. Am.* **88**, 1543–1546 (1990).
- <sup>16</sup>A. E. Hay, "Turbidity currents and submarine channel formation in Rupert Inlet, British Columbia. I. Surge observations," *J. Geophys. Res.* **92**(C3), 2875–2881 (1987).
- <sup>17</sup>C. S. Clay and H. Medwin, *Acoustical Oceanography: Principles and Applications* (Wiley, New York, 1977).
- <sup>18</sup>T. K. Stanton, R. D. M. Nash, R. L. Eastwood, and R. W. Nero, "A field examination of acoustical scattering from marine organisms at 70 kHz," *IEEE J. Ocean Eng.* **12**, 339–348 (1987).
- <sup>19</sup>R. C. Anderson and E. V. Browell, "First- and second-order backscattering from clouds illuminated by finite beams," *Appl. Opt.* **11**, 1345–1351 (1972).
- <sup>20</sup>H. P. Knudsen, "The Bergen Echo Integrator: an introduction," *J. Cons. Int. Explor. Mer* **47**, 167–174 (1990).
- <sup>21</sup>R. Brede, "Simrad EK400 scientific echo sounder," *FAO Fish. Circ.* **778**, 44–56 (1984).
- <sup>22</sup>H. Bodholt, H. Nes, and H. Solli, "A new echo-sounder system," *Proc. IOA* **11**(3), 123–130 (1989).
- <sup>23</sup>K. G. Foote, H. P. Knudsen, G. Vestnes, D. N. MacLennan, and E. J. Simmonds, "Calibration of acoustic instruments for fish density estimation: a practical guide," *ICES Coop. Res. Rep.* **144** (1987).
- <sup>24</sup>N. R. Draper and H. Smith, *Applied Regression Analysis* (Wiley, New York, 1981), 2nd ed.
- <sup>25</sup>K. G. Foote, "Fish target strengths for use in echo integrator surveys," *J. Acoust. Soc. Am.* **82**, 981–987 (1987).
- <sup>26</sup>O. Nakken and K. Olsen, "Target strength measurements of fish," *Rapp. P.-v. Reun. Cons. Int. Explor. Mer* **170**, 52–69 (1977).
- <sup>27</sup>K. G. Foote, "Effects of fish behaviour on echo energy: the need for measurements of orientation distributions," *J. Cons. Int. Explor. Mer* **39**, 193–201 (1980).
- <sup>28</sup>K. G. Foote and J. J. Traynor, "Comparison of walleye pollock target strength estimates determined from *in situ* measurements and calculations based on swimbladder form," *J. Acoust. Soc. Am.* **83**, 9–17 (1988).
- <sup>29</sup>R. J. Urick, *Principles of Underwater Sound* (McGraw-Hill, New York, 1983), 2nd ed.
- <sup>30</sup>E. Oma, "Physiological factors causing natural variations in acoustic target strength of fish," *J. Mar. Biol. Assoc. U.K.* **70**, 107–127 (1990).

# Ambient noise measurements from 100 Hz to 80 kHz in an Alaskan fjord

Steven O. McConnell

*Areté Associates, P.O. Box 8050, La Jolla, California 92038*

Michael P. Schilt

*David Taylor Research Center, Puget Sound Detachment, Bremerton, Washington 98314*

J. George Dworski

*Applied Physics Laboratory, College of Ocean and Fishery Sciences, University of Washington, 1013 N.E. 40th Street, Seattle, Washington 98105*

(Received 8 January 1991; accepted for publication 22 November 1991)

Measurements covering a broad frequency range from 100 Hz to 80 kHz have been made in Behm Canal, Alaska. This site represents a fairly deep embayment (400 m) with a soft bottom (porosity of about 0.8) and, hence, the noise detected at the hydrophones is affected negligibly by multipath contributions except possibly at the lowest frequencies. Data were gathered over a wide range of wind speeds (0 to 15 m/s) and during periods of rain and snow. Several unique and noteworthy results were obtained. Foremost was the observation that the wind-generated noise level measured during the winter was approximately 5 dB lower than during the summer for the same wind speeds and air-sea temperature differences (air temperature about the same as or colder than the sea surface). The summer data agree well with the most recent published measurements and are approximately 2 dB higher than the standard Knudsen/Wenz reference spectra. It appeared that below-freezing air temperatures and snow were responsible for the 5 dB offset between the summer and winter data. Most reported wind noise measurements are restricted to frequencies less than 20 kHz. Those that go beyond this frequency display a noticeable hump above the usual -17 dB/decade power-law slope, and the Behm Canal measurements show that this hump continues to 80 kHz where the spectrum rejoins the extension of the canonical power-law slope.

PACS numbers: 43.30.Nb, 43.30.Pc

## INTRODUCTION

Ambient noise has received much attention recently, particularly with regard to identification of source mechanisms and quantification of source levels at the sea surface.<sup>1</sup> Noise generated by the action of wind on the water surface has been extensively studied and has usually been parameterized as a function of wind speed,<sup>2</sup> although the air-sea temperature difference also clearly plays a role.<sup>3</sup> Wind stress is probably the more relevant environmental parameter.<sup>4</sup> These parameterizations are helpful, especially in practical applications, and can be used to identify source mechanisms. Because of the complexity of processes occurring at and close to the air-sea interface, such as wave-breaking events and associated bubble formation which have been linked to ambient noise generation,<sup>5,6</sup> it is extremely difficult to obtain measurements of these processes directly. Thus inferences using accurate environmental parameterizations are often the best tools for identifying and quantifying source mechanisms. These inferences can be strengthened when combined with the use of a variety of noise measurement techniques.

The measurements reported herein employed a variety of measurement techniques and also enjoyed a wide range of environmental conditions, including periods of snow and rain. Wind speeds ranged from 0–15 m/s during the three trips to Behm Canal, Alaska—one in winter, one in spring, and one in summer. In addition to the use of an omnidirectional hydrophone to cover the frequency range 100 Hz–80 kHz, a vertical array of four hydrophones and a vertical line array were employed. These additional instruments provide information on the source radiation pattern. Perhaps the most interesting finding was the effect of snow or below freezing air temperatures or both on the wind-generated noise levels. Under these conditions the noise levels were suppressed by 5 dB or more compared with other measurements. This effect has not been reported elsewhere.

## I. EXPERIMENTAL DESCRIPTION

The measurements were made in the western arm of Behm Canal, Alaska, at a location near Ketchikan as shown in Fig. 1. This site represents a fairly wide and deep fjord with a water depth of about 400 m in the general vicinity of the measurement location. Core samples of the upper few feet of the seabed have shown the sediment to be a very fine organic clay or clay/silt with a typical median grain size of 0.01 mm.<sup>7</sup> This implies that the bottom is quite soft<sup>8</sup> and has a high associated bottom bounce loss (e.g., losses are greater than 20 dB at angles above 10° and frequencies above 10 kHz based on grain size alone).<sup>9</sup> The sediment layering to basement rock is fairly thick, with thickness values ranging between 15 and 60 m surrounding the measurement site.<sup>10</sup> This site was nearly ideal for measuring noise generated at the sea surface by wind or precipitation, even down to 100 Hz, since man-made and biological noise sources were ab-

# Acoustic sampling volume

Kenneth G. Foote

Institute of Marine Research, 5024 Bergen, Norway

(Received 5 April 1990; accepted for publication 10 April 1991)

Knowledge of the acoustic sampling volume is necessary in many quantitative applications of acoustics. In general, the sampling volume is not merely a characteristic of the transmitting and receiving transducers, but also depends on the concentration and scattering properties of the target, the kind of signal processing performed on the echo, and the detection threshold. These dependences are stated explicitly in formulas for the sampling volume and a differential measure, the effective equivalent beam angle. Numerical examples are given for dispersed or dense concentrations of both point scatterers and directional fish scatterers. Application of theory to optical and other remote sensing techniques is mentioned.

PACS numbers: 43.30.Ft, 43.30.Gv, 43.30.Xm

## INTRODUCTION

A number of practical uses of acoustics require knowledge of the sampling volume. In fluid-processing applications these include determinations of the concentration of monodispersed scatterers and the size distribution and concentration of polydispersed scatterers, e.g., of human red blood cells<sup>1</sup> and other small particles,<sup>2-5</sup> such as contaminants of industrial fluids. In oceanographic applications these include analogous determinations of scatterer concentration and size distribution, e.g., of bubbles,<sup>6</sup> fish,<sup>7-9</sup> plankton,<sup>10-13</sup> and suspended sediment.<sup>14-17</sup> Some of the cited applications involve bistatic sonar, others monostatic sonar, but the problem is the same: describing how large the particular sampling volume is.

In the case of high signal-to-noise ratio (SNR), as with acoustically powerful scatterers, the sampling volume may be identical to the available or accessible volume. However, in the case of low or marginal SNRs, the sampling volume will in general be less than the high-SNR volume. The reason is simply that some echoes from relatively weak scatterers, singly or aggregated, will lie below the detection threshold. This is not an academic situation either, for what technique in acoustics, or in science for that matter, is not at some time pushed to its limit: smaller, larger, weaker, stronger, thinner, denser, nearer, farther.

The problem of defining the acoustic sampling volume is especially timely in fisheries acoustics. Several years ago, when the Northeast Arctic cod (*Gadus morhua*) was surveyed during its annual migration to spawning grounds in Lofoten, the fish was observed at depths exceeding 400 m, which is much deeper than usual. Since the echo sounding equipment begins to be severely limited with respect to the detection of single cod at this range, only a fraction of the stock was registered, as was later demonstrated by the catch. Other evidence for the importance of sampling-volume considerations for cod has been presented by Ona.<sup>18</sup>

Defining the sampling volume for fish registration is also particularly illustrative for the general problem because of the involved scattering regime. This is characterized by size-wavelength ratios of about 1–100, which are due to the use of ultrasonic survey frequencies in the approximate

range 30–200 kHz. Consequently, a scatterer that gives a strong echo when in one orientation may give a very weak or unobservable echo when in another, despite being in the same position in the beam. Differences in backscattering cross sections due to ordinary changes in tilt angle will moreover be slight for small size-wavelength ratios and potentially large for big ratios, thus nearly spanning the range of effects intrinsic to the scatterer itself.

The dependence of the sampling volume on the backscattering characteristics of observed fish, in addition to transducer properties, has already been recognized.<sup>7,18-25</sup> Dependence of the sampling volume on the minimum detectable signal level or so-called detection threshold has also been recognized. However, notwithstanding several different approaches to the problem, computations are scarce, and there is a distinct lack of concise or comprehensive expressions for the sampling volume or threshold effect.

A notable, overtly statistical approach to a different but related problem is that by Weimer and Ehrenberg.<sup>26</sup> For a given threshold, the effect on a distribution of target strengths is described by an integral. This is evaluated numerically for a specific normal target strength distribution for each of several thresholds.

The present approach attempts to address both the particular fisheries acoustics application and the more general problem of defining the sampling volume. Following a description of the first-order role of the sampling volume in two methods of scatterer density determination, the theory of the sampling volume is developed. General issues concerned with integration are discussed. The volume associated with acoustic sampling by fish is computed through a derived differential measure, the effective equivalent beam angle, for a particular computational model. This is intended both to illustrate the method of numerical evaluation and to reveal some important dependences of the sampling volume on the underlying scatterer characteristics.

## I. THEORY

Two common methods of determining scatterer concentration are those of echo counting and echo integration.<sup>27,28</sup> In the case of sufficiently dispersed scatterers, the echo

counting method may be used. According to this, the scatterer density  $\rho$  is measured by the average number of echoes  $\bar{N}$ , obtained from the sampled volume  $V_s$  per sounding,

$$\rho = \bar{N}/V_s.$$

The echo integration method may be applied in the general case of scatterers of arbitrary concentration.<sup>29</sup> Accordingly, the column scattering coefficient  $s_o$  is obtained by integrating the volume backscattering coefficient  $s_v$  over an accessible range interval. The fundamental quantity  $s_v$  relates the mean cumulative backscattering cross section  $\bar{\sigma}$  per sounding to the sampled volume  $V_s$ ,<sup>12</sup>

$$s_v = \bar{\sigma}/(4\pi V_s),$$

assuming, for the sake of simplicity only, negligible extinction. Usually  $s_v$  is expressed as a function of range, or depth, by limiting  $V_s$  by a succession of generally narrow range intervals. These two methods are well known in underwater acoustics, but possess exact analogs for the sampling of other media, whether by acoustical or optical means.

In the following, the theory of the sampling volume is first developed without reference to any particular method or application. It thus encompasses the bistatic case of separate transmitting and receiving transducers. The derived expression for the sampling volume is then specialized to the monostatic case of a single transducer or collocated transmitting and receiving transducers.

### A. Bistatic case

In the general bistatic case, separate transducers are used for transmission and reception. The respective directional characteristics are contained in the one-way beam patterns  $b_T$  and  $b_R$ . A received echo is registered if its strength exceeds a minimum signal level or threshold  $t$ . The received echo strength is expressed as the product of a gain or geometric factor  $g$ , product of transmit and receive beam patterns  $b^2$ , and bistatic, or differential, cross section  $\sigma$ .

For a nondirectional scatterer with constant  $\sigma$ , the sampling volume  $V_s$  is a fraction of the total available or accessible volume  $V_0$ :

$$V_s = \int_{V_0} H(gb^2\sigma - t)dV. \quad (1)$$

The integrand is a counting function: the Heaviside step function,  $H(x) = 0, 1$  as  $x < 0, x = 0, x > 0$ , respectively. Thus, for echo strengths  $gb^2\sigma$  exceeding  $t$ , the contribution is fully registered.

For directional scatterers,  $\sigma$  varies with orientation. To account for this in  $V_s$ , the integration in Eq. (1) is also performed over the range of orientations determining the sampled values of  $\sigma$  according to the cumulative distribution function  $F$ . Thus

$$V_s = \int \int H(gb^2\sigma - t)dF dV. \quad (2)$$

This is tantamount to Eq. (7) in Ref. 30, although with differences in nomenclature. For the case of constant  $\sigma$ , the integration over  $dF$  yields unity and Eq. (1) results.

### B. Monostatic case

The expression for  $V_s$  in Eq. (2) is complete and unambiguous. However, its incorporation in echo counting and integration schemes,<sup>7,28</sup> in their usual monostatic forms, requires adapting the equivalent beam angle  $\psi_0$ , which is defined entirely in terms of the transducer beam pattern,<sup>31</sup>

$$\psi_0 = \int b^2 d\Omega. \quad (3)$$

Since this applies at a constant, far-field range, and  $dV = r^2 dr d\Omega$ , the solid-angle analog to Eq. (2) is

$$\int \int H(gb^2\sigma - t)dF d\Omega,$$

where  $\sigma$  is the backscattering cross section. Comparing this with Eq. (3), it is clear that the effective equivalent beam angle is

$$\psi = \int \int b^2 H(gb^2\sigma - t)dF d\Omega. \quad (4)$$

This quantity can, in one sense, be regarded as a generalization of the equivalent beam angle defined in Eq. (3). However, its origin is in the concept of sampling volume, described in Eq. (2), and, when  $\psi$  is multiplied by  $r^2 \Delta r$ , the product is equal to the sampling volume within a spherical shell of infinitesimal thickness  $\Delta r$ .

The gain factor  $g$  in the several equations is exemplified by two extreme, but not uncommon, monostatic situations of detection in the usual far field of the transducer: (1) for a single scatterer,  $g = 10^{-\alpha r/5} r^{-4}$ , where  $\alpha$  is the coefficient of absorption given in decibels per meter and  $r$  is the range in meters to the scatterer; and (2) for a layer of identical scatterers,  $g = 10^{-\alpha r/5} r^{-2}$ .

The detection threshold  $t$  has the same units as the product  $gb^2\sigma$ . At the very threshold, detection occurs essentially on the acoustic axis, where  $b = 1$ . The scatterer, if directional, is moreover in its most favorable aspect, where  $\sigma = \sigma_{\max}$ . Here, at the maximum detection range,  $g$  is a minimum. Thus  $t = g_{\min} \sigma_{\max}$ . In the limit that  $t$  vanishes, or the SNR becomes very large,  $V_s \rightarrow V_0$  and  $\psi \rightarrow \psi_0$ .

## II. INTEGRATION ISSUES

In both the general expression for  $V_s$  in Eq. (2) and the associated differential measure for the monostatic case,  $\psi$  in Eq. (4), the spatial integrals are shown without explicit limits, and the Heaviside step function  $H$  appears in the integrand. The integration with respect to the volume element  $dV$  in Eq. (2) is understood to be performed over the entire volume that is accessible between the range intervals of interest. Similarly, the integration with respect to the solid-angle element  $d\Omega$  in Eq. (4) is assumed to be performed over that accessible at the particular range of interest. The physically available space, either volume or solid angle, constitutes an upper bound to the respective integrals.

The Heaviside step function, or counting function, describes the details of the sampling process. If and only if the received echo strength  $gb^2\sigma$  exceeds the detection threshold  $t$  is the echo fully registered. In the case that  $gb^2\sigma = t$ , the echo is registered with one-half weight or count, corresponding to

the statistical registration of such marginal echoes 50% of the time.

For generally directive scatterers with random orientations, echoes arising from the same scatterer at the same fixed position in space may or may not be registered. In a favorable orientation, for example, the scattering cross section  $\sigma$  may be so large that  $gb^2\sigma$  exceeds  $t$  and the echo is registered. In an unfavorable orientation at the same position,  $gb^2\sigma$  may be less than  $t$ , and the echo will not be registered. It is therefore not generally possible to remove the Heaviside step function from the integrand and impose precise limits on the volume or solid-angle integrals. That is,  $V_s$  and  $\psi$  are not sharply defined regions of space. Nonetheless, they are well-defined quantities, as described in the several integrals.

The discussed integrals, if analytically intractable, are, in fact, easy to compute by means of an algorithm. The physically available space is first partitioned into small cells. Each cell is then examined separately with respect to the received echo level relative to the detection threshold for the range of scatterer orientations specified by the distribution function  $F$ . The several continuous variables involved in this are discretized in the usual manner, as illustrated by the example in Sec. IV. Received echo levels are, respectively, counted or ignored as  $gb^2\sigma$  exceeds or is less than  $t$ .

### III. COMPUTATIONAL MODEL FOR ACOUSTIC SAMPLING OF FISH

An immediate application of theory is in the acoustic measurement of fish density. It is convenient to evaluate numerically the effective equivalent beam angle in Eq. (4). This is done through the following model.

**Medium.** This consists of seawater of salinity 35 ppt and temperature 5 °C. The sound speed is thus 1470 m/s.<sup>32</sup> At 38 kHz, therefore, the absorption coefficient  $\alpha$  is 0.0106 dB/m.<sup>33</sup>

**Transducer.** The transducer is assumed to be circular, with half-beamwidth of 4 deg or full beamwidth between opposite -3-dB levels of 8 deg. The beam pattern thus depends only on the polar angle  $\theta$ , and  $b = [2J_1(ka \sin \theta)/(ka \sin \theta)]^2$ , where  $ka = 1.61/\sin(\pi/45) = 23.1$ . Performance of the integration in Eq. (3) yields the nominal equivalent beam angle  $\psi_0 = 0.0108$  sr or -19.66 dB.

**Fish backscattering cross section.** The source of data consists of measurements by Nakken and Olsen<sup>34</sup> of the tilt angles

TABLE I. Characteristics of four subsets of target strength functions for gadoids at 38 kHz, used in computations for Figs. 1-4. The minimum and maximum lengths  $l_{\min}$  and  $l_{\max}$  refer to criteria applied in selecting the subsets. The number of included functions is denoted  $n_i$ . The mean and standard deviation of lengths  $l$  in each subset are shown. Units of length are centimeters.

Subset	$\bar{l}$				
	$l_{\min}$	$l_{\max}$	$n_i$	mean	s.d.
1	5	15	27	10.7	2.3
2	15	25	29	21.5	3.0
3	35	45	29	39.0	3.1
4	55	65	21	59.0	3.2

gle dependence of the dorsal aspect target strength function, which are tabulated in Ref. 35. Of these, 171 apply to the gadoids cod (*Gadus morhua*), saithe (*Pollachius virens*), and pollack (*Pollachius pollachius*), at 38 kHz. Four subsets of these functions are selected to illustrate the effect of fish length, thence directionality of scattering pattern, on  $\psi$ . These are described in Table I. The backscattering cross section  $\sigma$  of fish at tilt angle  $\theta'$  is derived from the target strength value  $TS$  ( $\theta'$ ) according to the definition<sup>36</sup>  $TS = 10 \log \sigma / 4\pi$ , but with use of SI units.

**Fish behavior.** This is characterized in the usual way by a normal probability density function of tilt angle  $N(\bar{\theta}', s_{\theta'})$ . Two sets of parameters are used:  $(\bar{\theta}', s_{\theta'}) = (0, 5)$  and  $(-4.4, 16.2)$  deg. The empirical bases of the two sets are described in Refs. 37 and 38, respectively. The tilt angle distribution is assumed to be truncated at two standard deviations from the mean. Thus the probability density function  $f$  in  $dF = f d\theta'$  is  $f = 0.95^{-1} \exp[-(\theta' - \bar{\theta}')^2/2s_{\theta'}^2]$ .

### IV. NUMERICAL METHOD

The integration in Eq. (4) is effected in the following way. For the range  $r$ , less than the maximum detection range  $r_{\max}$ , the equation  $gb^2 = t$  is solved for  $\theta$ . Specifically, the equation

$$2J_1(ka \sin \theta)/ka \sin \theta = 10^{-\alpha(r_{\max} - r)/20} (r/r_{\max})^q$$

is solved numerically, where  $q = 1$  for a single point scatterer and  $q = 1/2$  for a scattering layer. The solution, denoted  $\theta_r$ , is then used to limit the  $\theta$  integration in Eq. (4), for the target at  $r$  cannot be detected anywhere outside the cone  $\theta = \theta_r$ .

Equation (4) is evaluated in the following discrete version:

$$\begin{aligned} \psi_r &= 2\Delta\theta\Delta\phi \sum_{i=1}^{n_j} b^2(\theta_i) \sin \theta_i \\ &\times \sum_{j=1}^{n_j} \left\{ \left[ \sum_{k=1}^{n_k} H \left( b^2(\theta_i) \frac{\sigma(\chi_{ijk})}{\sigma_{\max}} - \frac{g_{\min}}{g_r} \right) f'(\theta'_k) \right] \right. \\ &\left. \times \left( \sum_{k=1}^{n_k} f'(\theta'_k) \right)^{-1} \right\}, \end{aligned} \quad (5)$$

where

$$\Delta\theta = \theta_r/n_j, \quad \theta_i = (i - 1/2)\Delta\theta, \quad \Delta\phi = \pi/n_j,$$

$$\phi_j = (j - 1/2)\Delta\phi, \quad \Delta\theta' = 4s_{\theta'}/n_k,$$

$$\theta'_k = \bar{\theta}' - 2s_{\theta'} + (k - 1/2)\Delta\theta',$$

$$\chi_{ijk} = \pi/2 - \cos^{-1}(\sin \theta_i \cos \phi_j \cos \theta'_k - \cos \theta_i \sin \theta'_k).$$

The subscript is attached to  $\psi$  and  $g$  to emphasize their applicability at range  $r$ . In the computations reported below,  $n_j = 20$ ,  $n_j = 6$ , and  $n_k = 40$ .

### V. RESULTS

The effective equivalent beam angle  $\psi$  is examined first for a single point scatterer and a layer of point scatterers. Equation (4), thence Eq. (5) also, is immediately simplified, for the scattering is independent of orientation; hence, the integration over  $dF$  yields unity. Since  $b$  only depends on

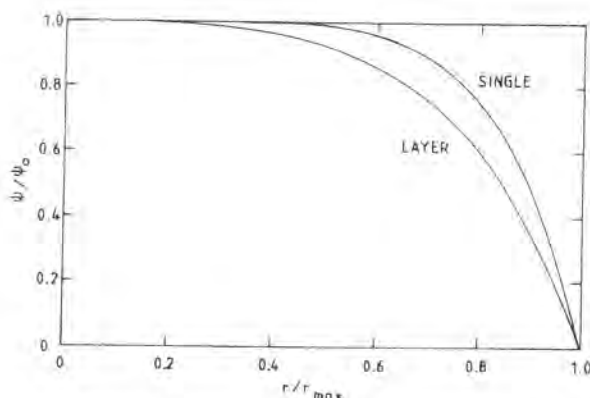


FIG. 1. Effective equivalent beam angle  $\psi$  normalized to the nominal transducer value  $\psi_0$  as a function of range  $r$  relative to the maximum detectable range  $r_{\max} = 400$  m for both a single point scatterer and a layer of identical point scatterers. Other parameters are specified in Sec. III.

$\theta$ , integration over  $\phi$  yields  $2\pi$ . Given a maximum range of detectability,  $\psi$  is reduced to the following:

$$\psi_r = 2\pi \int b^2(\theta) H \left( b^2 - \frac{g_{\min}}{g_r} \right) \sin \theta d\theta.$$

This, or rather its discrete version, analogous to Eq. (5), is evaluated for  $r_{\max} = 400$  m. The results, after normalization to the ideal limit  $\psi_0$ , are presented in Fig. 1.

What is to be remarked on here, with force for the other computations too, is that an absolute comparison of the scattering strengths of the point scatterer and layer of point scatterers is not undertaken. Rather, each of two problems is examined, where each scatterer type has its detection threshold at 400 m. Under ordinary conditions, without this constraint, if the point scatterers in the layer were identical with the single point scatterer, the detection thresholds would of course be different.

The effect of directionality in scattering by fish on  $\psi$  is illustrated in Figs. 2–4 for the single-scatterer case, hence with  $g = 10^{-\alpha r/5} r^{-4}$ . Figure 2 applies to the tilt angle distribution  $N(0,5)$ ; Fig. 3 applies to the distribution

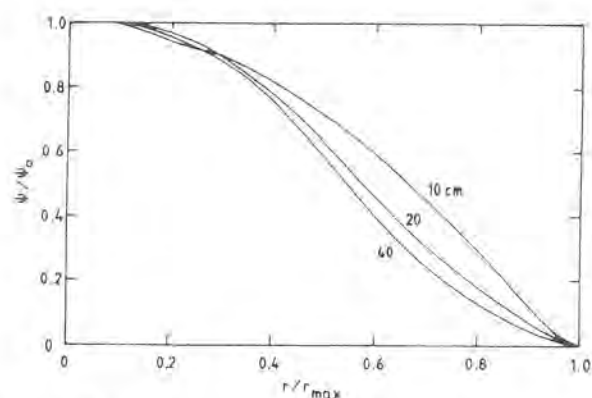


FIG. 3. Effective equivalent beam angle  $\psi$  after normalization, versus range  $r$  relative to  $r_{\max} = 400$  m, as in Fig. 2, but with the tilt angle distribution  $N(-4.4,16.2)$  deg.

$N(-4.4,16.2)$ . The effect of behavior on  $\psi$  is shown directly for gadoids of nominal length 60 cm in Fig. 4.

## VI. DISCUSSION

A number of systematic dependences expected from Eq. (4) are confirmed by the computations. To elucidate these more strongly, the dependence on the backscattering cross section  $\sigma$  is essentially eliminated in the computations for Fig. 1 by consideration of identical point scatterers. For these, the value of the product  $gb^2$ , when compared with the threshold value  $t$ , is decisive for determining whether an echo strength lies above or below  $t$ , hence is or is not detected. Since the so-called gain or geometric factor  $g$  decreases with increasing range, the maximum angle of detection,  $\theta = \theta_r$  in the beam pattern  $b$ , also decreases with increasing  $r$ . This is evident in Fig. 1.

The curves in Figs. 1–4, which are ogives in Figs. 2–4, show the expected monotonic decrease in  $\psi$  with increasing  $r$ . In addition,  $\psi$  is seen to vanish at the maximum range  $r_{\max}$  and to approach the nominal transducer value  $\psi_0$  asymptotically as  $r$  decreases.

Another systematic dependence seen in Fig. 1 is the effect of scatterer type, single or layer, on  $\psi$ . The mechanism

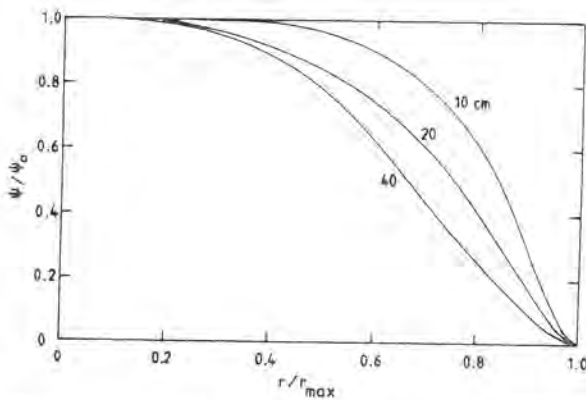


FIG. 2. Effect of directionality in scattering by fish on the normalized effective equivalent beam angle  $\psi$ , after normalization, versus range  $r$  relative to  $r_{\max} = 400$  m for gadoid target strength functions at 38 kHz, as described in subsets 1–3 in Table I, with respective nominal mean lengths 10, 20, and 40 cm, assuming the tilt angle distribution  $N(0,5)$  deg.

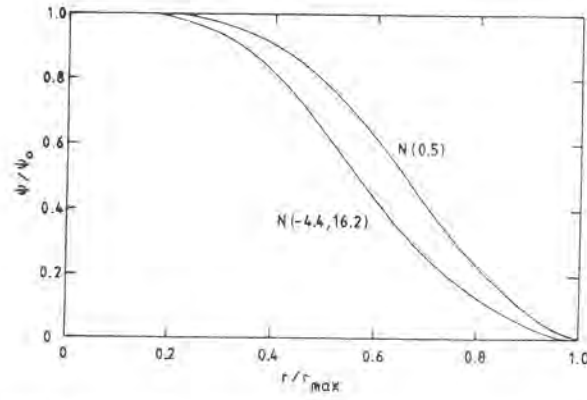


FIG. 4. Comparison of the normalized effective equivalent beam angle  $\psi$  versus range  $r$  relative to  $r_{\max} = 400$  m for gadoid target strength functions, with nominal mean length 60 cm, as computed for each of two tilt angle distributions.

for this is the range dependence of  $g$ . For the same range,  $g$  for the single point scatterer is less than  $g$  for the layer of identical point scatterers, hence  $\psi$  for the single-point scatterer exceeds that for the layer. If this result seems contrary in the context of overall backscattering strength, it must be remembered that the maximum detection range is assumed to be the same for the two scatterer types. This assumption is artificial for, all things being equal, the layer of identical scatterers would be detected at a greater range than the single scatterer would be. However, it was not felt necessary to illustrate this fact here.

Repetition of the computations in Fig. 1 for different values of  $r_{\max}$  yields very similar results. For example, for a single point scatterer with  $r_{\max} = 500$  m,  $\psi$  is within 1 dB of  $\psi_0$  for ranges less than 390 m, or 78% of  $r_{\max}$ , while with  $r_{\max} = 200$  m,  $\psi$  departs from  $\psi_0$  by 1 dB at 150 m, or 75% of  $r_{\max}$ . The trend is indeed similar; the small difference is due to the absorption part of  $g$ , which does not scale with  $r$  in the same way that the spreading part does.

Having established and shown how the effective equivalent beam angle  $\psi$  varies for identical point scatterers, different single-fish scatterers are now considered. Comparison of the single-scatterer curve in Fig. 1 with any of the other curves in Figs. 2–4 shows that the effect of directionality in fish scattering is to decrease  $\psi$  below that of the point scatterer. In addition, for the same orientation distribution, the larger the scatterer and more directional the scattering pattern, the smaller  $\psi$  tends to be at the same  $r$ , assuming identical values for  $r_{\max}$ . This general trend clearly holds in Figs. 2 and 3, except for small values of  $r/r_{\max}$  in Fig. 3, where the differences are not significant. The corresponding curves for 60-cm fish in Fig. 4 also deviate somewhat from the trend, but again only to an insignificant degree. The discrepancies reflect variations in scattering properties, especially with respect to scatterer orientation, that are intrinsic to the scattering process, but which are not so strong as to upset the described general trend.

Behavior, as described by the orientation distribution, is also an important factor affecting  $\psi$  in Eq. (4). For broad tilt angle distributions, such as that in Fig. 3, the chance of sensing lower values of backscattering cross section is much greater than for rather narrow distributions, such as that in Fig. 2, hence the general displacement of the two sets of curves. This is illustrated directly in Fig. 4, where the curve for  $N(-4.4, 16.2)$  lies significantly below that for  $N(0, 5)$  for the same set of fish target strength functions, subset number 4 in Table I.

As described in Sec. III, the computations presented in Figs. 1–4 are based on an ideal circular transducer with 4-deg half-beamwidth, measured from the acoustic axis to –3-dB level. Repetition of the computations for other narrow transducer beams, with half-beamwidths over the range 2.5–10 deg, shows no or only negligible differences with the present results.

The several functions described graphically can also be approximated. One successful function that has been used to model  $\psi$  for cod target strength functions is the following:<sup>39</sup>

$$\psi/\psi_0 = \hat{\psi}_1 + \hat{\psi}_2, \quad (6a)$$

where

$$\hat{\psi}_1 = 1 - [1 + (Q\Delta)^2]^{-1}, \quad (6b)$$

$\Delta = r/r_{\max} - r_{\max}/r$ , and  $Q$  is a measure of the steepness of falloff of  $\psi/\psi_0$ . The function  $\hat{\psi}_2$  is determined by fitting a Fourier series, such as finite cosine series, to the residual function

$$\psi_{\text{res}} = \psi/\psi_0 - \hat{\psi}_1. \quad (6c)$$

A fairly reasonable agreement can be obtained for a seven-term series, for example, but values near the threshold are most difficult to fit, both because of the smallness of the data sample and the sensitivity of  $\psi$  near the threshold to the exact form of the target strength function.

While the model and computational example are directed to acoustic scattering, analogs exist in optical and other systems using irradiation and scattering for the remote sensing of scatterer concentration or size. Acknowledgment of the importance of the sampling volume is evident in the study of a forward-scattering system by Hirleman *et al.*<sup>40</sup> Application to size and concentration measurements, by like forward scattering<sup>41</sup> or by backscattering lidar or laser radar,<sup>42,43</sup> is apparent.

- <sup>1</sup>M. S. Roos, R. E. Apfel, and S. C. Wardlaw, "Application of 30-MHz acoustic scattering to the study of human red blood cells," *J. Acoust. Soc. Am.* **83**, 1639–1644 (1988).
- <sup>2</sup>L. R. Abts, R. T. Beyer, P. D. Richardson, P. M. Galletti, and K. E. Karlsson, "Microparticle detection with focused ultrasound," *J. Acoust. Soc. Am. Suppl. 1* **60**, S53–S54 (1976).
- <sup>3</sup>L. R. Abts, R. T. Beyer, P. D. Richardson, P. M. Galletti, and K. E. Karlsson, "Reflections from microparticles in a flowing liquid," *J. Acoust. Soc. Am. Suppl. 1* **64**, S62 (1978).
- <sup>4</sup>P. L. Edwards and J. Jarzynski, "Scattering of focused ultrasound by spherical microparticles," *J. Acoust. Soc. Am.* **74**, 1006–1012 (1983).
- <sup>5</sup>M. S. Roos, "A technique for the study of acoustic scattering from microparticles," *J. Acoust. Soc. Am.* **83**, 770–776 (1988).
- <sup>6</sup>J. Y. Chapelon, P. M. Shankar, and V. L. Newhouse, "Ultrasonic measurement of bubble cloud size profiles," *J. Acoust. Soc. Am.* **78**, 196–201 (1985).
- <sup>7</sup>S. T. Forbes and O. Nakken, Eds., "Manual of methods for fisheries resource survey and appraisal. Part 2. The use of acoustic instruments for fish detection and abundance estimation," FAO Man. Fish. Sci. **5**, 1–138 (1972).
- <sup>8</sup>M. L. Peterson, C. S. Clay, and S. B. Brandt, "Acoustic estimates of fish density and scattering function," *J. Acoust. Soc. Am.* **60**, 618–622 (1976).
- <sup>9</sup>J. E. Ehrenberg, "A review of *in situ* target strength estimation techniques," FAO Fish. Rep. **300**, 85–90 (1983).
- <sup>10</sup>D. V. Holliday, "Extracting bio-physical information from the acoustic signatures of marine organisms," in *Oceanic Sound Scattering Prediction*, edited by N. R. Andersen and B. J. Zahuranec (Plenum, New York, 1977), pp. 619–624.
- <sup>11</sup>R. E. Pieper, "Euphausiid distribution and biomass determined acoustically at 102 kHz," *Deep-Sea Res.* **26**, 687–702 (1979).
- <sup>12</sup>T. K. Stanton, R. D. M. Nash, R. L. Eastwood, and R. W. Nero, "A field examination of acoustical scattering from marine organisms at 70 kHz," *IEEE J. Ocean. Eng.* **OE-12**, 339–348 (1987).
- <sup>13</sup>D. V. Holliday, R. E. Pieper, and G. S. Kleppel, "Determination of zooplankton size and distribution with multifrequency acoustic technology," *J. Cons. Int. Explor. Mer* **46**, 52–61 (1989).
- <sup>14</sup>J. R. Proni, F. C. Newman, D. C. Rona, D. E. Drake, G. A. Berberian, C. A. Lauter, Jr., and R. L. Sellers, "On the use of acoustics for studying suspended oceanic sediment and for determining the onset of the shallow thermocline," *Deep-Sea Res.* **23**, 831–837 (1976).
- <sup>15</sup>M. H. Orr and R. R. Hess, "Remote acoustic monitoring of natural suspensate distributions, active suspensate resuspension, and slope/shelf water intrusions," *J. Geophys. Res.* **83(C8)**, 4062–4068 (1978).
- <sup>16</sup>A. E. Hay, "On the remote acoustic detection of suspended sediment at long wavelengths," *J. Geophys. Res.* **88(C12)**, 7525–7542 (1983).

- <sup>1</sup>J. Sheng and A. E. Hay, "An examination of the spherical scatterer approximation in aqueous suspensions of sand," *J. Acoust. Soc. Am.* **83**, 598–610 (1988).
- <sup>2</sup>E. Ona, "The equivalent beam angle and its effective value when applying an integrator threshold," *Counc. Meet. Int. Counc. Explor. Sea* **1987/B-35**, Copenhagen, Denmark.
- <sup>3</sup>D. H. Cushing, "Computations with a sonar equation," *J. Cons. Int. Explor. Mer* **35**, 22–26 (1973).
- <sup>4</sup>D. H. Cushing, "The present state of acoustic survey," *J. Cons. Int. Explor. Mer* **38**, 28–32 (1978).
- <sup>5</sup>K. I. Yudanov and I. L. Kalikhman, "Sound scattering by marine animals," in *Proceedings of the Meeting on Hydroacoustical Methods for the Estimation of Marine Fish Populations*, edited by J. B. Suomala, Jr. (C. S. Draper Lab., Cambridge, MA, 1981), Vol. 2, pp. 53–95.
- <sup>6</sup>I. L. Kalikhman, W. D. Tesler, and K. I. Yudanov, "Methods of determining the density of fish concentrations," in *Proceedings of the Meeting on Hydroacoustical Methods for the Estimation of Marine Fish Populations*, edited by J. B. Suomala, Jr. (C. S. Draper Lab., Cambridge, MA, 1981), Vol. 2, pp. 533–573.
- <sup>7</sup>A. Aglen, "Echo/integrator threshold and fish density distribution," *FAO Fish. Rep.* **300**, 35–44 (1983).
- <sup>8</sup>I. L. Kalikhman and W. D. Tesler, "The effective parameters of the real acoustic beam," *FAO Fish. Rep.* **300**, 9–17 (1983).
- <sup>9</sup>H. Lassen, "Signal threshold in echointegration," *Counc. Meet. Int. Counc. Explor. Sea* **1986/B-35**, Copenhagen, Denmark.
- <sup>10</sup>R. T. Weimer and J. E. Ehrenberg, "Analysis of threshold-induced bias inherent in acoustic scattering cross-section estimates of individual fish," *J. Fish. Res. Board Can.* **32**, 2547–2551 (1975).
- <sup>11</sup>C. S. Clay and H. Medwin, *Acoustical Oceanography: Principles and Applications* (Wiley, New York, 1977).
- <sup>12</sup>D. N. MacLennan, "Acoustical measurement of fish abundance," *J. Acoust. Soc. Am.* **87**, 1–15 (1990).
- <sup>13</sup>K. G. Foote, "Correcting acoustic measurements of scatterer density for extinction," *J. Acoust. Soc. Am.* **88**, 1543–1546 (1990).
- <sup>14</sup>K. G. Foote, "Biasing of fish abundance estimates derived from use of the sector scanning sonar in the vertical plane," in *Proceedings of the Conference Progress in Sector Scanning Sonar* (Institute of Acoustics, Edinburgh, 1979), pp. 44–52.
- <sup>15</sup>E. J. Simmonds, "A comparison between measured and theoretical equivalent beam angles for seven similar transducers," *J. Sound Vib.* **97**, 117–128 (1984).
- <sup>16</sup>K. V. Mackenzie, "Nine-term equation for sound speed in the oceans," *J. Acoust. Soc. Am.* **70**, 807–812 (1981).
- <sup>17</sup>R. E. Francois and G. R. Garrison, "Sound absorption based on ocean measurements... Part II: Boric acid contribution and equation for total absorption," *J. Acoust. Soc. Am.* **72**, 1879–1890 (1982).
- <sup>18</sup>O. Nakken and K. Olsen, "Target strength measurements of fish," *Rapp. P.-v. Réun. Cons. Int. Explor. Mer* **170**, 52–69 (1977).
- <sup>19</sup>K. G. Foote and O. Nakken, "Dorsal aspect target strength functions of six fishes at two ultrasonic frequencies," *Fiskeri og havet, Ser. B* **1978/1**, 1–95.
- <sup>20</sup>R. J. Urick, *Principles of Underwater Sound* (McGraw-Hill, New York, 1975), 2nd ed.
- <sup>21</sup>K. G. Foote and E. Ona, "Tilt angles of schooling penned saithe," *J. Cons. Int. Explor. Mer* **43**, 118–121 (1987).
- <sup>22</sup>K. Olsen, "Orientation measurements of cod in Lofoten obtained from underwater photography and their relation to target strength," *Counc. Meet. Int. Counc. Explor. Sea* **1971/B-17**, Copenhagen, Denmark.
- <sup>23</sup>K. G. Foote, "Acoustic sampling volume for cod," *Counc. Meet. Int. Counc. Explor. Sea* **1989/B-5**, Copenhagen, Denmark.
- <sup>24</sup>E. D. Hirleman, V. Oechsle, and N. A. Chigier, "Response characteristics of laser diffraction particle size analyzers: optical sample volume extent and lens effects," *Opt. Eng.* **23**, 610–619 (1984).
- <sup>25</sup>B. A. Weiss, P. Derov, D. DeBiase, and H. C. Simmons, "Fluid particle sizing using a fully automated optical imaging system," *Opt. Eng.* **23**, 561–566 (1984).
- <sup>26</sup>H. Nakane and Y. Sasano, "Structure of a sea-breeze front revealed by scanning lidar observation," *J. Meteorol. Soc. Jpn.* **64**, 787–792 (1986).
- <sup>27</sup>P. Qing, H. Nakane, Y. Sasano, and S. Kitamura, "Numerical simulation of the retrieval of aerosol size distribution from multiwavelength laser radar measurements," *Appl. Opt.* **28**, 5259–5265 (1989).

# Importance of the swimbladder in acoustic scattering by fish: A comparison of gadoid and mackerel target strengths

Kenneth G. Foote

Department of Applied Mathematics, University of Bergen, 5014 Bergen, Norway

(Received 3 December 1979; accepted for publication 7 March 1980)

Previous determinations of the swimbladder contribution to the fish backscattering cross section have been hindered by ignorance of the acoustic boundary conditions at the swimbladder wall. The present study circumvents this problem by direct comparison of target strengths of three gadoid species and mackerel — anatomically comparable fusiform fish which respectively possess and lack a swimbladder. The relative swimbladder contribution to both maximum and averaged dorsal aspect backscattering cross sections is shown to be approximately 90% to 95%, which is higher than most other estimates. The new results were established for fish of 29- to 42-cm length and acoustic frequencies of 38 and 120 kHz.

PACS numbers: 43.80.Jz, 43.30.Dr, 43.30.Gv

## INTRODUCTION

The importance of the swimbladder in acoustic scattering by physoclistous and physostomatous fish has long been recognized.<sup>1-17</sup> There is conflicting evidence, however, for the magnitude of its contribution to the fish backscattering cross section. This may be due in part to systematic species and frequency differences in scattering properties, but undoubtedly also reflects the variety of methods which have been applied in its determination.

Experimental studies have been essentially comparative. Backscattering cross sections or target strengths of fish with intact swimbladders have been compared with measurements of the same fish with deflated,<sup>2,5,14</sup> flooded,<sup>6</sup> or model-substituted<sup>2,4</sup> swimbladders. Comparisons have also been made with measurements on air-filled sacs with an equivalent volume<sup>1,13</sup> and solid

swimbladder models.<sup>2</sup> Theoretical studies have modeled the swimbladder as a gas-filled cylinder,<sup>7,8</sup> spherical air bubble in water<sup>9</sup> or in an elastic medium,<sup>6</sup> spheroidal gas bubble,<sup>12</sup> and spherical viscoelastic shell.<sup>13,14</sup> Several of these models are examined further, in the light of measurements, in Refs. 15, 18, and 19. Estimates of the swimbladder contribution derived from some of the cited studies are presented in Table I.

The problem common to the various investigations, which is also a cause of the differing results, is that of preserving boundary conditions. The swimbladder is generally aspherical<sup>1,15,16</sup> and cannot be approximated by a simple geometric shape except possibly at rather low frequencies. In addition, the swimbladder is supported unequally by the surrounding tissue.<sup>20</sup> This was observed dramatically in a recent series of radiographic observations of the swimbladder of several fish sub-

TABLE I. Estimates of the swimbladder contribution to fish backscattering cross sections derived from earlier studies.

Method	Objects of acoustic comparison	Frequencies (kHz)	Swimbladder contribution (percentage)	Ref.
Experiment	Gutted cod of 60–75 cm length and model swimbladders with equivalent swimbladder volume	10, 14, 30	35–70	1
Experiment	Perch of 20 cm length with full and deflated swimbladders	30	50	2
Experiment	1 crappie (32 cm), 1 large mouth bass (40 cm), and 2 yellowfin tuna (69 and 73 cm) with full and deflated swimbladders	20, 40, 50, 280	20–80	5
Experiment	Rubber cylinders of lengths from 14 to 30 acoustic wavelengths with and without air-filled cylindrical cavities	1480	30–90	8
Theory	Same rubber cylinders as above	1480	96	8
Experiment	1 cod (62 cm) with and without its swimbladder	278	20	10
Experiment	140 "Fun" of lengths from about 1 to 20 acoustic wavelengths at each frequency with and without their swimbladders	50, 200	68	14

jected to large external pressure changes.<sup>21</sup>

The present study attempts to preclude all considerations of boundary conditions by direct comparison of measured backscattering cross sections of gadoids and mackerel, which respectively possess and lack a swimbladder, but are otherwise similar in size, shape, and, to an extent, anatomy.

## I. DATA BASE AND ANALYSIS

The data base of this study consists in Nakken and Olsen's measurements of the dorsal aspect target strength functions of three gadoid species and mackerel at 38 and 120 kHz.<sup>22,23</sup> Only those measurements corresponding to fish with lengths from 29 to 42 cm are used. This length range represents the extent of the mackerel measurements, which is more limited than that of any of the gadoid species. The numbers of available target strength functions are described by species and frequency in Table II.

These data have been prepared for further analysis by extraction of maximum values and by averaging of each dorsal aspect function. The averaging proceeds according to the model described in detail in Ref. 24 and used elsewhere.<sup>25-30</sup> For present purposes it is sufficient to consider ensonification of fish by a directional echo sounder. The position and orientation of fish in the echo sounder beam are described by probability distribution functions which are, respectively, uniform and essentially normal in tilt angle. Independence of the two distributions, which is tantamount to neglecting avoidance reaction,<sup>30,31</sup> is also reasonable for the intended computations here.

The tilt angle distribution is defined precisely as a normal distribution which is truncated at angles departing from the mean by three standard deviations. Empirical justification for use of this distribution is presented in Refs. 32 and 33. The mean and standard deviation of the nontruncated distribution are chosen to be 0 and 10 deg, which are characteristic of a rather loose aggregation.<sup>28</sup> For these parameter values the noted deficiencies of some of the mackerel data in Ref. 23 are entirely negligible.

The echo sounder is represented by beam patterns equivalent to that of an ideal circular piston with half-beamwidth, or angular distance from acoustic axis to -3 dB level, of 2.5 deg.

TABLE II. Numbers of available and analyzed target strength functions of gadoids and mackerel with lengths from 29 to 42 cm as distinguished by species and frequency.

Species	Numbers of target strength functions	
	Frequency = 38 kHz	Frequency = 120 kHz
Cod ( <i>Gadus morhua</i> )	22	12
Saithe ( <i>Pollachius virens</i> )	17	12
Pollack ( <i>Pollachius pollachius</i> )	11	11
Mackerel ( <i>Scomber scombrus</i> )	35	24

Possible systematic species differences in the gadoid target strength data are ignored. The merged data are distinguished only by target strength type and frequency. These are compared with corresponding target strengths for mackerel. To facilitate this comparison, the target strengths of each set are regressed linearly on fish length according to the prescription

$$TS = m \log l + b, \quad (1)$$

where TS is the target strength predicted for fish of length  $l$ , expressed in centimeters, and  $m$  and  $b$  are the estimated regression coefficients. Evidence for the validity of linear regression analysis of similar target strength data is cited in Ref. 26.

In order to determine the contribution of the swimbladder to the backscattering cross section, the target strength of Eq. (1) is expressed as a cross section  $\sigma$  according to the definition

$$TS = 10 \log(\sigma/4\pi). \quad (2)$$

The units of TS are decibels and  $\sigma$ , square meters, such that the idealized perfectly reflecting sphere of 2 m radius has a target strength of 0 dB.

### Swimbladder contribution

The contribution of the swimbladder to the backscattering cross section is defined here by the relative quantity

$$1 - \sigma_2/\sigma_1,$$

where  $\sigma_1$  and  $\sigma_2$  are the respective backscattering cross sections of gadoids and mackerel of the same length. Since  $\sigma_1$  and  $\sigma_2$  are derived from data which are intrinsically stochastic on the scale size of measurement, the swimbladder contribution is specified within limits that obtain with a given probability, say  $1 - \alpha$ . If the cumulative distribution function of the gadoid target strength variable  $y_1$  is denoted  $F_1(y_1)$  and the probability density function of the mackerel target strength variable  $y_2$  is denoted  $f_2(y_2)$ , then

$$1 - 10^{-d_1/10} \leq 1 - \sigma_2/\sigma_1 \leq 1 - 10^{-d_2/10} \quad (3)$$

with probability  $1 - \alpha$ , where  $d_1$  and  $d_2$  are determined by numerical solution of the equation

$$\int_{-\infty}^{\infty} F_1(y+d) f_2(y) dy = \begin{cases} \alpha/2, & \text{for } d = d_1, \\ 1 - \alpha/2, & \text{for } d = d_2. \end{cases} \quad (4)$$

This last equation simply expresses the probability that the difference of the two independent random variables  $y_1$  and  $y_2$  does not exceed the values  $d_1$  or  $d_2$ .<sup>34</sup> According to the plausible hypotheses on which the linear regression analyses are based, each distribution is normal. For fish of length  $l$  in the interval [29, 42] cm the defining parameters of the distribution of target strength variable  $y$  are the mean

$$\bar{y} = m \log l + b \quad (5)$$

and standard deviation

$$s_y = s_{y,x} \left( n^{-1} + (l - \bar{x})^2 / \sum_i (x_i - \bar{x})^2 \right)^{1/2}, \quad (6)$$

where  $s_{y,x}$  is the standard error of the regression,  $x_i$  is the logarithm of length for a single datum, and  $\bar{x}$  is the mean of the logarithmically transformed lengths of all  $n$  data underlying the regression.

## II. RESULTS

Target strengths corresponding to the data enumerated in Table II are presented on scatter diagrams in Figs. 1–4. The maximum dorsal aspect target strengths of Figs. 1 and 3 were derived by simple extraction from the data presented in Ref. 23. The target strengths of Figs. 2 and 4 were derived from the data of the same reference by the averaging method outlined above and described fully in Ref. 24.

Results of regressing both the merged gadoid target strengths and mackerel target strengths on fish length for the various data sets are described in Table III. There the estimated standard errors of estimated regression coefficients are denoted  $s_m$  and  $s_b$ . The standard error of the regression is denoted SE. The correlation coefficient  $\rho$  of data is attached for reference. The described linear regressions are shown on the figures.

The principal results of the study are shown in Fig. 5. This is composed of four sets of figures, corresponding to Figs. 1–4, which express the relative swimbladder contribution as a percentage. The contribution is described within limits that obtain with probability 0.95.

TABLE III. Regression analyses of maximum and averaged target strengths on fish length for gadoid and mackerel data at 38 and 120 kHz.  $m$  and  $b$  are the estimated regression coefficients, cf. Eq. (1);  $s_m$  and  $s_b$ , the corresponding standard errors; SE, the standard error of the regression; and  $\rho$ , the correlation coefficient.

TS-type	Fish	Frequency (kHz)	$m$	$s_m$	$b$	$s_b$	SE	$\rho$
Maximum	Gadoids	38	27.1	5.6	-71.7	8.6	1.8	0.572
Maximum	Mackerel	38	39.6	13.9	-100.7	21.5	2.8	0.445
Average	Gadoids	38	23.8	5.5	-71.3	8.4	1.7	0.532
Average	Mackerel	38	39.8	14.9	-106.3	23.0	3.0	0.423
Maximum	Gadoids	120	27.2	7.1	-70.4	10.9	1.8	0.553
Maximum	Mackerel	120	54.7	17.8	-125.0	27.6	3.3	0.547
Average	Gadoids	120	22.9	6.2	-71.2	9.5	1.6	0.541
Average	Mackerel	120	53.7	19.5	-130.2	30.2	3.6	0.506

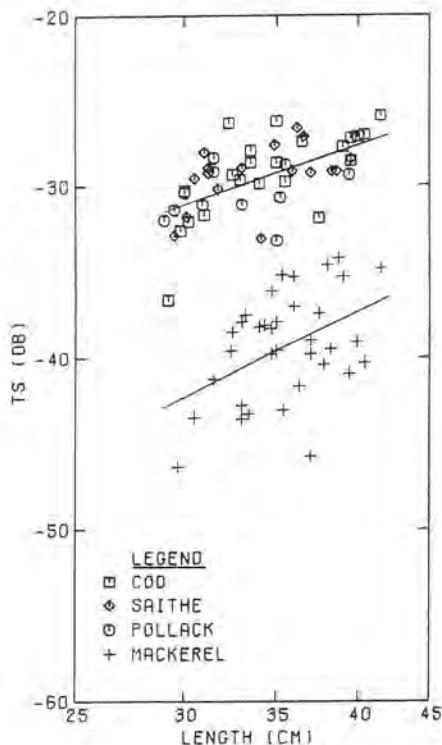


FIG. 1. Scatter diagrams with regressions of maximum dorsal aspect target strengths on length for merged gadoids and for mackerel at 38 kHz.

## III. DISCUSSION

The target strength data of each of Figs. 1–4 are divisible into two groups with only a small "gray zone" of possible ambiguity or overlap. The gadoid data are apparently homogeneous, which justifies their merging. General systematic species differences among gadoid target strength data<sup>26–28</sup> are probably absent in the present case because of the particular, narrow, length range of the data. The mackerel data are similarly homogeneous, although more dispersed. Both the gadoid and mackerel target strength data are assumed to be amenable to linear regression analysis, which is supported by the analysis of Table III and other computations.<sup>26</sup>

The backscattering cross sections and associated statistics derived from the regression analyses were used, as in Eqs. (3) and (4), to determine the swimbladder contribution to the backscattering cross section. It is reasoned that this contribution can be estimated as the difference in cross sections of anatomically comparable fish, of the same length or mass, which respectively possess and lack a swimbladder. The cross section of a bladderless fish is thus taken to be a measure of the cumulative scattering power of fish flesh, bone, and other organs. While the backscattering cross section of an individual fish is a sensitive function of its precise composition,<sup>7,10,17</sup> it is reasonable to assume that individual variations are smoothed out through the kind of regression analysis performed here. Because gadoids and mackerel are approximately similar in their gross anatomy and fusiform shapes, the difference in cross sections may be accepted as a measure of the scattering strength of the swimbladder. The similarity in condition factors for the mackerel and gadoids of measurement<sup>35</sup> supports the comparison of the target strengths, as presented in Figs. 1-4, both for fish of the same mass and for fish of the same length.

From the several parts of Fig. 5, the swimbladder contribution to the backscattering cross sections of gadoids is observed to be about 90% to 95%. This is higher than that of many earlier studies, cf. Table I, for example, but is entirely consistent with Yudanov's *a posteriori* assertion that the swimbladder contributes at least 90%, and often much more, to the backscattering cross section.<sup>36</sup>

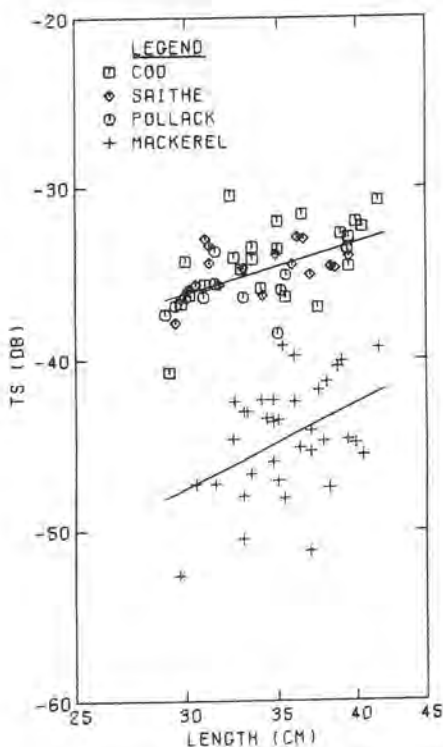


FIG. 2. Scatter diagrams with regressions of averaged dorsal aspect target strengths on length for merged gadoids and for mackerel at 38 kHz.

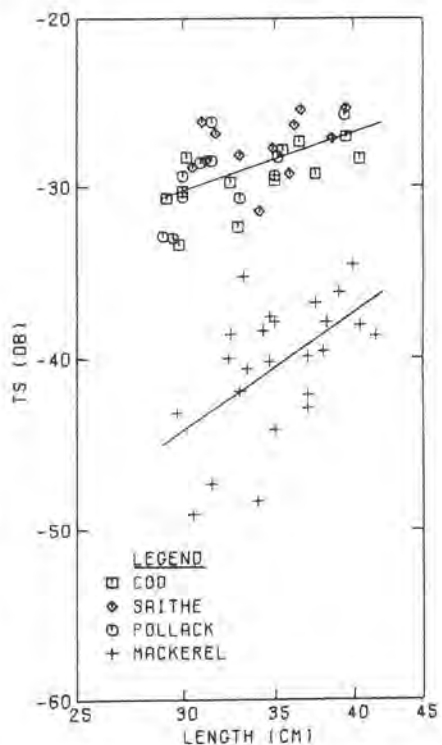


FIG. 3. Scatter diagrams with regressions of maximum dorsal aspect target strengths on length for merged gadoids and for mackerel at 120 kHz.

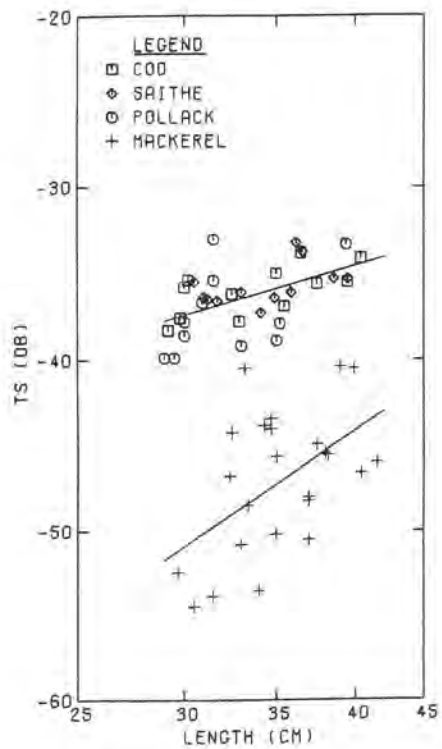


FIG. 4. Scatter diagrams with regressions of averaged dorsal aspect target strengths on length for merged gadoids and for mackerel at 120 kHz.

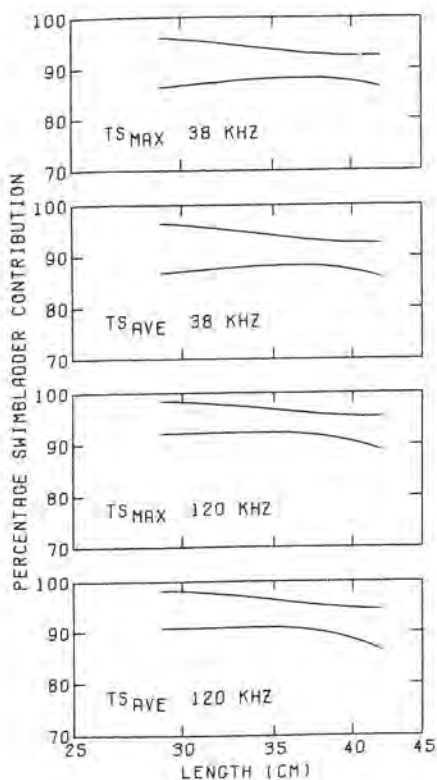


FIG. 5. Percentage swimbladder contribution to maximum and averaged dorsal aspect backscattering cross sections of fish at 38 and 120 kHz, with 95% confidence as defined by the data of Figs. 1-4.

Differences in results between this study and the cited earlier studies are attributed both to differences in the particular species and acoustic frequencies of investigation and to the methods of analysis. The advantage of the present method is that it avoids altering the basic boundary conditions at the swimbladder wall—the interface between the acoustically lossy and elastic fish flesh and strongly reflecting gas sac of the swimbladder.

In revising upwards previous estimates of the scattering contribution of the swimbladder, at least for gadoids at typical ultrasonic survey frequencies, the present study may provide a new impetus to acoustic modelling of swimbladder-bearing fish. This is anticipated to be equally applicable to physoclists and physostomes.

- <sup>1</sup>D. H. Cushing and I. D. Richardson, "Echo sounding experiments on fish," *Fish. Invest. Lond.*, Ser. 2 18(4), 1-34 (1955).
- <sup>2</sup>F. R. Harden Jones and G. Pearce, "Acoustic reflexion experiments with perch (*Perca fluviatilis* Linn) to determine the proportion of the echo returned by the swimbladder," *J. Exp. Biol.* 35, 437-450 (1958).
- <sup>3</sup>L. Midttun and I. Hoff, "Determination of the reflection of sound by fish," *Fiskdir. Skr. Ser. Havunders*, 13(3), 1-18 (1962).
- <sup>4</sup>D. H. Cushing, F. R. Harden Jones, R. B. Mitson, G. H. Ellis, and G. Pearce, "Measurements of the target strength of fish," *J. Br. Inst. Radio Eng.* 25, 299-303 (1963).

- <sup>5</sup>H. W. Volberg, "Target strength measurements of fish," Straza Industries, El Cajon, California, Report R-101 (1963).
- <sup>6</sup>I. B. Andreeva, "Scattering of sound by air bladders of fish in deep sound-scattering ocean layers," *Sov. Phys.-Acoust.* 10, 17-20 (1964).
- <sup>7</sup>R. W. G. Haslett, "Acoustic backscattering cross sections of fish at three frequencies and their representation on a universal graph," *Br. J. Appl. Phys.* 16, 1143-1150 (1965).
- <sup>8</sup>R. W. G. Haslett, "Acoustic backscattering from an air-filled cylindrical hole embedded in a sound-translucent cylinder," *Br. J. Appl. Phys.* 17, 549-561 (1966).
- <sup>9</sup>R. W. G. Haslett, "Automatic plotting of polar diagrams of target strength of fish in roll, pitch and yaw," *Rapp. P.-V. Reun. Cons. Int. Explor. Mer.* 170, 74-81 (1977).
- <sup>10</sup>R. W. G. Haslett, "The fine structure of sonar echoes from underwater targets, such as fish," in *Ultrasonics International 79 Conference Proceedings* (IPC, Guildford, England, 1979), pp. 307-320.
- <sup>11</sup>R. L. Capen, "Swimbladder morphology of some mesopelagic fishes in relation to sound scattering," Navy Electronics Laboratory, San Diego, California, Report 1447 (1967).
- <sup>12</sup>D. E. Weston, "Sound propagation in the presence of bladder fish," in *Underwater Acoustics*, edited by V. M. Albers (Plenum, New York, 1967), Vol. 2, Chap. 5, pp. 55-88.
- <sup>13</sup>B. S. McCartney and A. R. Stubbs, "Measurements of the acoustic target strengths of fish in dorsal aspect, including swimbladder resonance," *J. Sound Vib.* 15, 397-420 (1971).
- <sup>14</sup>K. Shibata, "Experimental measurement of target strength of fish," in *Modern Fishing Gear of the World: 3*, edited by H. Kristjansson [Fishing News (Books) Ltd., London, 1971], pp. 104-108.
- <sup>15</sup>A. D. Hawkins, "Fish sizing by means of swimbladder resonance," *Rapp. P.-V. Reun. Cons. Int. Explor. Mer.* 170, 122-129 (1977).
- <sup>16</sup>R. H. Love, "Resonant acoustic scattering by swimbladder-bearing fish," *J. Acoust. Soc. Am.* 64, 571-580 (1978).
- <sup>17</sup>K. I. Yudanov and I. L. Kalikhman, "Acoustic characteristics of marine animals," in *Proceedings of the Meeting on Hydroacoustical Methods for the Estimation of Marine Fish Populations*, edited by J. B. Suomala, Jr. (Draper Laboratory, Cambridge, MA, in press), Vol. 2.
- <sup>18</sup>O. Sand and A. D. Hawkins, "Acoustic properties of the cod swimbladder," *J. Exp. Biol.* 58, 797-820 (1973).
- <sup>19</sup>G. Sundnes and O. Sand, "Studies of a physostome swimbladder by resonance frequency analyses," *J. Cons. Int. Explor. Mer.* 36, 176-182 (1975).
- <sup>20</sup>P. Tytler and J. H. S. Blaxter, "The effect of swimbladder deflation on pressure sensitivity in the saithe *Pollachius virens*," *J. Mar. Biol. Assoc. U. K.* 57, 1057-1064 (1977).
- <sup>21</sup>K. G. Foote and E. Ona, "Radiographic study of gross changes in swimbladder shape under systematic pressure changes," (in preparation).
- <sup>22</sup>O. Nakken and K. Olsen, "Target strength measurements of fish," *Rapp. P.-V. Reun. Cons. Int. Explor. Mer.* 170, 52-69 (1977).
- <sup>23</sup>K. G. Foote and O. Nakken, "Dorsal aspect target strength functions of six fishes at two ultrasonic frequencies," *Fisk og Havet, Ser. B.*, 1978, No. 3, 95 pp.
- <sup>24</sup>K. G. Foote, "Averaging of fish target strength functions," *J. Acoust. Soc. Am.* 67, 504-515 (1980).
- <sup>25</sup>K. G. Foote, "Effect of fish behaviour on echo energy: the need for measurements of orientation distributions," *J. Cons. Int. Explor. Mer.* 39 (in press).
- <sup>26</sup>K. G. Foote, "On representing the length dependence of acoustic target strengths of fish," *J. Fish. Res. Board Can.* 36, 1490-1496 (1979).
- <sup>27</sup>K. G. Foote, "Fish target strength-to-length regressions for application in fisheries research," in *Ultrasonics International 79 Conference Proceedings* (IPC, London, 1979), pp. 327-332.

- <sup>28</sup>K. G. Foote, "Systematic species and frequency dependent differences among gadoid target strength functions," in *Proceedings of the Meeting on Hydroacoustical Methods for the Estimation of Marine Fish Populations*, edited by J. B. Suomala, Jr. (Draper Laboratory, Cambridge, MA, in press), Vol. 2.
- <sup>29</sup>K. G. Foote, "Evidence for the influence of fish behaviour on echo energy," in *Proceedings of the Meeting on Hydroacoustical Methods for the Estimation of Marine Fish Populations*, edited by J. B. Suomala, Jr. (Draper Laboratory, Cambridge, MA, in press), Vol. 2.
- <sup>30</sup>K. G. Foote, "Biasing of fish abundance estimates derived from use of the sector scanning sonar in the vertical plane," in *Proceedings of the Conference 'Progress in Sector Scanning Sonar'* (Institute of Acoustics, Edinburgh, 1979), pp. 44-52.
- <sup>31</sup>K. Olsen, "Observed avoidance behaviour in herring in relation to passage of an echo survey vessel," ICES C. M. 1979/B:18, 10 pp.
- <sup>32</sup>K. Olsen, "Orientation measurements of cod in Lofoten obtained from underwater photography and their relation to target strength," ICES C. M. 1971/B:17, 8 pp.
- <sup>33</sup>A. K. Beltestad, "Feeding, vertical migration, and schooling of 0-group herring (*Clupea harengus* L.) in relation to light intensity," Dissertation, University of Bergen (1974) (in Norwegian).
- <sup>34</sup>S. S. Wilks, *Mathematical Statistics* (Wiley, New York, 1962), 644 pp.
- <sup>35</sup>E. Bakken (unpublished data).
- <sup>36</sup>K. I. Yudanov, statement at the Meeting on Hydroacoustical Methods for the Estimation of Marine Fish Populations, Draper Laboratory, Cambridge MA, 1979 (unpublished).

# Measurement of fish target strength with a split-beam echo sounder

Kenneth G. Foote, Asgeir Aglen, and Odd Nakken

Institute of Marine Research, 5011 Bergen, Norway

(Received 17 November 1985; accepted for publication 10 April 1986)

Data derived with a 38-kHz split-beam echo sounder have been analyzed to yield target strengths suitable for use with echo integrators. This has required compensation for both thresholding and saturation, since these operations can significantly bias data intended for use with systems, such as echo integrators, whose dynamic ranges are much larger. A nonparametric statistical method is introduced for this purpose. Pure-species acoustic data are extracted in several two-species cases by a method for separating superimposed frequency distributions. Mean *in situ* target strengths are presented for cod, saithe, Norway pout, herring, redfish, and greater silver smelt. For comparison with other data, these are expressed through the standard equation  $\bar{TS} = 20 \log l + b$ , where  $\bar{TS}$  is the mean target strength in decibels, and  $l$  is the fish length in centimeters. For gadoids of lengths from 10 to over 105 cm,  $b = -67.5$  dB. For herring of lengths from 24 to 34 cm,  $b = -72.1$  dB. The often-ignored problem of obtaining unambiguous biological data by trawl sampling is discussed.

PACS numbers: 43.30.Dr, 43.20.Fn, 43.30.Sf, 43.80.Jz

## INTRODUCTION

The need for knowledge of fish target strength is well known.<sup>1</sup> *In situ* measurements are particularly valuable for representing the acoustic scattering properties of fish under the actual conditions of their surveying. Such data acquire a greater significance when used to determine the length dependence of target strength, as the resulting relation can then be used on fish of different lengths than originally observed and also, under certain circumstances, on fish of different species.

Development of the first commercial split-beam echo sounder, by SIMRAD, was therefore welcomed for its evident usefulness in determining *in situ* target strengths. By providing a means of direct measurement, the split-beam technique avoids many of the problems intrinsic to indirect methods.<sup>2</sup> It is additionally superior in principle, if not in practice too, to the only other direct *in situ* method, that of dual beams,<sup>3</sup> when the effect of noise is considered.<sup>4</sup>

Data derived with the split-beam echo sounder cannot be used immediately in ordinary echo surveying work, however, because of general differences in thresholds. The same is true of data derived with the dual-beam echo sounder.<sup>5</sup> An additional problem associated with a limited dynamic range in direct-target-strength-measuring systems is the presence of a maximum-signal level. For the split-beam system, this resembles saturation, and each echo whose pressure exceeds the maximum registration level is recorded at this maximum level.

The two problems of thresholding and saturation are addressed here, with the aim of showing how the split-beam echo sounder can be used to determine target strengths for application in echo surveying. In the course of analyzing data from the first research cruises with the new instrument, the problem of separating two superimposed target strength distributions is also addressed, although for a prescribed but still important case. A very tangible result of this study is a

set of mean *in situ* target strengths for six species of fish at 38 kHz, for use in interpreting echo integrator data.

## I. MATERIALS

The primary materials consist of the acoustic and biological data collected on a number of species during cruises on R/V G. O. SARS, a 75-m-long stern trawler, about Lofoten in March 1984 and the Shetland Islands in July 1984, cf. Fig. 1.

### A. Biological data

The biological data, like the acoustic data, were collected from R/V G. O. SARS. The ensonified fish aggregations

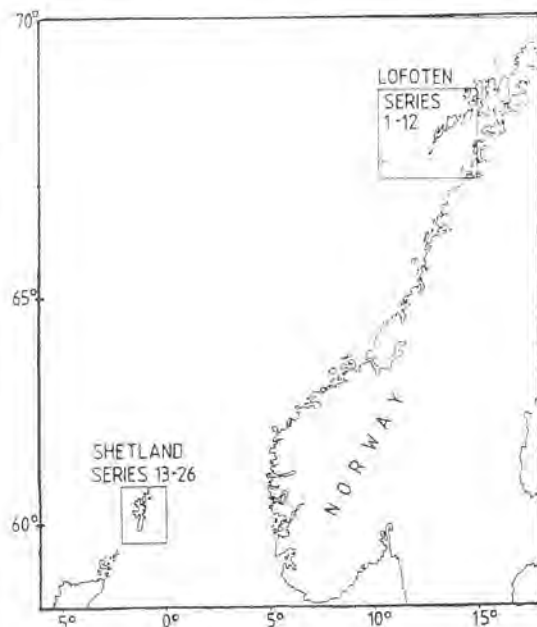


FIG. 1. Regions of data collection.

TABLE I. Biological data accompanying *in situ* target strength measurements made during two 1984 cruises.

Data series	Survey date	Fish	No. specimens		Fish length (cm)				N (mean, s.d.)		Assumed length distribution in simulations	
			Caught	Sized	Mean	s.d.	Min.	Max.	Mean	s.d.	Min.	Max.
1	12/3	{Norway pout Saithe}	223	223	17.6	1.6	10	21	17.6	1.6	14.4	20.8
			52	52	59.7	4.9	48	69	57.2	6.0	45.2	69.2
2	13/3	Saithe	1863	73	57.2	6.0	45	91	57.2	6.0	45.2	69.2
			92	92	19.7	8.7	9	43	19.7	8.7	11.0	37.1
3	13/3	{Redfish Saithe}	15	15	56.3	5.1	46	65	57.2	6.0	45.2	69.2
			13	13	81.7	10.6	60	98	81.6	11.4	58.8	104.4
7	15/3	Cod	1813	1813	37.2	4.4	25	50	37.2	4.4	28.4	46.0
			[Unspec.]	953	81.6	11.4	50	105 + ]	81.6	11.4	58.8	104.4
8	15/3	G. s. smelt	165	165	28.8	2.0	24	34	28.5	2.0	24.5	32.5
			22	22	28.0	2.7	25	34	28.5	2.0	24.5	32.5
11	18/3	Cod	2250	107	14.8	1.1	12	19	14.8	1.1	12.6	17.0

were sampled by trawls immediately prior to, during, or immediately after the target strength collection runs. The type of trawl to be used, either bottom or pelagic, was chosen from the vertical distribution of the fish shown on the echo sounder paper record.

The bottom trawl was a shrimp trawl with 80-mm mesh size, circumference of 1800 meshes in front, and 20-mm mesh size in the cod end. When towed at a speed of 3 kn, its horizontal and vertical openings are, respectively, 18 and 4 m. The pelagic trawl was a herring trawl with a rectangular opening of 21 × 10 meshes of 6400-mm mesh size in the front and 22-mm mesh size in the cod end. When towed at 3–4 kn, its horizontal and vertical openings are approximately 35 and 20 m, respectively.

Along the Lofoten Islands, spawning cod (*Gadus morhua*) of lengths generally exceeding 70 cm were observed in pure concentrations between 100- and 200-m depth. On the outer banks, immature saithe (*Pollachius virens*) of 50- to 65-cm length were found in schools and scattering layers below 100-m depth. In some cases, the recordings of saithe overlapped scattered concentrations of Norway pout (*Trisopterus esmarkii*) and small redfish (*Sebastes marinus*) closer to the bottom. In the deeper parts of Vestfjord, the body of water between the Lofoten Islands and the mainland, at bottom depths of 250 m and more, scattering layers of greater silver smelt (*Argentinasilus*) were observed. All species showed the usual diurnal behavior, forming small schools usually close to the bottom during the day, but ascending somewhat and dispersing at night, thus giving suitable conditions for single-fish target strength measurements.

About the Shetland Islands, suitable observing conditions were only obtained at night and generally only for the darkest hours. For the present observations, which were obtained in an area off the southeastern coast of Shetland, a mixture of plankton and 0-group gadoids consisting of Norway pout, haddock (*Melanogrammus aeglefinus*), and whiting (*Merlangius merlangus*) dominated the echo recordings in the upper 50 m, while adult Norway pout were caught in quantities close to the bottom. Additionally, in parts of the area, dispersed herring (*Clupea harengus*) were recorded

and caught in layers of depth 15–45 m and 65–95 m.

The acoustic data are valuable only when accompanied by good biological data on rather pure fish aggregations. The species and length compositions in each trawl haul and the corresponding echo sounder paper record were therefore carefully examined. Only catches showing a clearly dominant single species or two species of distinct length groups which also could be recognized on the paper record were accepted for further use.

Thus, of the 11 data series from the March Lofoten cruise, only five, numbered 1, 2, 3, 7, and 8 in Table I, qualify unconditionally here for further analysis. Biological data for series 11 were taken from commercial Danish seine catches over the period 8–14 March in the same areas as the acoustic data were sampled. As this is the main area of commercial fishing for spawning cod, trawling was impossible. The authors are nonetheless confident that the species and length composition determined by Danish seining are representative for the recorded fish. The similarity of these data with those determined by trawling by R/V G. O. SARS in an area slightly further east on 15 March is also noted.

Of the 14 data series collected during the July Shetland Islands cruise, only three are sufficiently clean for analysis here. Data series 15 was collected on herring dispersed in the 65- to 95-m layer, while series 25 was collected on herring from the same layer immediately after rising to the 15- to 45-m layer. The herring catch was rather small, but the length distributions of the fish from the respective layers were essentially identical and also equivalent to those from daytime catches in the same area. The mean of the combined length data is 28.5 cm; the standard deviation is 2.0 cm. The catch from the upper layer also contained some 0-group gadoids of mean length 6.8 cm and standard deviation 1.6 cm. Data series 26 represents adult Norway pout dispersed in a layer from the bottom to a height 15 m over the bottom. The trawl haul showed by numbers 96% Norway pout and 4% whiting of mean length 31.1 cm and standard deviation 4.7 cm.

All measurements of fish length reported here refer to the so-called total length.<sup>6,7</sup> For work performed at the Institute of Marine Research, this is essentially the distance from

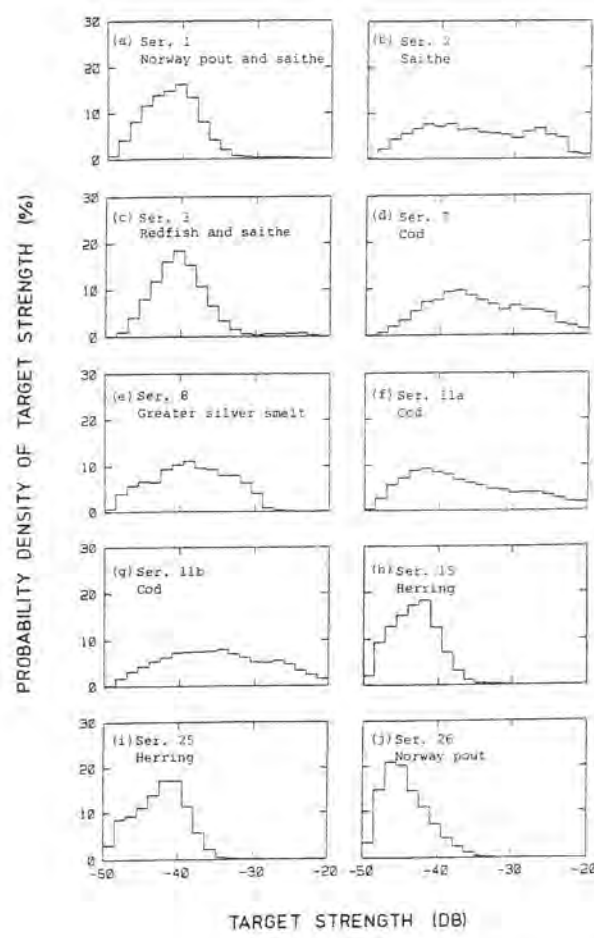


FIG. 2. Target strength histograms of ten data sets derived with the split-beam echo sounder. See Tables I and II for further details.

and the target range. However, since targets are accepted by the ES380 system only if lying within 4.94 deg of the acoustic axis, the depth estimate is only very slightly biased.

Generally, fewer data were analyzed than were available. One reason for this was the desire to maintain a homogeneous data set, as for example by limiting the vessel speed

to a narrow range or by limiting the fish echoes to a narrower depth range than was actually employed during the observations.

## II. METHODS

Two basic problems must be addressed in analyzing the data presented in Fig. 2.

### A. Separation of composite target strength histograms

In the case of those data consisting of mixed species, namely those of series 1 and 3, the target strength data in Fig. 2(a) and (c) must be assigned to the individual fishes. The solution to this problem is referred to as the "method of separation."

It is apparent from Table I that the saithe length distributions of series 1 and 3 resemble those of series 2. In fact, the geographical areas of the three series are essentially the same, being the fishing banks west of Lofoten. Thus the relative contribution of the saithe to the composite target strength histograms of Fig. 2(a) and (c) is known. Because the second species of the two data series, Norway pout and redfish, respectively, is smaller than the saithe, the greatest target strengths of the largest Norway pout and redfish will undoubtedly be substantially less than the greatest target strengths of the largest saithe.<sup>13</sup>

The difference in peak dorsal aspect target strengths of the several fishes can be estimated by reference to Nakken and Olsen's target strength data.<sup>13,14</sup> The appropriate equations share the common form

$$TS_{\max} = m \log l + b, \quad (1)$$

where  $TS_{\max}$  is the maximum dorsal aspect target strength in decibels,  $l$  is the fish length in centimeters, and the coefficients  $m$  and  $b$  are determined by a least-mean-squares regression analysis. For saithe the result is

$$TS_{\max} = 23.4 \log l - 65.1, \quad (2a)$$

or, requiring that  $m = 20$ ,

$$TS_{\max} = 20 \log l - 60.2. \quad (2b)$$

If a nominal length of 70 cm is used for the largest saithe in each of data series 1 and 3, then the maximum dorsal aspect target strength is expected to be about -23 or -22 dB.

TABLE II. Conditions of acoustic data collection.

Data series	Measuring time			Starting position		No. single-fish data		Depth range (m)		Boat speed (kn)	
	Date	Hour	Duration (min)	Lat. (°N)	Long. (°E)	Total	Analyzed	Min.	Max.	Mean	s.d.
1	12/3	2103	81	68.73	12.86 E	10400	9179	105	240	3.9	2.6
2	13/3	0031	23	68.54	12.43 E	3400	3000	105	130	2.9	0.2
3	13/3	1837	78	67.43	10.30 E	8600	7584	165	225	4.4	3.0
7	15/3	1912	48	68.11	14.58 E	5400	4400	70	165	2.7	0.2
8	15/3	2217	47	67.97	14.60 E	7800	2600	265	360	2.4	0.1
11a	18/3	1736	87	68.10	14.52 E	9600	9600	85	160	11.3	0.4
11b	18/3	2155	65	68.10	14.46 E	9000	9000	85	160	3.3	0.3
15	26/7	0021	104	59.96	1.14 W	10600	6545	65	95	7.1	2.9
25	29/7	2353	99	60.24	0.70 W	5800	2687	15	45	5.5	3.8
26	30/7	2248	104	60.61	0.63 W	24000	4201	85	115	4.2	3.7

the anteriormost extremity, e.g., tip of the snout if protruding beyond the end of the lower jaw, to the end of the tail fin. In the case of fish with a forked tail, the two lobes are moved into the position which gives the maximum length measurement.

## B. Acoustic data

### 1. Split-beam echo sounder

The acoustic data were gathered with the SIMRAD ES380 split-beam echo sounder, with hull-mounted transducer resonant at 38 kHz.<sup>8</sup> In this device, essentially a  $2 \times 2$  element phased array, each quadrant signal is separately amplified according to the same time-varied-gain function. The four quadrant beams are combined in pairwise fashion by simple summing to form a total of four half beams. The zero crossings of corresponding half-beam signals are detected and used to determine the alongships and athwartships phase differences, thence angles. Together, these two numbers specify the angular location of the detected scatterer, if present. The same numbers serve as an address for accessing a programmable-read-only memory (PROM) containing the measured beam pattern values.

Simultaneous with the operations on the half-beam signals, the port and starboard half-beam signals are summed to produce a total-signal output. Following envelope detection and analog-to-digital conversion, another PROM is accessed to determine the logarithm of the signal amplitude. This and the beam pattern compensation value form a set of addresses for a third PROM, which provides the target strength value, in coded form, for the particular time sample. A sequence of target strength values spanning the interval from the start of echo-signal reception to its termination by arrival of the bottom echo is derived for each individual transmission. For the fixed sampling frequency of 7.3625 kHz and design sound speed of 1472.5 m/s, the nominal depth resolution is 10 cm.

The sequence of target strength values is reduced by software before the next transmission, which is governed by the pulse repetition frequency, nominally 50/min for the depths encountered during the measurements. The purpose of this data processing is the extraction of all single-fish echoes lying within the operator-specified depth interval.

To describe the criteria for extracting single-fish echoes, it is useful to introduce two quantities. The minimum detectable signal (MDS) is that corresponding to the least target strength of representation, -50 dB, when detected at the maximum allowable angle, 4.94 deg, where the two-way beam pattern loss is -12 dB. For angles greater than 4.94 deg, a zero code is generated. The duration of a single-fish echo is measured at the MDS level and is compared with the duration of the transmit signal as measured at the one-half power points of the detected envelope.

For the present application, a single-fish echo was defined as that set of contiguous nonzero-coded target strengths, whose duration lay within 75% and 175% of the transmit pulse duration and which was bordered by at least four zero-coded target strengths on either side. For the

transmit pulse duration of 1 ms, the minimum distance of separation between scatterers was thus greater than 1 m.

Each single-fish echo is characterized by three data: the ping number, echo range to the nearest decimeter, and target strength, expressed as one of 80 target strength classes evenly spread over the range from -50 to -20 dB, hence with 0.375-dB resolution. The target strength is, in fact, an approximation, being the largest of the arithmetical means of target strengths computed for each pair of adjacent samples. Given the described resolution in target strength, this averaging is expected to incur only a slight negative bias, estimated to be less than 0.1 dB in magnitude, and neglected elsewhere in this paper.

### 2. Calibration

The split-beam echo sounder was calibrated with a 60-mm copper sphere<sup>9,10</sup> on axis in the exact manner of Ref. 11 at least once during each cruise. Direct measurement of the two-way beam pattern during a cruise in November 1985 revealed irregularities in beam shape consistent with the manufacturing specifications but requiring an overall adjustment of measured target strengths by -0.4 dB. This is moderated by the bias of -0.1 dB introduced by a hardware operation in the echo sounder. Measurements of target strength thus had to be reduced by 0.3 dB, which has been done in all computations reported here. In referring, in text and figures, to the measurements as made, however, the original target strength scale and class division are retained.

Detailed analysis of the errors due to measurement of the on-axis value and overall beam-pattern correction factor disclosed a calibration error due to procedure of  $\pm 0.6$  dB with 95% confidence. This may be compared with the figure derived by Simmonds *et al.* for a calibration performed under more controlled conditions, namely  $\pm 0.2$  dB, which was also estimated to apply with 95% confidence.<sup>12</sup>

The basic quantization level or step of the echo sounder is 0.375 dB, implying an additional error of  $\pm 0.2$  dB. The combined error due to calibration procedure and quantization is thus established to be  $\pm 0.6$  dB with 95% confidence.

### 3. Fish target strength

Acoustic data corresponding to the catch data in Table I are summarized through histograms of *in situ* target strength in Fig. 2. Additional data in the form of ping number and depth, which were attached to each respective target strength datum, are neglected here. Thus, according to Ref. 8, some of the measurements included in the histograms derive from the same fish observed repeatedly during passage of the vessel and echo sounder beam. Such multiple observations, which may involve from about 15% to more than 50% of the total number of single-fish data, are not expected to bias the results, although reference to the original data and recomputation could decide the matter if necessary.

Some circumstances of the acoustic data collection are given in Table II. Both the depth range and ship speed refer to the analyzed data. The depth is actually the sum of the depth of the hull-mounted transducer, which is about 5 m,

This agrees well with the observations in Fig. 2(a) and (c), if requiring some squinting to confirm.

Maximum dorsal aspect target strengths of Norway pout and redfish are not reported in the literature. Norway pout is a gadoid, hence for present purposes might be represented as having a target strength roughly comparable to that of other gadoids of similar length. For want of a closer kinship, the maximum target strength relation for Norway pout is based on the combined cod, saithe, and pollack (*Pollachius pollachius*) data of Nakken and Olsen. It is

$$TS_{\max} = 24.5 \log l - 67.1 \quad (3a)$$

or, requiring that  $m = 20$ ,

$$TS_{\max} = 20 \log l - 60.5 \quad (3b)$$

Thus, for the largest observed Norway pout, with  $l = 21$  cm, the maximum target strength is expected to be about  $-35$  or  $-34$  dB.

Redfish is not a gadoid. If gadoid data are appropriate, however, a maximum target strength of about  $-28$  or  $-27$  dB could be expected from the largest caught specimen of 43 cm. However, comparison of the target strength histograms of Fig. 2(b) and (c) suggests a possible greatest redfish target strength of  $-30.5$  dB.

Separation of the saithe contribution from the composite histograms in Fig. 2(a) and (c) is accomplished by attributing all data above the likely greatest target strength of the second, lesser fishes to saithe. The number of represented saithe data above this cutoff represents the same fraction of the entire saithe distribution as does the comparable part of the pure-saithe target strength histogram in Fig. 2(b). The pure-saithe histogram can thus be scaled absolutely, and the part below the cutoffs in Fig. 2(a) and (c) can be subtracted directly from the composite histogram. The result of applying this procedure to the composite data in Fig. 2(a) and (c) is shown in Fig. 3(a) and (b), respectively.

## B. Threshold and saturation compensation

### 1. Background

The problem of extracting the mean target strength is common to all data sets. This would be trivial, indeed, if the intended application involved the same threshold and saturation effects. However, since echo integrators generally register both weaker and stronger signals than the split-beam echo sounder does, the matter cannot be ignored.

Consideration of the range in fish sizes and likely corresponding target strengths<sup>13,14</sup> suggests that the target strengths of the largest cod have not been correctly represented because of saturation at  $-20$  dB. Similarly, the target strengths of fish shorter than 30 cm often lie well below the lower threshold of  $-50$  dB. Thus there is particular justification for investigating the effects of thresholding and saturation on the underlying target strength data of this study.

Weimer and Ehrenberg have approached the problem of thresholding by means of parametric statistics.<sup>5</sup> Under the assumptions of a normal distribution in target strength and equally likely probability of occurrence in the echo sounder

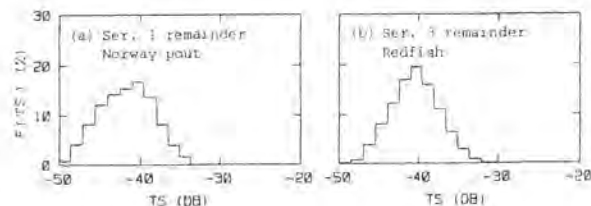


FIG. 3. Target strength histograms derived from Fig. 2(a) and (c) by removal of the saithe contributions.

beam, they derived an exact expression for the threshold effect. The effect of saturation could be incorporated in this, although less simply than by a mere change in the upper limit of integration. In addition, the assumed normal distribution could be replaced by the actual observed distribution,<sup>15</sup> although generally incomplete because of the several delimiting operations.

The empirical data of this study, shown in Figs. 2 and 3, appear for the most part to be non-normally distributed. This should not be surprising, perhaps, for Clay and Heist have found the echo amplitude to be distributed according to Ricean statistics,<sup>16</sup> and other recent modeling work based on representing a fish by its swimbladder and assuming the usual normal tilt-angle distribution has confirmed the non-normal nature of target strength.<sup>17</sup> Extrapolation of the target strength distributions by application of the methods in Refs. 16 and 17 was not attempted for want of sufficient behavioral and morphometric data. Thus a different approach has been pursued here.

### 2. Plan

The effect of thresholding and saturation by the split-beam echo sounder at  $-50$  and  $-20$  dB is estimated by comparing the pure-species target strength histograms of Figs. 2(b), (d)–(j), and 3 with target strength histograms simulated for comparable species from Nakken and Olsen's data.<sup>13</sup> Computation of the simulated target strength histograms, or theoretical distributions, is reviewed in the next section.

In essence, an observed target strength histogram, or empirical distribution, is first trimmed at one or both ends to avoid the biasing influence of target strengths over  $-50$  dB or under  $-20$  dB, affected, respectively, by thresholding or saturation. The trimmed empirical distribution is then extended by appending the tails of the theoretical distributions. Proper allowance must be made for the relative proportions of truncated and added endpieces of the distributions. This is discussed in Sec. II B 4.

Additional compensation of the final, averaged target strengths for the threshold and saturation levels of the intended devices of application, modern echo-integrating systems, is unnecessary. The reason, simply, is that these levels lie far beyond the ordinary range of single-fish target strengths.

### 3. Simulating target strength histograms

The target strength simulation data were derived directly from Nakken and Olsen's data.<sup>13</sup> To form a uniform basis

having the same length distribution as that observed, only those target strength functions were used whose corresponding fish lengths lay within the truncation limits shown in Table I. The measured target strength functions were then scaled in both angle and magnitude to simulate the functions of a series of fish spanning the length range. Simulation of the target strength function  $TS'(\theta')$  of tilt angle  $\theta'$  for a fish of length  $l'$  from the measured function  $TS(\theta)$  for a fish of length  $l$  was accomplished by the transformation:

$$\begin{aligned} l &\rightarrow l', \\ \theta - \theta_{\max} &\rightarrow (l'/l)(\theta' - \theta_{\max}), \\ TS &\rightarrow TS' = 20 \log(l'/l). \end{aligned}$$

The angle of maximum target strength, denoted by  $\theta_{\max}$ , is assumed to be unchanged under the transformation. Target strength values lost in cases of contraction of the original function were replaced by values derived from the very approximate relation  $TS_{\min} = 30 \log l' - 100$ , where  $l'$  is expressed in centimeters. This was established by cursory inspection of the data in Ref. 14.

For each of these simulated functions, a target strength histogram was computed in an analogous manner to that of Ref. 17. These theoretical histograms were subsequently compounded according to a truncated normal distribution of fish length having the characteristics given in Table I.

Representation of the several fishes in the simulation was one-to-one for cod, saithe, and herring. For both Norway pout and the non-gadoid but physoclistous redfish and greater silver smelt, Nakken and Olsen's<sup>13</sup> combined data for cod, saithe, and pollack were used.

In order to compute a target strength histogram from simulated data, a specific behavior mode has to be assumed. Because of the present use of a vertical echo-sounding system, this is described adequately by the distribution of tilt angle.<sup>18,19</sup> Notwithstanding broad recognition of its importance, and recent development of a transponding tilt-angle-measuring tag by R. B. Mitson at the Fisheries Laboratory in Lowestoft, England, tilt angle distributions have been determined at sea for only three species.<sup>20-22</sup> Given the sensitivity of the tilt angle distribution to behavior, for example, directed horizontal swimming *contra* feeding *contra* diving, this is clearly unknown for the observed fish.

The state of nearly total ignorance of fish behavior was remedied by assuming a range of behavioral modes, performing the described computations for each, and averaging the results over the entire set. A single assumption was made about the behavior: that it was not extreme. This hypothesis was theoretically sustained, in fact, for simulated target strength distributions with mean tilt angles greater than 10 deg from the horizontal generally lack or under-represent the largest observed target strengths. Therefore, if the target strength measurements of Nakken and Olsen<sup>13</sup> and their applicability<sup>23</sup> can be believed, then strong avoidance reactions with diving<sup>24,25</sup> are simply incompatible with the observations. The nonextreme behavior modes were characterized by normal distributions in tilt angle with means of -10, -5, 0, 5, and 10 deg and standard deviations of 5, 10, and 15 deg.

In simulating the target strength histograms with respect to normal distributions of tilt angle, the effect of per-

spective<sup>19</sup> was incorporated by increasing the first two standard deviations to 5.5 and 10.2 deg, while leaving the third unchanged. These values were determined for an ideal circular beam pattern with sharp edge 5 deg from the acoustic axis, assuming an equally likely probability of occurrence anywhere in the horizontal plane.

#### 4. Mean target strengths

All averaging was accomplished in the intensity domain, hence with respect to the backscattering cross section  $\sigma$ . The relation between target strength  $TS$  and  $\sigma$  assumed throughout this paper is that given by the traditional and usual definition,

$$TS = 10 \log(\sigma/4\pi),$$

as in Urick,<sup>26</sup> but with SI units. The mean target strength  $\bar{TS}$  for a particular behavior mode is defined in terms of the average backscattering cross section  $\bar{\sigma}$  by analogy,

$$\bar{TS} = 10 \log(\bar{\sigma}/4\pi). \quad (4)$$

For the special case of a uniform target strength distribution over the interval from  $TS_1$  to  $TS_2$ , the mean backscattering cross section  $\sigma$  is

$$\bar{\sigma} = \frac{40\pi}{\ln 10} \frac{10^{TS_2/10} - 10^{TS_1/10}}{TS_2 - TS_1}. \quad (5)$$

This is, in fact, the prescription used in assigning mean backscattering cross sections to the various target strength classes of the several distributions. The basic target strength interval,  $TS_2 - TS_1$ , used in the computations was 1.5 dB.

Compensation for thresholding and saturation is applied in the determination of  $\bar{\sigma}$ , which begins with the straightforward averaging of the observed target strength histogram, or empirical distribution, with result  $\bar{\sigma}_e$ . The two compensations are now described.

a. *Lower tail.* This compensation involves extrapolating the observed target strength distribution below the nominal threshold of -50 dB. As the effect of the threshold is sharp only for scatterers with target strengths greater than about -47 dB, and since scatterers with target strengths between -50 and -47 dB are unequally registered by the echo sounder, the effective threshold may exceed -50 dB. This quantity, referred to as the lower cutoff, was chosen to optimize the agreement of empirical and theoretical distributions at their junction. Six discrete levels were examined, from -50 to -42.5 dB in steps of 1.5 dB. In practice, the cutoff was determined from among the three lowest levels, the higher ones always giving a much poorer agreement.

The contributions of the lower tails of the empirical and theoretical distributions to their respective averages were computed for target strengths not exceeding the chosen cut-off. These are denoted  $\Delta\sigma_{e,a}$  and  $\Delta\sigma_{t,a}$ , respectively. The proportions of the histograms, or distributions, represented by the several contributions,  $p_{e,a}$  and  $p_{t,a}$ , were also computed.

Compensation for the threshold is effected by lopping off the lower tail of the empirical distribution and appending the lower tail of the theoretical distribution. When allowance is made for the change in the number of basis data,

$$\bar{\sigma}_e \rightarrow \frac{1-p_{t,a}}{1-p_{e,a}} (\bar{\sigma}_e - \Delta\sigma_{e,a}) + \Delta\sigma_{t,a}$$

describes the effect on the uncompensated mean backscattering cross section  $\bar{\sigma}_e$ .

b. *Upper tail.* In compensating for saturation, the empirical distribution is terminated at  $-21.5$  dB, which reduces  $\bar{\sigma}_e$  by the amount  $\Delta\sigma_{e,b}$ . The corresponding proportion of the histogram is  $p_{e,b}$ . This is to be replaced by the upper tail of the theoretical distribution, lying above  $-21.5$  dB, with contribution  $\Delta\sigma_{t,b}$  to the theoretical mean. The effective contribution is determined by scaling  $\Delta\sigma_{t,b}$  in proportion to  $p_{e,b}$  since, in saturation, no data are lost, but only wrongly classified in the highest target strength class. If the proportion of the theoretical distribution above  $-21.5$  dB is denoted  $p_{t,b}$ , then

$$\bar{\sigma}_e \rightarrow \bar{\sigma}_e - \Delta\sigma_{e,b} + (p_{e,b}/p_{t,b})\Delta\sigma_{t,b}$$

describes the transformation of  $\bar{\sigma}_e$  due solely to saturation.

c. *Combined effect.* The result of applying the two transformations is the fully compensated value

$$\bar{\sigma}'_e = \frac{1-p_{t,a}}{1-p_{e,a}} \left( \bar{\sigma}_e - \Delta\sigma_{e,a} - \Delta\sigma_{e,b} + \frac{p_{e,b}}{p_{t,b}} \Delta\sigma_{t,b} \right) + \Delta\sigma_{t,a} \quad (6)$$

This quantity was computed for each of the 15 investigated, nonextreme behavior modes. The ensemble average  $\sigma^*$  was then computed as a simple arithmetic mean, and the sample variation due to ignorance of the behavior mode was estimated by computing the standard deviation  $\Delta\sigma^*$  in  $\sigma^*$ . Corresponding target strengths were determined analogously to Eq. (4), hence

$$TS^* = 10 \log (\sigma^*/4\pi) \quad (7a)$$

and

$$TS^*_{\pm} = 10 \log [(\sigma^* \pm \Delta\sigma^*)/4\pi]. \quad (7b)$$

### III. RESULTS

Threshold- and saturation-compensated mean *in situ* target strengths derived with the new split-beam echo sounder are shown in Table III. The uncertainty in target strength includes three effects: (1) error in calibration procedure, (2) quantization error, and (3) uncertainty over the exact behavioral mode or tilt angle distribution assumed in the course of complementing the original, generally truncat-

ed, data series. The combined error due to the first two sources was established above to be  $\pm 0.6$  dB with 95% confidence. The error due to the third source was determined as the arithmetic mean of  $(TS^*_+ - TS^*)$  and  $(TS^* - TS^-)$ . The number shown in the table as an uncertainty in mean target strength is derived by combining the standard deviations of each of the three sources through the root-mean-square operation.

For comparison purposes, the quantity

$$b_{20}^* = TS^* - 20 \log \bar{l}, \quad (8)$$

where  $\bar{l}$  is the mean fish length, is included in Table III. Its error is composed of the uncertainties in both target strength estimate  $TS^*$  and mean length  $\bar{l}$ . As this last error depends on the representability of biological sampling by trawling, which remains unknown, no confidence limits are given.

The mean target strength derived by equal weighting of the three cod data is  $-30.6$  dB. If this is used together with the tabulated data for the other gadoids, then the result of regressing the mean target strength on the logarithm of mean fish length is

$$TS_{\text{gadoids}} = 20.2 \log l - 67.8, \quad (9a)$$

which obtains with a standard error of 1.7 dB. If the length dependence is constrained to be  $20 \log \bar{l}$ , then

$$\bar{TS}_{\text{gadoids}} = 20 \log \bar{l} - 67.5, \quad (9b)$$

with the same standard error. If each of the six tabulated gadoid data is weighted equally, then the resulting equations are  $\bar{TS} = 18.9 \log \bar{l} - 66.2$  and  $\bar{TS} = 20 \log \bar{l} - 68.0$ , which obtain with respective standard errors of 1.4 and 1.5 dB.

If the matter of the depth dependence of the herring data is ignored, and the two target strengths are accorded equal weight, then the average target strength of a 28.5-cm herring is  $-43.0$  dB. If this single datum is allowed to determine the coefficient  $b$  in the equation  $\bar{TS} = 20 \log \bar{l} + b$ , then

$$\bar{TS}_{\text{herring}} = 20 \log \bar{l} - 72.1. \quad (10)$$

### IV. DISCUSSION

#### A. Biological sampling

The usefulness of *in situ* target strength measurements depends largely on the reliability of the accompanying biological data. In general, trawls are highly selective gears be-

TABLE III. Threshold-compensated mean *in situ* target strengths derived with the SIMRAD ES380 split-beam echo sounder.

Fish	Length (cm)	Depth (m)	Boat speed (kn)	No. data	Target strength (dB)	$b_{20}^*$ (dB)	Data series
Cod	$81.6 \pm 11.4$	70–165	$2.7 \pm 0.2$	4400	$-30.6 \pm 0.3$	-68.9	7
Cod	$81.6 \pm 11.4$	85–160	$11.3 \pm 0.4$	9600	$-31.0 \pm 0.3$	-69.2	11a
Cod	$81.6 \pm 11.4$	85–160	$3.3 \pm 0.3$	9000	$-30.3 \pm 0.3$	-68.5	11b
Saithe	$57.2 \pm 6.0$	105–130	$2.9 \pm 0.2$	3000	$-30.6 \pm 0.3$	-65.8	2
Norway pout	$17.6 \pm 1.6$	105–240	$3.9 \pm 2.6$	9179	$-42.2 \pm 0.9$	-67.1	1
Norway pout	$14.8 \pm 1.1$	85–115	$4.2 \pm 3.7$	4201	$-44.9 \pm 0.9$	-68.3	26
Redfish	$19.7 \pm 8.7$	165–225	$4.4 \pm 3.0$	7584	$-40.6 \pm 0.5$	-67.1	3
G. s. smelt	$37.2 \pm 4.4$	265–360	$2.4 \pm 0.1$	2600	$-36.6 \pm 0.4$	-68.0	8
Herring	$28.5 \pm 2.0$	65–95	$7.1 \pm 2.9$	6545	$-43.4 \pm 0.5$	-72.5	15
Herring	$28.5 \pm 2.0$	15–45	$5.5 \pm 3.8$	2687	$-42.6 \pm 0.5$	-71.7	25

cause of mesh selection and because of both species and length dependent herding by all components of the trawl system, including vessel, warps, otterboards, bridles, and net.<sup>27</sup> Hence, both species and length compositions in trawl hauls from areas where various species and size groups are mixed together are biased. Accordingly, also, the mean lengths calculated for such distributions are biased.

Hylen *et al.*<sup>28</sup> have shown that the bottom trawl used in the present experiments largely undersamples small cod. Their studies also indicate that the number of captured fish of 10- to 15-cm length must be multiplied by a factor of 8–10 in order to be comparable with the catch of 40- to 50-cm fish. A similar trend has been observed for haddock. With regard to the pelagic trawl, Hylen *et al.*<sup>28</sup> have shown that the largest cod are undersampled because these beasts are able to avoid the gear by diving beneath it during towing.

While these observations may give some general guidelines on the biases introduced by the sampling gear, the information is not sufficient for estimating the biases incurred for various species and length compositions, hence correction for such biases. Therefore, to ensure the quality of the biological data, only data from quite pure fish aggregations have been used. Additionally, it was required that the coefficient of variation of fish lengths in the respective catches be as low as possible. This was the case for all of the reported species except that of redfish, which has been included because of the rarity, if not uniqueness, of unambiguous acoustic observations on it.

#### B. Acoustic data analysis

Compensation for the threshold and saturation effects has been achieved through a combined comparison and extrapolation procedure based on simulated target strength distributions. These depend on the validity of the basis target strength data, presumed established,<sup>23</sup> and knowledge of the fish behavior as expressed through the tilt angle distribution. Given nearly complete ignorance of the particular behavior patterns, a range of nonextreme behavior modes has been assumed. Averaging of the respective mean target strengths has revealed a rather low variance, with maximum standard deviation due only to uncertainty in behavior mode of 0.9 dB. Given the standard deviation due to other causes of 0.3 dB, the standard deviation in estimated mean due to all error sources is therefore less than 1.0 dB in all cases, as shown in Table III. This is fortunate for indicating a basic insensitivity of threshold- and saturation-compensated *in situ* target strengths to the particular behavior mode, which is both unknown and difficult to know.

There is, however, clear support for the exclusion of extreme behavior patterns from the analysis of each data series here: It is the presence of relatively large target strengths in the distributions. If the mean tilt angle were, for instance, to deviate from the horizontal by more than about 10 deg, then it would be difficult, if not impossible, to explain the large target strengths that were observed. In a word, the present analysis indicates that fish detected within the acoustic beam were not seriously affected by the passage of the vessel. It is noteworthy in the same context that most of the data were collected at moderate speeds. In the case of

TABLE IV. Adjustments to the uncompensated mean target strengths according to two methods: the present nonparametric method and Weimer and Ehrenberg's method<sup>5</sup> based on assumption of normality in target strength data. NC denotes not computed.

Fish	Length (cm)	Adjustment to target strength	
		Nonparametric method	Parametric method
Cod	81.6 ± 11.4	0.2	NC
Cod	81.6 ± 11.4	0.2	NC
Cod	81.6 ± 11.4	0.1	NC
Saithe	57.2 ± 6.0	0.0	-1.5
Norway pout	17.6 ± 1.6	-1.5	-1.1
Norway pout	14.8 ± 1.1	-1.7	-1.4
Redfish	19.7 ± 8.7	-1.0	-0.8
G. s. smelt	37.2 ± 4.4	-0.6	-1.3
Herring	28.5 ± 2.0	-1.2	-1.2
Herring	28.5 ± 2.0	-1.2	-1.2

cod, however, data were collected at each of several distinct speeds, varying from less than 3 knots to more than 11 knots, yet neither systematic nor significant differences in target strength were found.

Justification for the threshold and saturation compensation is provided by a comparison of the compensated mean target strengths with the corresponding mean target strengths as computed directly from the uncompensated split-beam data. The result is shown in Table IV under the heading "nonparametric method." Only in the case of saithe are the estimates identical, which indicates that the principal part of the target strength distribution for saithe is expected to lie within the acceptance range of the echo sounder. For the other fishes, the effect of compensation, as based solely on the mean values, varies from -1.7 to 0.2 dB.

Included in Table IV are compensation factors derived from Weimer and Ehrenberg's parametric approach.<sup>5</sup> In performing the computations, the true mean values were assumed to be those given in Table III, and the standard deviations were assumed equal to those characterizing the distributions in Figs. 2(b), (d)–(j), and 3. The value used for the factor  $c$  in Eq. (30) of Ref. 5 is 0.895, as given in Ref. 29, since the present 3-dB beamwidth is less than the specified 20 deg. Except for the case of cod, which was not computed, and that of saithe, which was, the agreement of corresponding nonparametric and parametric results is quite good.

While preparing the split-beam data for averaging, two instances of mixed-species data were encountered. In each of these, the distribution form of the component with the larger target strengths, namely saithe, was well known. This allowed subtraction of the entire large-fish contribution, leaving the small-fish distribution as the remainder for further analysis.

A degree of justification for this procedure lies in the final results: The target strengths of the Norway pout of 17.6-cm mean length and the redfish are in line with other physoclist *in situ* target strengths, both as determined in this study and as determined elsewhere. Exemplary, independently derived target strength data are provided by a series of measurements of walleye pollock (*Theragra chalcogramma*) with the dual-beam echo sounder.<sup>2,15,29–31</sup>

## C. Comparisons

The similarity of target strengths of cod and saithe, with respective mean lengths of 82 and 57 cm, deserves particular comment, for according to Eqs. (9a) and (9b) the difference in length suggests a difference in target strength of more than 2 dB, yet none is found.

Two general causes of this discrepancy are discussed. (1) Behavior. Avoidance reaction is believed unlikely because of the depth of saithe, in excess of 100 m, and the demonstrably ship-speed-independent mean target strength of the shallower cod. Differences in less-extreme behavior modes, as related, for example, to ambient light intensity, feeding conditions, or migratory phase, may explain only part of the discrepancy when account is taken of possible species-based differences in target strength.<sup>19</sup> (2) Swimbladder state. A difference in relative degrees of swimbladder inflation, due solely to depth, is also believed unlikely because of the similar physoclistous nature of the two gadoids, which are expected to maintain inflated swimbladders to remain neutrally buoyant. However, differences in the biological states of the two fishes, as due, for example, to the presence of spawning products, extent of stomach filling, or level of lipids, may explain considerable variations in both form and size of the swimbladder.<sup>32,33</sup> These synoptic variations may account for the discrepancy, although detailed scattering computations in the manner of Ref. 17 have not been performed for want of suitable data.

Systematic comparison of the present results with other *in situ* data is foregone for the sake of brevity. Instead, several rather recent measurement results are quoted.

### 1. Gadoid target strength

The relation derived on the sole basis of 13 pollack swimbladders and 2 saithe swimbladders, and assumption of cod behavior as described by Olsen,<sup>20</sup> is<sup>17</sup>

$$\overline{TS}_{\text{gadoids}} = 20 \log \bar{l} - 66.9, \quad (11)$$

which is to be compared with Eq. (9b).

### 2. Herring target strength

The relation recommended by the 1983 Planning Group on ICES-coordinated Herring and Sprat Acoustic Surveys, albeit anonymously, is<sup>34</sup>

$$TS_{\text{herring}} = 20 \log \bar{l} - 71.2, \quad (12)$$

which is to be compared with Eq. (10). Degnbol, Lassen, and Stæhr have, through an indirect *in situ* measurement method, determined the constant in this equation to be -72.6 dB for herring in the Kattegat-Skagerrak<sup>35</sup> and -70.8 dB for herring in the Baltic Sea.<sup>36</sup> For herring in the North Sea, Forbes has recently completed a preliminary study with the dual-beam system which indicates a value of -73.6 dB.<sup>37</sup> Forbes regards this result as being quite tentative because of the problem of species identification in the surveyed, mixed-species environment.

The variance in the several numbers reported here may be due to measurement error, of course, but may also reflect, in the words of Traynor,<sup>31</sup> the dynamic nature of fish target strength.

## D. Future work and afterword

Much more remains to be done with the data analyzed here. Three examples of future studies are the following: (1) determination of the depth dependence of the herring target strength, (2) compensation for thresholding and saturation on the basis of data simulated from swimbladder morphometries, and (3) investigation of avoidance reactions through a statistical analysis of echo trace lengths.<sup>1,38</sup> Another study which could be profitably undertaken, were better behavioral data forthcoming, is a refinement of the present target strength values based on more certain specification of the applicable tilt angle distributions.

It is interesting retrospective of the introduction of the split-beam echo sounder one year ago<sup>8</sup> to note that the potential of the instrument is being realized. However, it is also exceedingly important to call the attention of current and future users of the equipment to the hazards of ignoring thresholding and saturation, the Scylla of -50 dB, the Charybdis of -20 dB.

## ACKNOWLEDGMENT

A. Raknes is thanked for collecting the acoustic data on cod on 18 March 1984. This paper is an expanded version of a report presented at the Statutory Meeting of the International Council for the Exploration of the Sea, held in London, 7-16 October 1985.

- <sup>1</sup>L. Midttun, "Fish and other organisms as acoustic targets," Rapp. P.-v. Réun Cons. Int. Explor. Mer. **184**, 25-33 (1984).  
<sup>2</sup>J. E. Ehrenberg, "A review of *in situ* target strength estimation techniques," FAO Fish. Rep. (300), 85-90 (1983).  
<sup>3</sup>J. E. Ehrenberg, "Two applications for a dual beam transducer in hydro-acoustic fish assessment systems," Proc. 1974 IEEE Conf. Eng. Ocean Environ. **1**, 152-155 (1974).  
<sup>4</sup>J. E. Ehrenberg, "A comparative analysis of *in situ* methods for directly measuring the acoustic target strength of individual fish," IEEE J. Ocean. Eng. **OE-4**(4), 141-152 (1979).  
<sup>5</sup>R. T. Weimer and J. E. Ehrenberg, "Analysis of threshold-induced bias inherent in acoustic scattering cross-section estimates of individual fish," J. Fish. Res. Board Can. **32**, 2547-2551 (1975).  
<sup>6</sup>T. Laevastu, "Manual of methods in fisheries biology," FAO Man. Fish. Sci. (1) (1965).  
<sup>7</sup>K. F. Lagler, "Capture, sampling and examination of fishes," in *Methods for the Assessment of Fish Production in Fresh Waters*, edited by T. Bagenaal (Blackwell, Oxford, England, 1978), 3rd ed., Chap. 2, pp. 7-47.  
<sup>8</sup>K. G. Foote, F. H. Kristensen, and H. Solli, "Trial of a new, split-beam echo sounder," Coun. Meet. Int. Coun. Explor. Sea **1984/B:21**, Copenhagen, Denmark.  
<sup>9</sup>K. G. Foote, H. P. Knudsen, G. Vestnes, R. Brede, and R. L. Nielsen, "Improved calibration of hydroacoustic equipment with copper spheres," Coun. Meet. Int. Coun. Explor. Sea **1981/B:20**, Copenhagen, Denmark.  
<sup>10</sup>K. G. Foote, "Optimizing copper spheres for precision calibration of hydroacoustic equipment," J. Acoust. Soc. Am. **71**, 742-747 (1982).  
<sup>11</sup>K. G. Foote, "Maintaining precision calibrations with optimal copper spheres," J. Acoust. Soc. Am. **73**, 1054-1063 (1983).

- <sup>12</sup>E. J. Simmonds, L. B. Petrie, F. Armstrong, and P. J. Copland, "High precision calibration of a vertical sounder system for use in fish stock estimation," *Proc. Inst. Acoust.* **6**(5), 129–138 (1984).
- <sup>13</sup>O. Nakken and K. Olsen, "Target strength measurements of fish," *Rapp. P.-v. Réun. Cons. Int. Explor. Mer.* **170**, 52–69 (1977).
- <sup>14</sup>K. G. Foote and O. Nakken, "Dorsal aspect target strength functions of six fishes at two ultrasonic frequencies," *Fisker og Havet, Ser. B* **1978**(3), 1–95.
- <sup>15</sup>J. J. Traynor and J. E. Ehrenberg, "Evaluation of the dual beam acoustic fish target strength measurement method," *J. Fish. Res. Board Can.* **36**, 1065–1071 (1979).
- <sup>16</sup>C. S. Clay and B. G. Heist, "Acoustic scattering by fish—Acoustic models and a two-parameter fit," *J. Acoust. Soc. Am.* **75**, 1077–1083 (1984).
- <sup>17</sup>K. G. Foote, "Rather-high-frequency sound scattering by swimbladdered fish," *J. Acoust. Soc. Am.* **78**, 688–700 (1985).
- <sup>18</sup>K. G. Foote, "Effects of fish behavior on echo energy: The need for measurements of orientation distributions," *J. Cons. Int. Explor. Mer.* **39**, 193–201 (1980).
- <sup>19</sup>K. G. Foote, "Averaging of fish target strength functions," *J. Acoust. Soc. Am.* **67**, 504–515 (1980).
- <sup>20</sup>K. Olsen, "Orientation measurements of cod in Lofoten obtained from underwater photographs and their relation to target strength," *Coun. Meet. Int. Coun. Explor. Sea* **1971/B:17**, Copenhagen, Denmark.
- <sup>21</sup>J. E. Carscadden and D. S. Miller, "Estimates of tilt angle of capelin using underwater photographs," *Coun. Meet. Int. Coun. Explor. Sea* **1980/H:50**, Copenhagen, Denmark.
- <sup>22</sup>U. Buerkle, "First look at herring distributions with a bottom referencing underwater towed instrumentation vehicle 'BRUTIV,'" *FAO Fish. Rep.* **(300)**, 125–130 (1983).
- <sup>23</sup>K. G. Foote, "Linearity of fisheries acoustics, with addition theorems," *J. Acoust. Soc. Am.* **73**, 1932–1940 (1983).
- <sup>24</sup>K. Olsen, "Observed avoidance behavior in herring in relation to passage of an echo survey vessel," *Coun. Meet. Int. Coun. Explor. Sea* **1979/B:18**, Copenhagen, Denmark.
- <sup>25</sup>K. Olsen, "The significance of fish behavior in the evaluation of hydro-acoustic survey data," *Coun. Meet. Int. Coun. Explor. Sea* **1981/B:22**, Copenhagen, Denmark.
- <sup>26</sup>R. J. Urick, *Principles of Underwater Sound* (McGraw-Hill, New York, 1975), 2nd ed.
- <sup>27</sup>C. S. Wardle, "Fish reactions to towed fishing gears," in *Experimental Biology at Sea*, edited by A. G. MacDonald and I. G. Priede (Academic, London, 1983), Chap. 4, pp. 167–195.
- <sup>28</sup>A. Hylen, T. Jakobsen, O. Nakken, and K. Sunnanå, "Preliminary report of the Norwegian investigations on young cod and haddock in the Barents Sea during the winter 1985," *Coun. Meet. Int. Coun. Explor. Sea* **1985/G:68**, Copenhagen, Denmark.
- <sup>29</sup>J. E. Ehrenberg, T. J. Carlson, J. J. Traynor, and N. J. Williamson, "Indirect measurement of the mean acoustic backscattering cross section of fish," *J. Acoust. Soc. Am.* **69**, 955–962 (1981).
- <sup>30</sup>J. J. Traynor and N. J. Williamson, "Target strength measurements of walleye pollock (*Theragra chalcogramma*) and a simulation study of the dual beam method," *FAO Fish. Rep.* **(300)**, 112–124 (1983).
- <sup>31</sup>J. J. Traynor, "Dual beam measurement of fish target strength and results of an echo integration survey of the eastern Bering Sea walleye pollock (*Theragra chalcogramma*)," Ph. D. thesis (University of Washington, 1984).
- <sup>32</sup>E. Ona, "Mapping the swimbladder's form and form-stability for theoretical calculations of acoustic reflection from fish," Ph. D. thesis (University of Bergen, 1982), in Norwegian.
- <sup>33</sup>E. Ona, "In situ observations of swimbladder compression in herring," *Coun. Meet. Int. Coun. Explor. Sea* **1984/B:18**, Copenhagen, Denmark.
- <sup>34</sup>Report of the 1983 planning group on ICES-coordinated herring and sprat acoustic surveys," *Coun. Meet. Int. Coun. Explor. Sea* **1983/H:12**, Copenhagen, Denmark.
- <sup>35</sup>P. Degnbol, H. Lassen, and K. -J. Stæhr, "In situ determination of target strength of herring and sprat at 38 kHz and 120 kHz," *Dana* **5**, 45–54 (1985).
- <sup>36</sup>H. Lassen and K. -J. Stæhr, "Target strength of Baltic herring and sprat measured in situ," *Coun. Meet. Int. Coun. Explor. Sea* **1985/B:41**, Copenhagen, Denmark.
- <sup>37</sup>S. T. Forbes, "Progress in dual-beam target-strength measurement on herring and blue whiting," *Coun. Meet. Int. Coun. Explor. Sea* **1985/B:22**, Copenhagen, Denmark.
- <sup>38</sup>M. Aksland, "Basic echo-trace-length statistics," *Coun. Meet. Int. Coun. Explor. Sea* **1985/B:32**, Copenhagen, Denmark.

# Linearity of fisheries acoustics, with addition theorems

Kenneth G. Foote

Institute of Marine Research, 5011 Bergen, Norway

(Received 16 May 1982; accepted for publication 6 February 1983)

An experiment to verify the basic linearity of fisheries acoustics is described. Herring (*Clupea harengus* L.) was the subject fish. Acoustic measurements consisted of the echo energy from aggregations of encaged but otherwise free-swimming fish, and the target strength functions of similar, anesthetized specimens. Periodic photographic observation of the encaged fish allowed characterization of their behavior through associated spatial and orientation distributions. The fish biology and hydrography were also measured. Computations of the echo energy from encaged aggregations, derived by exercising the linear theory with the target strength functions of anesthetized fish and gross behavioral characteristics of encaged fish, agreed well with observation. This success was obtained for each of four independent echo sounders operating at frequencies from 38 to 120 kHz and at power levels from 35 W to nearly 1 kW. In addition to demonstrating the basic linearity of fisheries acoustics, the experiment verified both conventional acoustic measurements on anesthetized fish, at least for averaging purposes, and the echo integration method. Two simple theorems summarizing the meaning of linearity for use with the echo integration method are stated.

PACS numbers: 43.20.Fn, 43.30.Dr, 43.80.Jz

## INTRODUCTION

Assessment of fish stocks by means of the echo integration method demands detailed knowledge about the back-scattering cross section or target strength of fish.<sup>1</sup> A popular means of acquiring such information is by direct measurement on anesthetized, stunned, or killed specimens.<sup>2,3</sup> While such measurements allow a high degree of control, the extent to which they are representative of free-swimming fish in the wild is unknown.

It was to resolve this matter for the important class of swimbladder-bearing fish that the present investigation was undertaken. In particular, it was hoped that the connection between measurements on anesthetized fish and measurements on encaged but otherwise free-swimming fish could be established unambiguously. Thus, recognizing that the two prominent extrinsic dependences of fish target strength are the orientation and depth-or depth-history-related state of the swimbladder, it was apparent at the outset that the one effect must be isolated from the other.

Given the distinguished history of attempts to elucidate depth-induced effects on the target strength,<sup>4-6</sup> which are still unclear, it was decided to avoid depth effects entirely by conducting all measurements near the surface, in the manner of Röttingen<sup>7</sup> and Nakken and Olsen.<sup>3</sup> Transferring fish from pens to the tilting suspension or net cage could then be accomplished swiftly, and the acoustic measurements commenced immediately upon positioning the fish or net cage in the center of the transducer beam.

Naturally, the measurements would have to be made ventrally; but as the purpose of the experiment was verification of a methodology, and not derivation of target strengths to be applied directly to field measurements, this was no drawback. In fact, the configuration of ventrally executed measurements had everything to recommend it—from the principal advantage of being able to maintain the subject fish near the surface at all times, to the very practical advantage

of precluding bubble entrapment by the transducers or their housings due to disturbances beneath them. In addition, if the ventral aspect measurements on the anesthetized fish were found to be representative of the encaged, free-swimming fish, then accompanying measurements of the dorsal aspect function could presumably be applied in survey work, given sufficient knowledge about the circumstances of fish occurrence.

For the sake of redundancy, the measurements were to be performed on each of two species, with each of four echo sounders operating at frequencies from 38–120 kHz and at power levels spanning a wide range. A large number of data were to be collected to establish possible forthcoming results with a high degree of confidence. In the event, the redundant design proved its worth, and useful data were collected in abundance.

Although the original major objective was verification of the target strength functions of anesthetized fish, it was discovered early that the linearity of the whole acoustical process would be tested. Success with this would also enable the basic echo integration method to be verified. Thus the theme of the work became establishment of the linearity of fisheries acoustics. In this, conventional measurements of target strength functions provide the fundamental acoustical knowledge about fish. In addition, the echo integration method is one of the consequences of linearity.

The plan of the paper is the following: presentation of the simple linear theory for acoustic scattering by fish aggregations, statement of the problem of verification, outline of an experimental design, description of materials and method, including data analysis and results, discussion of these, and listing of summary conclusions.

## I. THEORY

According to the hypothesis of linearity, the acoustic echo from an aggregation of fish is merely the sum of the

individual echoes.<sup>1,8-13</sup> If the process of reception is linear, then the equivalent received pressure field  $p_{rec}$  is just

$$p_{rec} = \sum_{i=1}^n p_{rec,i}, \quad (1)$$

where  $p_{rec,i}$  is the component due to the  $i$ th fish of  $n$ . In terms of the backscattering cross section  $\sigma$ , product of transmit and receive beam patterns  $b^2$ , and cumulative gain  $G$ , including reference pressure level of the source, receiver amplification, and possible time-varied gain (TVG),

$$p_{rec,i} = (Gb^2\sigma)_i^{1/2}s_i, \quad (2)$$

where  $s_i$  is the echo waveform, which is generally different from that of the ensonifying signal. The several factors in Eq. (2) are generally implicit or explicit functions of fish orientation and position in the beams of the acoustic source and receiver, not to mention physical state of the fish.

Compounding of the received echoes from individual fish by Eq. (1), squaring, and integrating in time, yields the well-known expression for the echo energy  $\epsilon$ ; namely,

$$\epsilon = \sum_{i=1}^n \sum_{j=1}^n (Gb^2\sigma)_i^{1/2} (Gb^2\sigma)_j^{1/2} c_{ij}, \quad (3)$$

where  $c_{ij}$  is the correlation coefficient of echo waveforms from the  $(i, j)$  pair of fish,

$$c_{ij} = \frac{2}{T} \int_{-\infty}^{\infty} s_i \left( t - \frac{2r_i}{c} \right) s_j \left( t - \frac{2r_j}{c} \right) dt, \quad (4)$$

where  $T$  is the duration of the transmit signal,  $t$  is the time,  $r_i$  is the range of the  $i$ th fish, and  $c$  is the speed of sound. The factor  $G$  in Eq. (3) has been scaled by incorporation of several multiplicative constants so that  $\epsilon$  has the units of energy.

Statistical evaluation of Eq. (3) for ordinary sonar signals is straightforward. In the mean of a large number of observations and in the absence of noise, assumed implicitly above,

$$\text{Av } \epsilon = n_0 \langle Gb^2\sigma \rangle, \quad (5)$$

where  $n_0$  is the average number of fish detected per ping and  $\langle Gb^2\sigma \rangle$  is the ensemble average of  $Gb^2\sigma$ . This is determined from the general distributional characteristics of the fish. In terms of the cumulative distribution function  $F$ ,

$$\langle Gb^2\sigma \rangle = \int (Gb^2\sigma)_{l,\beta} dF, \quad (6)$$

where the subscripts attached to the integrand denote the length  $l$  of the fish and other biological characteristics  $\beta$ , such as species, condition when observed acoustically, and behavior insofar as social interactions may influence the fish as acoustic scatterers. The probability element  $dF$  shares these described dependences together with the suppressed position and orientation dependences of the fish when being observed.

Higher-order moments of the echo energy can be computed. These are important for understanding the nature of variations in observations of fish aggregations, but do not, in themselves, influence the mean value. Since it is the correctness of this first-order moment, as expressed by Eq. (5), which determines the success or failure of the echo integra-

tion technique, further statistical development of Eq. (3) is unnecessary here.

## II. PROBLEM OF VERIFICATION

The gist of linearity in fisheries acoustics is expressed most succinctly in Eq. (5): given a sufficient number of acoustic observations on a fish aggregation, the mean density of sensed fish, or mean number per ensonification, can be estimated without bias. This consequence of linearity is a tenet of the echo integration method of estimating fish density, hence may deserve closer examination.

There is a mass of powerful, circumstantial evidence for the truth of Eq. (5). This lies in the early observations of Truskanov and Scherbino,<sup>14</sup> in many measurements of ensonified fish aggregations,<sup>7</sup> and in consistent, long-term successes with the echo integration method.<sup>15</sup> *A priori* support is derived from well-known and oft-confirmed acoustical and electromagnetic theories for echo formation by random collections of scatterers,<sup>16</sup> which have been traditionally accepted in fisheries acoustics.<sup>17,18</sup>

What hard evidence is there, however, for the truth of the equation, hence that of the echo integration method? In fact, what could constitute a proof or convincing demonstration of either, given the nearly mutually exclusive requirements for acoustically clean measurements on a fish aggregation and exact knowledge about these fish during their measurement? This is the problem of verification.

In order to verify the echo integration method as represented by Eq. (5), it must be possible to specify each term of the equation for the same conditions of observation of the same fish aggregation. The constituents of this specification are the following: measurement of the echo energy  $\epsilon$  from an aggregation of known number density  $n_0$ , determination of the cumulative gain  $G$  of the receiver and coupled echo integrator and of cumulative patterns  $b^2$  of the transmitter and receiver, simultaneous observation or determination of the behavior of the ensonified fish, i.e., of their collective states of orientation and position, and independent knowledge of the backscattering cross section  $\sigma$  of the aggregating fish.

To be convincing, these data must be gathered on a fish aggregation under nontrivial circumstances. Thus the aggregation density should be sufficiently high, or the duration of the ensonifying signal should be correspondingly long, so that fish echoes overlap and the correlation coefficient of Eq. (4) is not identically zero for all pairs of fish. Similarly, the ensonification frequency should be sufficiently high so that the phases of the overlapping echoes are not all identical, which would be equivalent to a unity correlation coefficient, another tautological situation. The frequency should also be sufficiently high so that echoes from individual fish are sensitive to their orientation. Within these limits, the potential complexity is great. This may incidentally explain why the only echo verification experiment considered by Swingler and Hampton,<sup>19</sup> in a refutation, involved tethered spherical polystyrene floats.

## III. AN EXPERIMENT

Given the desire to verify the echo integration method in a nontrivial manner, consistent with the above require-

ments, but also as simply as possible, a series of experiments on encaged fish was performed in the summer of 1980. As noted in the Introduction, the original motivation was a verification of the conventional method of determining fish target strength functions by measurement on anesthetized or stunned fish, tethered and tilted about a fixed position in the beam of an echo sounder.<sup>2,3</sup> This objective was supplanted, however, by the larger, more encompassing goal of verification of the basic linearity of fisheries acoustics.

In essence, the experiment consisted in simultaneous acoustic and photographic measurements of an encaged aggregation of otherwise free-swimming fish. The least considered density was sufficient for the net cage geometry and pulse duration to ensure 50% overlapping of fish echoes. The acoustic wavelength corresponding to the least ensonification frequency was less than the dimensions of dominant scattering features of individual fish, ensuring both the variable nature of the correlation coefficient between overlapping echoes and the very sensitive orientation dependence of the fish backscattering cross section.

To keep other variables of the measurement process as simple as possible, the beamwidths of the several transducers were required to be broad with respect to the transverse dimension of the net cage, yet narrow enough to permit placement of an underwater television camera near the net cage, in the acoustic shadow region between the main and first side lobes. The relative broadness of the beam facilitated collection of data with good statistics, since arbitrariness in the spatial distribution of fish within the net cage could not in itself produce large variations. Problems of the kind experienced in the narrow-beam measurement of encaged fish, cf. Refs. 20–23, for example, could thus be circumvented. Tailoring of the transducer beamwidths also facilitated acoustic hiding of the television camera, allowing simultaneous photography and acoustic measurement, hence determination of the spatial and orientation distributions of the fish during their acoustic measurement.

Measurement of single-fish target strength functions was performed immediately before or after each series of encaged fish measurements. Thus, were the acoustic properties of the fish to change over long periods of time, this could not prejudice the ultimate comparison of observed and computed effective backscattering strengths derived in testing Eq. (5). Short-term variations in the acoustic properties of the encaged and anesthetized single fish, especially those due to depth adaptation, were avoided by performing the measurements at nearly the precise depth of fish holding in a pen. As this was shallow, the acoustic measurements were performed ventrally, as by Röttingen<sup>7</sup> and Nakken and Olsen,<sup>3</sup> for the respective encaged and single-fish measurement types.

Performance of both encaged and single-fish measurements on successive days eliminated the need for long-term maintenance of equipment calibration. Additional performance of the calibration at least several times each day, without adjustment of equipment parameters, allowed absolute measurements to be made at all times, freeing the experiment as much as possible from unknown effects of equipment. The hydrography was also performed daily, for long-term moni-

toring of conditions which could change the physical condition of the fish, hence measurement results.

Finally, a large degree of redundancy was employed throughout the measurements, which were performed on two different species with a number of different echo sounding systems operating at different frequencies and different power levels. The choice of herring (*Clupea harengus* L.) and pollack (*Pollachius pollachius* (L.)) was convenient for its representation of the two classes of swimbladder-bearing fish, respectively the physostomes, which possess a duct between the swimbladder and alimentary canal, and the physoclists, which lack the same. Were depth adaptation or other behavioral modifications a problem with one species, then hopefully the very problem would be precluded by use of the other species. In any case, both kinds of acoustic measurements were performed with each species. The encaged fish measurements were performed at different times of the day, hence under different lighting conditions, over a range of densities. The single-fish measurements were conducted at similar times under similar conditions.

#### IV. MATERIALS

##### A. Experimental site

The measurements were performed from a raft anchored at the end of a sheltered fjord arm, Kvalvaagen, near Skogsvaagen on the island of Sotra, west of Bergen. The average water depth was 14 m. The typical tidal range of 0.75 m produced no measurable underwater currents anywhere near the anchorage. There were no other sources of underwater currents. The bottom was even and composed of deep, soft mud. Boat traffic in the fjord was negligible, consisting primarily in small fishing boats used only occasionally.

##### B. Availability of fish

The supply of living fish in good condition, undamaged by handling or even contact with the net, was ensured by the local abundance of fish and catching of these, for the experiment, by seining. Transfer of fish from the seine to holding nets or pens was accomplished by shepherding the fish over the submerged common border of the two nets when drawn together.

##### C. Selection of subject fish

Herring and pollack were the subjects of the measurements because of their abundance at the time of the experiment and their representation of physostomes and physoclists.

##### D. Measurement configuration

As noted above, two basic kinds of acoustic measurements involving fish were undertaken. These were measurements of the target strength functions of anesthetized fish and measurements of the echo energy from encaged aggregations of similar fish. Both kinds of measurements were performed with the same basic measurement and equipment configurations as those of the later "Calibration Sphere Project," reported in Ref. 24. The measurement configuration,

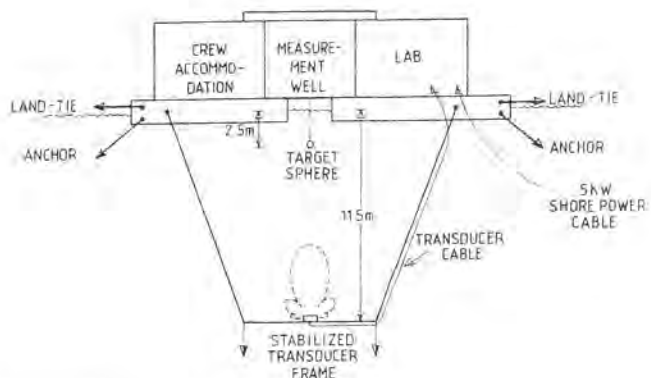


FIG. 1. Measurement configuration.

prepared to illustrate calibration of the echo sounders, is shown in Fig. 1. During fish measurements, additional equipment was present. For the single-fish target strength measurements, this was the tilting apparatus used by Nakken and Olsen,<sup>3</sup> although configured differently for the present investigation. The fish was held, during its tilting and measurement, at the exact 2.5 m depth and on-axis position of the calibration sphere.

During the aggregation measurements, the net cage was held on the acoustic axis with its center at the sphere position. The several net cages were designed similarly to those of Röttingen's study.<sup>7</sup> The height and diameter of the nearly cylindrical volume defined by the net cage were 1.10 and 0.90 m, respectively, implying a volume of 0.70 m<sup>3</sup>.

#### E. Acoustic equipment

The acoustic equipment consisted primarily of four Simrad echo sounding systems and the Simrad QD digital echo integrator. Each of the four transducers had a beam-width of approximately 20 deg at its resonant operating frequency. Some of the associated electronic equipment is indicated in Fig. 2. This is incomplete, however, for it does not include much additional, although nonessential equipment used variously during the fish measurements. This included a 14-channel instrumentation tape recorder, three hydrophones, separate transducer-signal amplifiers bypassing the receivers, a pair of four-channel oscilloscopes used for continual monitoring of signals under recording or processing, and signal amplifiers and detectors used with the hydrophones.

The parameters of the several transmit signals and power levels of the equipment are shown in Table I. Assuming an

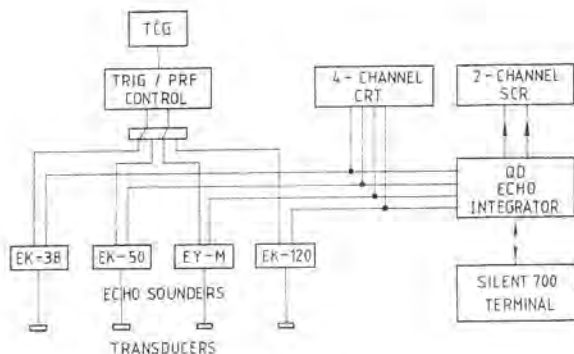


FIG. 2. Equipment configuration.

electroacoustical efficiency of 50%,<sup>1,2,5</sup> the range of acoustic power levels is seen to span the range from 17.5 to 434 W.

#### F. Photographic equipment

This consisted primarily of an underwater television system: a Telemation 1100 camera with specially constructed underwater housing, Cosmicar 25 mm lens, video monitor, and video recorder. During the behavioral observations, the television camera was hung at the same 2.5 m depth as the center of the net cage, but at a distance of several meters. Since the camera could not be hidden with respect to all four transducers, owing to small, but in this context, significant differences, a compromise placement was found. For this, the camera produced very weak echoes with the EK-50 and EK-120 systems, but sizeable echoes with the EK-38 and EY-M systems. In order to make clean measurements at all frequencies, the camera was generally kept in a raised position beneath the float, being lowered periodically for the crucial simultaneous acoustic and behavioral observations.

#### V. METHOD

Seven different series of measurements on engorged aggregations of herring or pollack were performed over a three-month period. In the first two series, fish escaped at unknown times, invalidating these and necessitating repair and reinforcement of the net cage. In the fourth and seventh series, the only two series with pollack, depth adaptation was apparently a severe problem, for the fish adopted extreme orientations approaching the frontal and the caudal. The corresponding target strength measurements on anesthetized specimens were limited to tilt angles within about 50 deg of the horizontal, hence could not be applied in a test of the linearity hypothesis. The sixth series was performed at

TABLE I. Characteristics of the four Simrad echo sounders used in the experiment.

Echo sounder	Center frequency (kHz)		Pulse duration (ms)		Peak electrical transducer power (W)
	Nominal	Measured	Nominal	Measured	
EK-38	38.0	38.0	0.6	0.64	35
EK-50	49.5	49.6	0.6	0.60	868
EY-M	70.0	68.5	0.6	0.60	89
EK-120	120.0	120.9	0.6	0.68	89

TABLE II. Numbers and biology of herring in the encaged fish measurement series and in the associated, analyzed single-fish measurements.

Type of measurement	Date	Total number of fish	Length $l \pm \Delta l$ (cm)	Weight $w \pm \Delta w$ (g)	Condition factor
Single fish target strength functions	15 July	25	$27.4 \pm 1.5$	$132.6 \pm 24.0$	0.00667
Encaged aggregation	16 July	40	$27.1 \pm 1.5$	$131.2 \pm 25.4$	0.00669

night, without photography, and with a high mortality, the only instance of its kind. Of the two remaining integral measurement series, only the data analysis for the third has been completed. This series, which was performed on 16 July, is the subject of the present inquiry.

Large numbers of measurements on anesthetized fish were performed before, after, and between the encaged fish measurement series. These were performed in the conventional manner, with a configuration similar to that of Nakken and Olsen,<sup>3</sup> but with a tauter suspension system innovated by E. Ona and A. Raknes. Because of the unknown effect of confinement on the physical state of the fish, hence on their acoustic properties, only single-fish measurements performed within one day of the subject encaged fish measurements are included in the analysis.

The number of herring involved in the two kinds of measurements associated with the encaged fish measurement series are listed in Table II together with several biological statistics. The condition factor is defined as the mean of the ratio of the weight in grams to the cube of length in centimeters for all fish in the group.

All acoustic measurements were performed absolutely, with an echo integrator that was calibrated several times daily by means of a steel ball bearing. This was later measured against copper spheres, whose target strengths are known *a priori*.<sup>24,26</sup>

The time-varied-gain functions of the four echo sounders were bypassed for the sake of simplicity. The nearness of the fish and the source levels of the transmitters made this amplification completely unnecessary. Fish echo levels were always high, generally exceeding the reverberation level by at least 10 dB in the mean for a single free-swimming fish.

Behavioral observations made with the underwater television were stored on videotape for later analysis. For the subject series of encaged aggregation measurements, the behavior was observed for each density, with varying degrees of resolution owing to changing lighting conditions. No artificial lighting was employed at any time during the measurements.

## VI. DATA ANALYSIS AND RESULTS

The fundamental ingredients for establishing the linearity of fisheries acoustics and for verifying the echo integration method are the separate factors of Eq. (5). The derivations of these are now described.

### A. Mean echo energy $\bar{A}v\epsilon$

The digital echo integrator was programmed to compute the energy in the total echo from the encaged fish aggregation. This was generally done in units of 500 pings, for which the variance was also computed. The mean and standard deviation were printed out on a typewriter/terminal at the end of each sequence of 500 pings. In the analysis of the subject encaged aggregation series, the measured average echo energy due to the empty net cage and reverberation were subtracted from the computed means. For convenience, the noise-corrected total echo energy is expressed below in units of square centimeters, to represent, in a familiar manner, the total effective scattering strength of the aggregation.

### B. Number density $n_0$

This quantity is defined as the number of fish in the net cage. To convert this to the absolute density or number of fish per cubic meter,  $n_0$  must be divided by the volume of the net cage; namely,  $0.70 \text{ m}^3$ .

### C. Gain factor $G$

In the absence of time-varied gain, this is the purely geometrical factor  $\exp(-2\alpha r)/r^4$ , where  $\alpha$  is the absorption coefficient at the center frequency and  $r$  is the instantaneous range of the single fish from the transducer. For the particular hydrographic conditions present during the July measurements,  $\alpha$  was computed according to Fisher and Simmonds.<sup>27</sup> In order of increasing frequency,  $\alpha = 0.0067, 0.0105, 0.018$ , and  $0.035 \text{ dB/m}$ . For convenience,  $G$  was normalized consistently with  $\epsilon$ , so that the ensemble average  $\langle Gb^2\alpha \rangle$  of Eq. (6) could be expressed in units of square centimeters.

### D. Beam patterns $b^2$

The product of transmit and receive beam patterns was assumed to be given by an ideal circular transducer with total beamwidth of 20 deg at the -3-dB level. This has been found from much earlier work and from theoretical simulation to be an excellent approximation.

### E. Backscattering cross section $\sigma$

The dependence of the backscattering cross section of anesthetized fish on the tilt angle was measured over a range from approximately -51 deg to +51 deg. Use of the logarithmic target strength TS, defined as  $10 \log \sigma/4\pi$ , facilitates

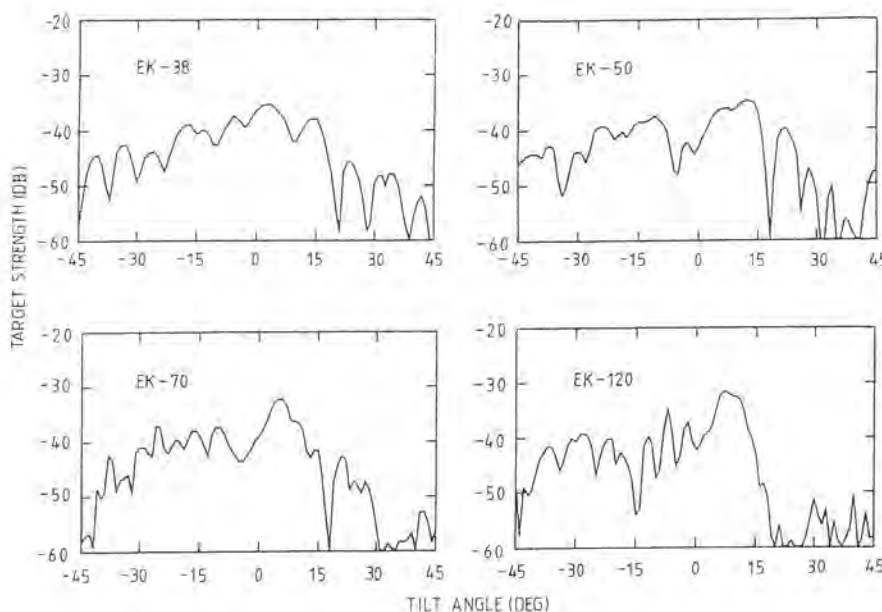


FIG. 3. Target strength functions of a 27-cm herring in ventral aspect. Positive angles denote the true head-up orientation.

ed expression of the measurements over their often large range of variation, sometimes exceeding 30 dB or a factor of 1000. These measurements are illustrated in Fig. 3 for a 27.0-cm herring measured on 15 July.

#### F. Fish distribution function $F$

Three dependences of this function necessary for use in Eq. (6) were obtained; namely, those of length, position, and orientation. The length distribution of the engaged fish aggregation has already been described in Table II. The spatial distribution of fish in the net cage was observed to be more or less uniform. The orientation distribution was characterized by a truncated Gaussian distribution in the tilt angle  $\theta$ . Values of  $\theta$  were obtained from representative still photographs extracted from the videotape. The three parameters of the distribution: the mean angle  $\bar{\theta}$ , standard deviation  $s_\theta$ , and excursion factor  $n_{s_\theta}$ , were determined by fitting a symmetrical Gaussian function to the observations. This is illustrated in Fig. 4. The results for the subject engaged aggregation series are summarized in Table III. That these are representative for the bulk of the acoustic measurements, which were made without photographic observation to avoid possible

biasing by the camera echo, was confirmed by detailed examination of the acoustic records of two echo sounders for which the echo was very weak; namely, the EK-50 and EK-120 systems. For these, there was essentially no difference in the measurements with or without the camera, which is significant since the camera was favorably placed with respect to the corresponding transducer beams.

#### G. Ensemble average $\langle Gb^2\sigma \rangle$

Averaging of the quantity  $Gb^2\sigma$  was performed according to Eq. (6) in the manner of Ref. 28. The ensemble average was computed for each anesthetized fish for which measurements of  $\sigma$  were available. These computations were repeated for each of the tilt angle distributions in Table III. Differences in the length distributions of the engaged aggregation and corresponding anesthetized fish were resolved by correcting the grand averages according to a quadratic length dependence of  $\sigma$ .

#### H. Results

The experimental and theoretical results are compared in Fig. 5. The confidence intervals of the experimental points are defined at the two-standard deviation level, where the standard deviation is defined as that of the series of means determined over 500-ping sequences. The variations in indi-

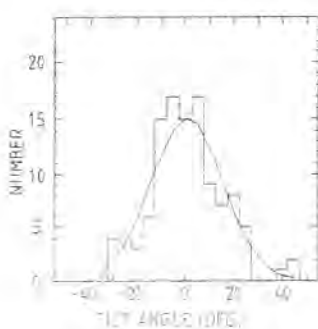


FIG. 4. Histogram of observed tilt angles for herring of number density 10, with fitted truncated Gaussian function.

TABLE III. Parameters of the tilt angle distributions of fish in the engaged aggregation measurements of 16 July.

Number density	Number of data	$\bar{\theta}$ (deg)	$s_\theta$ (deg)	$n_{s_\theta}$
10	113	0.8	15.0	2.5
20	228	3.3	14.0	2.7
30	106	2.7	14.7	2.9
40	296	3.0	14.1	3.2

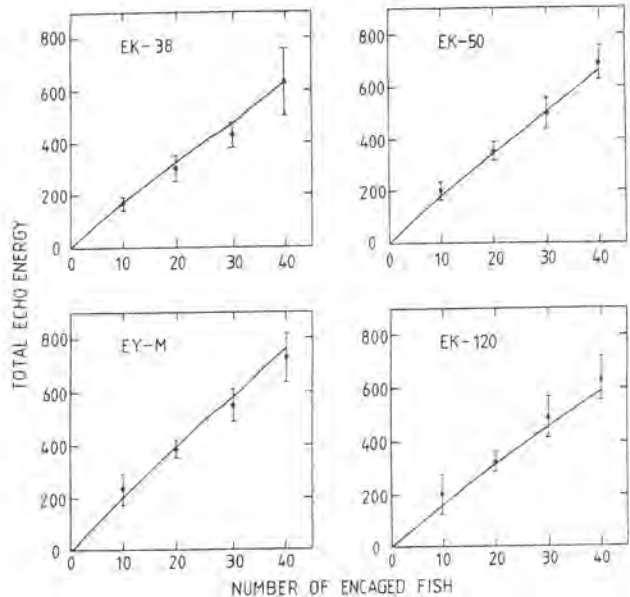


FIG. 5. Comparison of theoretical and measured values of total echo energy from the engaged herring aggregations. The echo energy has been expressed in units of square centimeters. Experimental points are indicated with confidence intervals defined at twice the estimated standard deviation. Theory is indicated by the solid line.

vidual pings were much larger, of course, but as a single datum is seldom significant in acoustics, the merging of data in 500-ping sequences was considered justified.

According to Eq. (5), the number of acoustically sensed fish can be estimated by dividing the average echo energy  $\bar{A}v\epsilon$  by the theoretically derived ensemble average  $\langle Gb^2\sigma \rangle$ . This is done in Fig. 6.

## VII. DISCUSSION

### A. Linearity of fisheries acoustics

The linearity of fisheries acoustics is evident from the agreement shown in Fig. 5. This is confirmed by goodness-of-fit testing, with no calculated statistic being significant even at the 0.25 level. Similar results obtain if the theoretical computations are repeated for a common, density-independent behavior, which may be described by treating the data underlying Table III as though belonging to the same set.

In its simplest form, the linearity principle asserts the proportionality of total echo energy and density of fish in an aggregation.<sup>1</sup> This assumes, of course, that a sufficient number of observations are made under low-noise conditions. According to the present theory, this also assumes a constancy of fish behavior and the negligibility of acoustic extinction.

In general, fish behavior will vary with the density of aggregation, for, at the least, the increasing proximity of fish must change the acoustically significant orientation distribution,<sup>28,29</sup> if only by delimiting it. The theory remains linear, however, but in the larger sense of Eq. (5). In the absence of extinction, then, the total echo energy is the sum of independent contributions for the constituent fish of the aggregation, where the contributions depend on fish behavior and

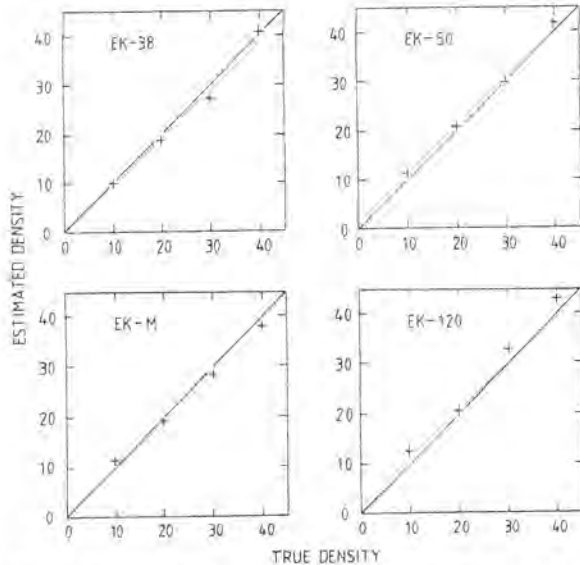


FIG. 6. Comparison of estimated and true number densities of the engaged herring aggregations. Estimates are indicated by the plus signs, and theory by the solid line.

other circumstances of their observation according to Eq. (6). This finding, which is supported by the comparison of theory with experiment in Fig. 5, is embodied in the following addition theorem, which obtains under the usual conditions of ensonification by a directional echo sounder:

**Theorem I:** In the absence of extinction, the total echo energy from an aggregation of  $N$  fish is, in the mean of a large number of observations,

$$\epsilon_{\text{tot}} = \sum_{i=1}^N \epsilon_i,$$

where  $\epsilon_i$  is the mean echo energy from the  $i$ th fish.

If the density, vertical extent, and mean extinction cross section of the fish are large enough so that extinction is significant, then the first theorem may be generalized by analogy with optics or quantum scattering theory. The following theorem represents a quite reasonable approximation for most applications:

**Theorem II:** For  $N$  fish uniformly distributed within a layer of thickness  $\Delta z$ , the total echo energy is, at least to the first order in the extinction parameter and in the mean of a large number of observations,

$$\epsilon_{\text{tot}} = \frac{1 - \exp(-2\nu\Delta z\sigma_e)}{2\nu\Delta z\sigma_e} \sum_{i=1}^N \epsilon_i,$$

where  $\nu$  is the fish density,  $\sigma_e$  is the mean extinction cross section of the fish, and  $\epsilon_i$  is the mean echo energy from the  $i$ th fish, were there no extinction.

There are at least two practical applications for the second theorem, which subsumes the first; namely, in the interpretation of certain net cage measurements, cf. Refs. 7 and 30, and for correcting underestimates of density in large pelagic schools.<sup>31</sup> The importance of this last-mentioned instance is recognized immediately by seagoing researchers who have probably witnessed weakening, if not premature triggering, of the bottom signal by dense schools.

It is remarked in passing that the linear phenomena observed in Fig. 5 were obtained at transmitter power levels spanning the range from about 50 W to 1 kW. In regard to the nearness of target fish in the experiment and the frequent use of more powerful transmitters in acoustic surveys, the range of depths typically encountered in large-scale surveys was thus simulated.

### B. Validity of target strengths derived by measurements on anesthetized fish

The fact of the agreement of theory with experiment in Fig. 5 also witnesses to another important finding. This is that the determination of fish backscattering cross sections or target strengths by measurement on anesthetized specimens is valid, at least for averaging purposes. Thus the particular methods of determining and applying target strength functions described by Midttun and Hoff,<sup>2</sup> Nakken and Olsen,<sup>3</sup> and Foote,<sup>28</sup> among others, are valid.

### C. Verification of the echo integration method

The experiment has also verified the echo integration method of determining fish density. This is illustrated in the most direct manner in Fig. 6. While the confidence intervals have not been finally determined, these are expected to be commensurate with those of Fig. 5, or perhaps better.

Admittedly, no time-varied gain was applied to the received signals, but this was of no consequence because of the measurement geometry, chosen by design. Theoretical simulation of the results with "20 log  $r'$ " and "40 log  $r'$ " TVG functions confirms this. That the echo sounder otherwise performed satisfactorily was confirmed by regular calibration with a target sphere, often at intervals of several hours. A further confirmation was provided by comparing the integrated, calibrated output signals with the same echo signal intercepted at the transducer, independently amplified, and processed in the same manner as the calibrated output signal. No difference could be discerned for sufficiently strong signals. For weaker signals, the independently amplified signal was inferior, which merely reveals the difficulty of performing the function of an echo sounder without duplicating its electronics.

The fact of the fish being ensonified ventrally is similarly immaterial to the verification of the echo integration method. Because of the shallowness of the fish-holding and measurement depth, the effects of depth change and depth adaptation were negligible for the herring. The scattering nature of the fish was thereby isolated, and interpretation of the encaged fish measurements by reference to behavior and measurements on similar, anesthetized specimens, facilitated. This process was further aided by the simultaneous acoustic and photographic observations, which confirmed the constancy of behavior throughout all of the encaged fish measurements at each density and justified use of the large number of acoustic measurements made without photography and the attendant burden of integration of the camera echo, however small.

Thus, there seems little doubt that when the several factors influencing the echo from a fish aggregation are tak-

en into account, whether intrinsic to the fish, medium, or equipment, it is possible to determine the density of that aggregation acoustically. Evidently, from Fig. 6, this determination is eminently feasible.

### D. Future work

The present findings are important to research in fisheries acoustics in several ways: they confirm the basic correctness of much earlier work in principle, if not in practice, and they provide directions for future work. In particular, the effects of depth change and depth adaptation on the target strengths of fish are still unknown. Granted success with these problems, conventional measurements of the target strengths of fish presumably could be adjusted for arbitrary depths and states of adaptation. Averaging of the corresponding backscattering cross section with respect to behavior, as characterized by the spatial and orientation distributions, would provide superior numbers for immediate use in the interpretation of measurements with echo integrators.

Determination of fish behavior is thus a key link in the envisaged improved application of target strength measurements. It is hoped that fisheries biologists and behaviorists will, in the future, be able to provide quantitative descriptions of the spatial and orientation distributions of fish under surveying conditions. Failing this, acoustical schemes for the determination of behavior may be realized.<sup>32</sup>

## VIII. CONCLUSIONS

The essential results are the following:

- (1) The phenomenon of acoustic scattering by fish under surveying conditions is strictly linear.
- (2) Mean acoustic backscattering cross sections of living, free-swimming fish can be determined from measurements on representative anesthetized specimens.
- (3) The echo integration method of determining fish density is valid.

A natural sequel to the present study would be elucidation of depth-induced effects. Such knowledge, when added to the present store and guided by descriptions of fish behavior, should effect an immediate, significant improvement in the acoustic estimation of fish abundance.

## ACKNOWLEDGMENTS

It is a privilege to acknowledge the steadfast support of L. Midttun and O. Nakken throughout the experiment and subsequent data analysis. G. Vestnes, H. P. Knudsen, and R. Brede are thanked for their contribution of equipment. H. Solli is thanked for his repeated contributions of programming to the prototype of the Simrad QD digital echo integrator. I. Hoff, H. P. Knudsen, and T. Lindem are thanked for getting the equipment running, and R. Pedersen, for keeping it that way for three months. E. Ona and A. Raknes are thanked for their tireless support, in and out of the water, including admirable construction of two nearly acoustically transparent net cages. For their supply of fish, I. Sangolt, I. B. Sangolt, and S. Sangolt are thanked. Of the many who visited Skogsvaag during the experiment, the author wishes particularly to thank M. Aksland, J. A. Hillman, K. Michal-

son, T. Neppelberg, and B. Robinson. The financial backing and other patient support of the Norwegian Council for Fisheries Research is gratefully acknowledged. This paper was presented at the Symposium on Fisheries Acoustics, Bergen, Norway, 21–24 June 1982.

- <sup>1</sup>S. T. Forbes and O. Nakken, "Manual of methods for fisheries resource survey and appraisal. Part 2. The use of acoustic instruments for fish detection and abundance estimation," FAO Man. Fish. Sci. (5), 1–138 (1972).
- <sup>2</sup>L. Midttun and I. Hoff, "Determination of the reflection of sound by fish," Fiskeri dir. Skr. Ser. HavUnders. 13 (3), 1–18 (1962).
- <sup>3</sup>O. Nakken and K. Olsen, "Target strength measurements of fish," Rapp. P.-v. Reun. Cons. Int. Explor. Mer 170, 52–69 (1977).
- <sup>4</sup>K. Olsen, "Some experiments on the effect on target strength of fish undertaking vertical migrations," Coun. Meet. Int. Coun. Explor. Sea 1976/B:42, Copenhagen, Denmark, 14 pp.
- <sup>5</sup>A. D. Hawkins, "Fish sizing by means of swimbladder resonance," Rapp. P.-v. Reun. Cons. Int. Explor. Mer 170, 122–129 (1977).
- <sup>6</sup>F. R. Harden Jones and P. Scholes, "The swimbladder, vertical movements, and the target strength of fish," in *Meeting on Hydroacoustical Methods for the Estimation of Marine Fish Populations, 25–29 June 1979*, edited by J. B. Suomala (Charles Stark Draper Laboratory, Inc., Cambridge, MA, 1981), Vol. II, pp. 157–181.
- <sup>7</sup>I. Röttingen, "On the relation between echo intensity and fish density," Fiskeri dir. Skr. Ser. HavUnders. 16, 301–314 (1976).
- <sup>8</sup>P. H. Moose and J. E. Ehrenberg, "An expression for the variance of abundance estimates using a fish echo integrator," J. Fish. Res. Board Can. 28, 1293–1301 (1971).
- <sup>9</sup>J. E. Ehrenberg and D. W. Lytle, "Acoustic techniques for estimating fish abundance," IEEE Trans. Geosci. Electron. 10, 138–145 (1972).
- <sup>10</sup>D. V. Holliday, "Resonance structure in echoes from schooled pelagic fish," J. Acoust. Soc. Am. 51, 1322–1332 (1972).
- <sup>11</sup>H. Bodholt, "Variance error in echo integrator output," Rapp. P.-v. Reun. Cons. Int. Explor. Mer 170, 196–204 (1977).
- <sup>12</sup>J. E. Ehrenberg and D. W. Lytle, "Some signal processing techniques for reducing the variance in acoustic stock abundance estimates," Rapp. P.-v. Reun. Cons. Int. Explor. Mer 170, 205–213 (1977).
- <sup>13</sup>K. G. Foote, "Energy in acoustic echoes from fish aggregations," Fish. Res. 1 (2), 129–140 (1982).
- <sup>14</sup>M. D. Truskanov and M. N. Scherbino, "Methods of direct calculation of fish concentrations by means of hydroacoustic apparatus," Res. Bull. Int. Comm. NW. Atlant. Fish. (3), 70–80 (1966).
- <sup>15</sup>O. Nakken and Ö. Ulltang, "A comparison of the reliability of acoustic estimates of fish stock abundances and estimates obtained by other assessment methods in the northeast Atlantic," presented at the Symposium on Fisheries Acoustics, Bergen, Norway, 21–24 June 1982 (in press).
- <sup>16</sup>P. M. Morse and H. Feshbach, *Methods of Theoretical Physics* (McGraw-Hill, New York, 1953).
- <sup>17</sup>W. D. Tesler, "Distribution of amplitudes and stability of fish echo signals," Mater. Ryb. Issled. Severn. Basseina. 17, 270–279 (1971).
- <sup>18</sup>I. L. Kalikhman, W. D. Tesler, and K. I. Yudanov, "Methods of determining the density of fish concentrations," in *Meeting on Hydroacoustical Methods for the Estimation of Marine Fish Populations, 25–29 June 1979*, edited by J. B. Suomala (Charles Stark Draper Laboratory, Inc., Cambridge, MA, 1981), Vol. II, pp. 533–573.
- <sup>19</sup>D. N. Swingler and I. Hampton, "Investigation and comparison of current theories for the echo-integration technique of estimating fish abundance, and of their verification by experiment," in *Meeting on Hydroacoustical Methods for the Estimation of Marine Fish Populations, 25–29 June 1979*, edited by J. B. Suomala (Charles Stark Draper Laboratory, Inc., Cambridge, Mass., 1981), Vol. II, pp. 97–156.
- <sup>20</sup>J. I. Edwards, "A preliminary investigation of the target strength of herring," Coun. Meet. Int. Coun. Explor. Sea 1981/B:12, Copenhagen, Denmark, 9 pp.
- <sup>21</sup>S. T. Forbes, E. J. Simmonds, and J. E. Edwards, "Progress in target strength measurements on live gadoids," Coun. Meet. Int. Coun. Explor. Sea 1980/B:20, Copenhagen, Denmark, 6 pp.
- <sup>22</sup>A. Aglen, O. Hagström, and N. Haakansson, "Target strength measurements and C-values determinations of live Skagerrak herring and cod," Coun. Meet. Int. Coun. Explor. Sea 1981/B:12, Copenhagen, Denmark, 9 pp.
- <sup>23</sup>J. I. Edwards and F. Armstrong, "Measurement of the target strength of herring and mackerel," Coun. Meet. Int. Coun. Explor. Sea 1981/B:26, Copenhagen, Denmark, 5 pp.
- <sup>24</sup>K. G. Foote, "Echo sounder measurements of backscattering cross sections of elastic spheres," Fiskeri Havet, Ser. B (6), 1–107 (1981).
- <sup>25</sup>R. J. Urick, *Principles of Underwater Sound* (McGraw-Hill, New York, 1975), 2nd ed.
- <sup>26</sup>K. G. Foote, "Optimizing copper spheres for precision calibration of hydroacoustic equipment," J. Acoust. Soc. Am. 71, 742–747 (1982).
- <sup>27</sup>F. H. Fisher and V. P. Simmons, "Sound absorption in sea water," J. Acoust. Soc. Am. 62, 558–564 (1977).
- <sup>28</sup>K. G. Foote, "Averaging of fish target strength functions," J. Acoust. Soc. Am. 67, 504–515 (1980).
- <sup>29</sup>K. G. Foote, "Effect of fish behavior on echo energy: the need for measurements of orientation distributions," J. Cons. Int. Explor. Mer 39 (2), 193–201 (1980).
- <sup>30</sup>K. G. Foote, "Analysis of empirical observations on the scattering of sound by encaged aggregations of fish," Fiskeri dir. Skr. Ser. HavUnders. 16, 423–456 (1978).
- <sup>31</sup>D. W. Lytle and D. R. Maxwell, "Hydroacoustic estimation in high density fish schools," in *Proc. IOA Underwater Acoustics Group Conf. "Acoustics in Fisheries"* (Institute of Acoustics, Edinburgh, Scotland, 1978), Chap. 1.2.
- <sup>32</sup>K. G. Foote, "Acoustic investigation of fish behaviour apropos avoidance reaction," Coun. Meet. Int. Coun. Explor. Sea 1981/B:21, Copenhagen, Denmark, 13 pp.

# Coincidence echo statistics

Kenneth G. Foote

Institute of Marine Research, 5024 Bergen, Norway

(Received 11 May 1995; accepted for publication 8 September 1995)

Two scatterers at similar range give an echo which may appear to be due to a single scatterer. Methods for determining target strength that depend on resolving single scatterers may fail in this instance. Statistics associated with the described special case of coincidence are derived and illustrated by theoretical computation for the SIMRAD EK500 echo sounder system with the ES38B split-beam transducer resonant at 38 kHz. Connections to angle measurement in radar and swath bathymetry and to bottom-scattering-strength measurement are noted. © 1996 Acoustical Society of America.

PACS numbers: 43.30.Sf, 43.30.Gv, 43.20.Fn

## INTRODUCTION

Many methods used to measure fish target strength *in situ* depend on resolution of single-target echoes. These include, for example, indirect methods, in which the effect of beam pattern is removed statistically,<sup>1</sup> and direct methods, for example, those of dual beams and split beams, in which the beam pattern effect is removed by means of phase measurement with multiple beams.<sup>2</sup>

It is generally appreciated that single-target selection criteria must be used with care, if not great care, to avoid effects due to the presence of multiple targets at similar ranges. A practical illustration of the effect of selection criteria on the resultant target strength distribution is obtained by changing the acceptance limits for echo length. Increasing the upper limit often increases the registration of large targets, while decreasing the same may radically decrease both the number and magnitude of accepted echoes. This illustration becomes vivid when fish are loosely concentrated, as during the process of nighttime dispersion. Dual-beam or split-beam echo sounding systems, with so-called target strength analyzers, generally continue to deliver target strength data whatever the state of concentration.

The interesting question thus arises as to the effect of multiple targets with coincident or near-coincident echoes, referred to forthwith simply as coincident echoes, on the apparent single-target target strength distribution. It is remarked at the outset that this problem has important antecedents both in radar and in swath bathymetry. For radars used in so-called very-high-precision tracking applications, multiple targets are known to be a source of error.<sup>3</sup> A multiple target may consist, for example, of two or more facets on the same target, differing in angle or range with respect to the transmitting or receiving antenna, or of different targets, such as two unresolved aircraft flying in formation. It is appreciated that the apparent angular location or range of the target may be outside the physical region of the target.

In swath bathymetry, interference due to multiple targets is recognized to be the major cause of depth error.<sup>4</sup> Multiple targets located at the same range on or in the bottom may cause a phase sample dispersion,<sup>5</sup> which is exactly analogous to the angle error or "glint" in the mentioned radar application. It may be significant that none of the methods described or developed by Masnadi-Shirazi *et al.*<sup>6</sup> is able to resolve

ambiguities due to multiple targets at the same range but different angles or same angle but different ranges, suggesting the fundamental nature of the problem.

In the present problem, the object of interest is the apparent target strength, determined in part by the angle error. This contrasts with the problem of angle error in radar and swath bathymetry applications, where the object of interest is the angle error *per se*. It is consequently necessary to specify a particular method for determining target strength. For definiteness in numerical computation, this is assumed to be the target strength analyzer in the SIMRAD EK500 echo sounder system with split-beam transducer resonant at 38 kHz.<sup>7</sup>

## I. THEORY

### A. Beam pattern of a transducer aperture

The transducer is defined as a shaded planar array of identical square elements. A subset of the elements defines an aperture. For the particular aperture A, the beam pattern amplitude factor in the direction  $\hat{k}$  is

$$D_A(\hat{k}) = \sum_{j \in A} w_j \int_A \exp(i\mathbf{k} \cdot \mathbf{r}) dA_j / \sum_{j' \in A} w_{j'}, \quad (1)$$

where  $\mathbf{k}$  is the wave vector,  $\hat{k} = \mathbf{k}/k$ ,  $w_j$  is the amplitude weight of the  $j$ th transducer element, and  $\mathbf{r}$  is the position of the differential surface element  $dA_j$ . In rectangular coordinates,  $\hat{k} = (\sin \theta \cos \phi, \sin \theta \sin \phi, \cos \theta)$ . Referring  $\mathbf{r}$  to the center  $\mathbf{r}_j$  of the  $j$ th transducer element, and integrating over the area,

$$D_A(\hat{k}) = D_1(\hat{k}) \sum_{j \in A} w_j \exp(i\mathbf{k} \cdot \mathbf{r}_j) / \sum_{j' \in A} w_{j'}, \quad (2)$$

where  $D_1 = \text{sinc}(ka \sin \theta \cos \phi) \text{sinc}(ka \sin \theta \sin \phi)$  is the beam pattern amplitude factor of a single, square array element of side length  $a$ ,  $\text{sinc}(x) = \sin(x)/x$ .

### B. Echo amplitude due to multiple targets at similar range

The echo pressure resulting from ensonification of an ensemble of targets can be expressed by the equation

$$p = \sum p_j s_j(t - 2r_j/c), \quad (3)$$

where  $p_j$  is the echo amplitude due to the  $j$ th target,  $s_j$  is the corresponding echo waveform,  $r_j$  is the range of the  $j$ th target, and  $c$  is the speed of sound. For the narrow-band operation implicit in use of a resonant transducer, the individual echo waveforms  $s_j$  are essentially identical, say, to the waveform

$$s(t) = \exp(i\omega_0 t) \operatorname{rect}\left(\frac{t - \tau/2}{\tau}\right),$$

where  $\omega_0 = ck$  is the angular frequency at resonance,  $\tau$  is the signal duration, and  $\operatorname{rect}(x) = 1$  for  $|x| \leq \frac{1}{2}$  and 0 for  $|x| > \frac{1}{2}$ . For targets at similar, sufficiently large ranges in the transducer far field, differing by no more than one-half wavelength,  $\lambda/2$ , then to a very good approximation and to within a constant of proportionality,

$$p_j = b_j \sigma_j^{1/2}, \quad (4)$$

where  $b_j = D_{Tj} D_{Rj}$ ,  $D_{Tj}$  and  $D_{Rj}$  are the beam pattern amplitude factors of the respective transmit and receive apertures in the direction of the  $j$ th target, and  $\sigma_j$  is the back-scattering cross section of the same. Substituting in Eq. (3) and ignoring common factors,

$$p = \sum b_j \sigma_j^{1/2} \exp(i\psi_j), \quad (5)$$

where  $\psi_j$  is the phase associated with the  $j$ th target, namely  $4\pi r_j/\lambda$ .

In the special case of just two targets, which is the one considered here, Eq. (5) can be simplified. To within a constant phase factor,

$$p = b_1 \sigma_1^{1/2} + b_2 \sigma_2^{1/2} \exp(i\chi), \quad (6)$$

where  $\chi$  is the relative phase.

It is noted here that for the case of  $n=2$  targets, a range of variation in  $\psi_j$  in Eq. (5) of  $\lambda/4$  is sufficient to encompass the entire range of possible interferences. In the more general case of  $n>2$  targets, a range of variation in  $\psi_j$  of  $\lambda/2$  is sufficient, as is immediately evident by construction of phasor diagrams.

### C. Split-beam echo processing

A split-beam transducer is electrically divided into quadrants. When transmitting, all quadrants are excited simultaneously, forming a single beam. When receiving, each quadrant acts independently to generate its own received echo signal. Half-beams are formed, and the phase difference between fore-and-aft halves and port-and-starboard halves detected. Knowing these two angles, hence target direction, the beam pattern is known *a priori*. The effect of the beam pattern on the sum-beam echo amplitude can thus be removed, resulting in an estimate for  $\sigma_j$ . A mathematical description follows.

For the assumed complex echo pressure  $p$ ,

$$p = |p| \exp\{i \tan^{-1}[\operatorname{Im}(p)/\operatorname{Re}(p)]\}. \quad (7)$$

The phase is  $\tan^{-1}[\operatorname{Im}(p)/\operatorname{Re}(p)]$ . The quadrants of the transducer are numbered sequentially from the forward starboard quarter (1), to forward port (2), to aft port (3), to aft starboard (4). The result of combining the echo pressure reg-

istered by quadrants 1 and 2 is the half-beam  $h_{12}$ , and so forth. The angle of the target relative to the transducer in the fore-and-aft plane is determined from the direction cosine

$$\begin{aligned} \alpha &= S^{-1} \{\tan^{-1}[\operatorname{Im}(h_{12})/\operatorname{Re}(h_{12})]\} \\ &= \tan^{-1}[\operatorname{Im}(h_{34})/\operatorname{Re}(h_{34})], \end{aligned} \quad (8)$$

where  $S$  is the so-called angle sensitivity factor, which is used to convert the phase difference to a spatial angle. The factor  $S$  is approximately equal to  $kd$ , where  $d$  is the effective distance between the transducer halves. The angle of the target in the port-and-starboard plane is determined from the direction cosine

$$\begin{aligned} \beta &= S^{-1} \{\tan^{-1}[\operatorname{Im}(h_{14})/\operatorname{Re}(h_{14})]\} \\ &= \tan^{-1}[\operatorname{Im}(h_{23})/\operatorname{Re}(h_{23})]. \end{aligned} \quad (9)$$

Equations (8) and (9) apply in the usual small-angle limit.

In a rectangular coordinate system with origin at the transducer center,  $x$  axis pointing to starboard,  $y$  axis forward, and  $z$  axis downward,

$$\alpha = \hat{k} \cdot \hat{y} = \sin \theta \sin \phi, \quad (10a)$$

$$\beta = \hat{k} \cdot \hat{x} = \sin \theta \cos \phi, \quad (10b)$$

hence

$$\theta = \sin^{-1}(\alpha^2 + \beta^2)^{1/2}, \quad (11a)$$

$$\phi = \tan^{-1}(\alpha/\beta). \quad (11b)$$

That is, the target position can be identified in ordinary polar coordinates based on measurement of half-beam phase differences, with immediate computation of  $\alpha$  and  $\beta$ .

Two targets at similar range but generally different angular locations  $(\theta_1, \phi_1)$  and  $(\theta_2, \phi_2)$  will produce echoes that appear to be due to a single scatterer at a third location  $(\theta, \phi)$ . If this lies in the main lobe of the split-beam transducer, it will, under the stated condition of similar range, be perceived as a single scatterer, and compensation for the apparent beam pattern loss accordingly applied. Larger apparent target angles are rejected. A series of measurements in the presence of multiple targets will thus in general produce a distribution of apparent single-target target strengths, at least some of which are spurious.

## II. COMPUTATIONAL METHOD

In order to investigate the effect of multiple targets on the target strength distribution derived by means of split-beam processing, the two-target case is considered according to the following model.

### A. Split-beam transducer

For definiteness, this is assumed to be the SIMRAD ES38B transducer. This is a truncated square array of identical square elements of side length 30 mm and center-to-center distance along rows and columns of 32 mm, with

100	100	70		
100	100	70	70	
100	100	100	70	70
100	100	100	100	100
100	100	100	100	100

FIG. 1. Amplitude weights of elements in the forward starboard quadrant of the SIMRAD ES38B transducer.

an operating resonant frequency of 38 kHz. The amplitude weights in the forward starboard quadrant are shown in Fig. 1.

### B. Transducer angle sensitivity factor

The nominal figure given by the manufacturer is 21.9.<sup>8</sup> For the sound speed assumed here, namely 1470.6 m/s, defined by temperature 5 °C, salinity 35 ppt, pH 8.8, and depth 0 m,<sup>9</sup> this factor was determined by the following procedure. For an assumed value of  $S$  and given target position, the four half-beams are computed, followed by computation of the direction cosines in Eqs. (8) and (9). Computation of  $\theta$  and  $\phi$  by Eq. (11) allows the beam pattern compensation value to be determined. Comparison with the beam pattern value at the given target position allows the beam pattern compensation error to be gauged. Repetition of this computation for each target position over a grid of points uniformly covering the transducer beam cross section allows the mean beam pattern compensation error to be determined. The described computations are repeated for a range of values of  $S$ . The value that produces no mean beam pattern compensation error is  $S=23.2$ . Use of this value ensures that the compensation method does not introduce a bias into the mean backscattering cross section of a single target.

### C. Spatial distribution

The target range is assumed to be constant and equal for the two targets to within one-quarter of the acoustic wavelength. The targets are assumed to be distributed with equal probability of occurrence anywhere in the cross section of the transducer beam within the -6-dB level, i.e., within the angular zone of acceptance for split-beam processing. For the ES38B transducer and medium sound speed of 1470.6 m/s, this zone is defined by a limiting polar angle that is to a fair approximation 4.66 deg.

### D. Target strength distributions

Each of two distributions is considered through the probability density function of target strength TS.

(1) Constant target strengths: The respective target strength distributions are

$$f_1(TS) = \delta(TS)$$

and

$$f_2(TS) = \delta(TS + \Delta TS),$$

where  $\delta$  is the Dirac delta function, and  $\Delta TS$  is the constant difference in TS.

(2) Normally distributed target strengths: Both target strengths independently follow the same normal distribution, namely,

$$f(TS) = (2\pi\sigma^2)^{-1/2} \exp[-(TS - \bar{TS})^2/(2\sigma^2)],$$

where  $\bar{TS}$  and  $\sigma$  denote the respective mean and standard deviation.

### E. Echo amplitude

The two-target form is computed according to Eq. (6), where  $\sigma = 4\pi 10^{TS/10}$ , and  $\chi$  is uniformly distributed over  $\pi$  rad. That is,

$$f(\chi) = \pi^{-1},$$

where  $0 \leq \chi \leq \pi$ .

### F. Simulation of split-beam processing

In addition to computing the sum beam for use with Eq. (6), the quadrant-beam responses are also computed. Half-beams are computed, assuming  $S=23.2$ , and the alongships and athwartships angles computed according to Eq. (10). Use of the resulting values in Eq. (11) determines the apparent single-target position  $(\theta, \phi)$ , thence the sum-beam compensation factor  $b$  if within the limiting angle. For a single realization of the described stochastic model, then, the apparent backscattering cross section is

$$\hat{\sigma} = |b_1 \sigma_1^{1/2} + b_2 \sigma_2^{1/2} \exp(i\chi)|^2/b^2, \quad (12)$$

and the corresponding apparent target strength, for  $\sigma$  in SI units, is

$$\hat{TS} = 10 \log \frac{\hat{\sigma}}{4\pi}. \quad (13)$$

### G. Apparent target strength distribution

Repeated exercise of the model determines a series of values for the apparent target strength. In this way the distribution  $f(TS)$  is generated. When simulated on a digital computer, the values are sorted in contiguous TS bins of width 0.5 dB.

### H. Numerical parameters

By simulation, two targets are allowed to occupy a range of paired positions entirely covering the transducer beam cross section with equal probability of occurrence. This is done by systematic and uniform variation of the polar angles  $\theta_1$  and  $\theta_2$  in 50 equal increments  $\Delta\theta$  over 4.66 deg. The azimuth  $\phi_1$  is varied over the range  $[0, \pi/4]$  in six increments  $\Delta\phi_1 = \pi/24$ , and  $\phi_2$  is moved over the range  $[\phi_1, \phi_1 + \pi]$  in 16 increments of size  $\Delta\phi_2 = \pi/16$ . The represented incremental area thus increases as  $\sin\theta_1 \sin\theta_2 \Delta\theta_1 \Delta\theta_2 \Delta\phi_1 \Delta\phi_2$ . The phase  $\chi$  is varied uniformly over the range  $[0, \pi]$  rad in 19 increments of size  $\Delta\chi = \pi/19$ . In the first case of constant target strengths, these are applied directly. In the second case of normally distributed target strengths, these are indepen-

dently drawn from the same distribution for each combination of values  $\theta_1$ ,  $\theta_2$ ,  $\phi_1$ , and  $\phi_2$ . A pseudorandom number generator of linear congruential type is employed, with simple realization on FORTRAN compiler f77 as implemented on SUN computers.

### III. RESULTS AND DISCUSSION

Apparent single-target target strength distributions are shown in Fig. 2 for the case of constant target strengths and in Fig. 3 for the case of normally distributed target strengths.

In the case of the constant target strengths, shown in Fig. 2, the strongest effect is observed for equal target strengths, in Fig. 2(a). With decreasing signal-to-noise ratio (SNR) in Fig. 2(b)–(d), the effect of the second, weaker target strength is seen to be progressively less, evidently serving as a minor perturbation to the single-target distribution  $f_1(TS) = \delta(TS)$ . The results are further illustrated by the change in average backscattering cross section of the apparent single target. For the distributions shown in Fig. 2(a)–(d), the corresponding logarithmic measure is 2.04, 0.91, 0.52, and 0.12 dB, respectively.

In the case of the normally distributed target strengths, the resultant distributions of apparent target strength in Fig. 3 display characteristics that are consistent with those in Fig. 2 and which can be understood in their light. First, the distribution in Fig. 3(a) closely resembles that in Fig. 2(a), as indeed it should since the case of constant and equal target strengths can be viewed as the limiting case of a normal distribution with vanishing standard deviation. Second, the distribution of apparent target strength in Fig. 3(e), due to the single-target distribution  $N(0,10)$ , bears a closer resemblance to the original single-target distribution than do any of the others. With increasing dispersion, the chance of two values being drawn from the same distribution being very similar is small, while that of being quite different is large, hence explaining the smaller effect, as also observed in Fig. 2(d) compared to that in Fig. 2(a). The mean values of the apparent single-target distribution, as computed in the intensity or  $\sigma$  domain, are 2.04, 5.12, 7.31, 9.45, and 15.33 dB for the five distributions arranged in order of increasing standard deviation. The corresponding values of the underlying single-target distribution are 0, 0.11, 1.00, 2.75, and 10.32 dB, as this distribution is log-normal, with increasing bias with increasing width.

The several distributions and computations of average measures include only those echoes that survive the detected-angle selection criterion, namely, that  $\theta$  not exceed 4.66 deg. In the cases represented by Fig. 2(a)–(d), the percentage of accepted echoes is 77.9%, 81.8%, 83.6%, and 86.8%, respectively. In the cases represented by Fig. 3(a)–(e), the acceptance number is in the range 77.7%–79.3%.

A detailed investigation identifies the nature of the rejection process for apparent single targets. When the quantities  $b_1\sigma_1^{1/2}$  and  $b_2\sigma_2^{1/2}$  in Eq. (6) are nearly equal, and the phase factor  $\chi$  is close to  $\pi$ , the sum becomes small and the apparent phase angle unstable. Out-of-range values can then result. These are rejected if greater than the threshold angle 4.66 deg, but other, irregular values not exceeding the threshold

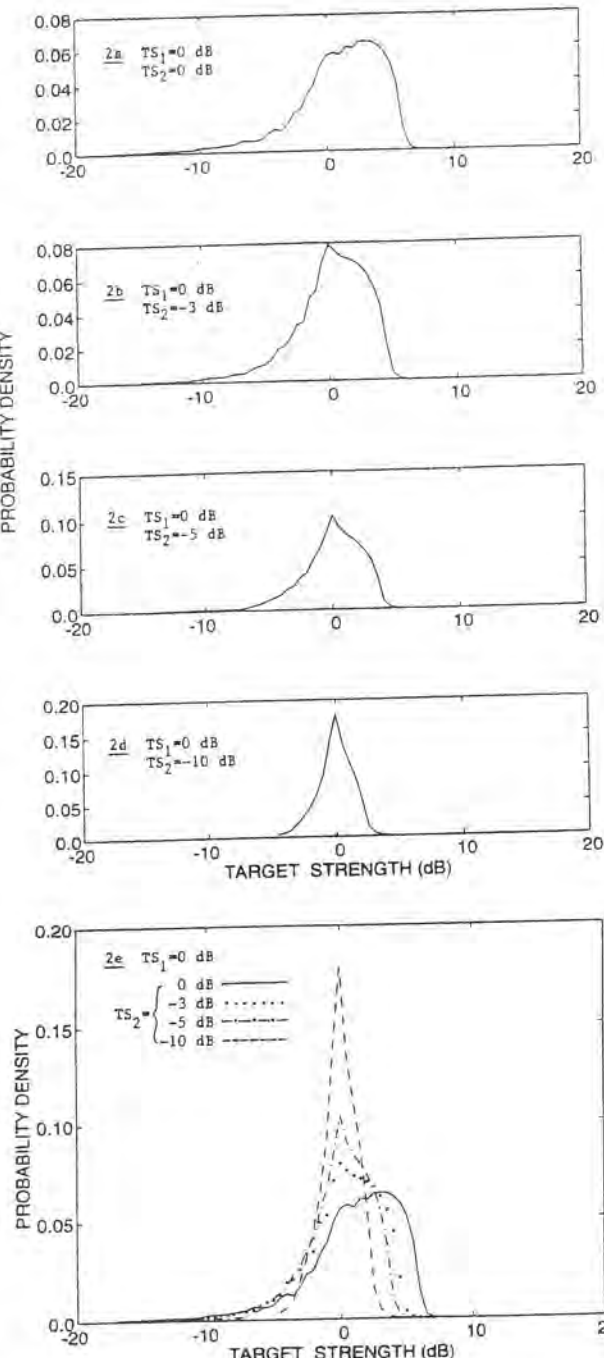


FIG. 2. Probability density functions of the apparent single-target target strength due to coincident echoes from two targets in the main beam of the SIMRAD ES38B split-beam transducer, with constant target strengths  $TS_1 = 0$  dB and  $TS_2$  as indicated in parts (a)–(d). Part (e) is a superposition of parts (a)–(d) but with the same scale.

angle break their damage on the apparent target strength distribution.

The particular mean levels of target strength assumed in the computations do not limit the results. In fact, the constant value  $TS_1 = 0$  dB assumed in the computations in Fig. 2 and mean distribution value  $TS = 0$  dB assumed for Fig. 3 may be viewed as arbitrary references. The displayed distributions

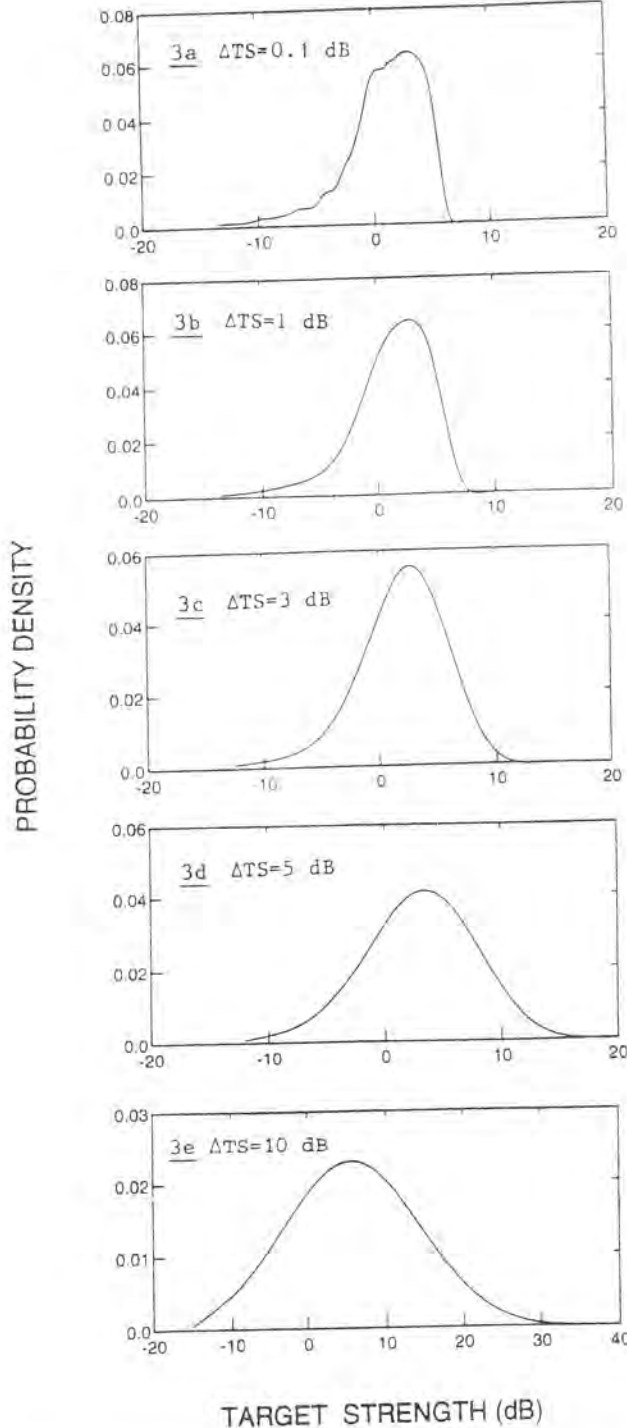


FIG. 3. Probability density function of the apparent single-target target strength due to coincident echoes from two targets in the main beam of the SIMRAD ES38B split-beam transducer, with target strengths independently drawn from the same normal distribution of target strength,  $N(TS, \Delta TS)$ , where  $TS=0$  dB and  $\Delta TS$  assumes the indicated values.

apply to other absolute levels by a simple translation in target strength domain.

In general, no matter what the application, simultaneous multiple-frequency measurements can help resolve situations of ambiguity. The phase is sensitive to frequency, so situa-

tions of multiple scatterers will differentiate themselves from single-scatterer situations through frequency-dependent phases. If the apparent target position varies with frequency, it can be assumed to be due to the presence of multiple scatterers at similar range, hence rejected.

While the present study involves angle errors due to interference, a problem common to both radar target-tracking and swath bathymetry, results for the effect of angle error on target strength may be directly applied to problems in acoustic scattering by the sea bottom. Makris and Berkson present an empirical histogram of scattering strength with standard deviation of 7 dB.<sup>10</sup> Were this the underlying distribution of each of two interfering targets, the result of coincidence would be a broadening of the apparent single-target target strength distribution to a degree intermediate to those in Fig. 3(d) and (e), with standard deviations of 5 and 10 dB. Direct measurements of bottom scattering strength, for example, of the type reported by Jackson *et al.*<sup>11</sup> may be corrupted by angle errors due to coincident echoes. Methods for determining seafloor roughness that depend on measurement of echo strength, for example, Stanton's method,<sup>12</sup> must also be affected by coincidences. Constructing maps of seafloor acoustic backscattering strength, mentioned by de Moustier,<sup>13</sup> is a further process that would be sensitive to coincident echoes.

#### IV. CONCLUSIONS

Clearly, the presence of multiple targets at similar range can change the character of a target strength distribution as determined with a split-beam echo sounder. Two consequences are broadening of the distribution and biasing of the average measure of target strength. The effect of digital signal processing on split-beam operation, not simulated here, is to produce a further, slight broadening of the distribution, but without significant bias.

While the present analysis aims to quantify the effects of coincidence in two-target echoes on target strength, as derived with a particular split-beam target strength analyzer, the effects are recognized to be common to other methods of target strength determination that depend on the resolution of single targets. Avoidance of multiple-target effects by operating only under unambiguous conditions of dispersion is the recommended practice.

#### ACKNOWLEDGMENTS

E. Ona is thanked for calling attention to the problem. Discussions with T. K. Stanton on the phenomenon of instability in detection angle of apparent single target are gratefully acknowledged. D. Chu, H. Nes, and D. Tang are thanked for information on other applications of the work. Ø. Østensen is thanked for assistance in preparing Fig. 3.

<sup>1</sup>K. G. Foote, "Summary of methods for determining fish target strength at ultrasonic frequencies," ICES J. Mar. Sci. **48**, 211–217 (1991).

<sup>2</sup>J. E. Ehrenberg, "A comparative analysis of *in situ* methods for directly measuring the acoustic target strength of individual fish," IEEE J. Ocean. Eng. **OE-4**, 141–152 (1979).

<sup>3</sup>D. D. Howard, "Tracking radar," in *Radar Handbook*, edited by M. I. Skolnik (McGraw-Hill, New York, 1990), 2nd ed., Chap. 18.

- <sup>4</sup>P. N. Denbigh, "Swath bathymetry: principles of operation and an analysis of errors," *IEEE J. Ocean. Eng.* **14**, 289–298 (1989).
- <sup>5</sup>H. Matsumoto, "Characteristics of SeaMARC II phase data," *IEEE J. Ocean. Eng.* **15**, 350–360 (1990).
- <sup>6</sup>M. A. Masnadi-Shirazi, C. de Moustier, P. Cervenka, and S. H. Zisk, "Differential phase estimation with the SeaMARC II bathymetric sidescan sonar system," *IEEE J. Ocean. Eng.* **17**, 239–251 (1992).
- <sup>7</sup>H. Bodholt, H. Nes, and H. Solli, "A new echo-sounder system," *Proc. IOA* **11**(3), 123–130 (1989).
- <sup>8</sup>H. Bodholt, "Split-beam transducer for target strength measurement," in *Scandinavian Cooperation Meeting in Acoustics XIII*, edited by H. Hobæk, Department of Physics Sci./Tech. Rep. 227 (University of Bergen, Bergen, Norway), p. 73.
- <sup>9</sup>K. V. Mackenzie, "A nine-term equation for sound speed in the oceans," *J. Acoust. Soc. Am.* **70**, 807–812 (1981).
- <sup>10</sup>N. C. Makris and J. A. Berkson, "Long-range backscatter from the Mid-Atlantic Ridge," *J. Acoust. Soc. Am.* **95**, 1865–1881 (1994).
- <sup>11</sup>D. R. Jackson, A. M. Baird, J. J. Crisp, and P. A. G. Thomson, "High-frequency bottom backscatter measurements in shallow water," *J. Acoust. Soc. Am.* **80**, 1188–1199 (1986).
- <sup>12</sup>T. K. Stanton, "Sonar estimates of seafloor microroughness," *J. Acoust. Soc. Am.* **75**, 809–818 (1984).
- <sup>13</sup>C. de Moustier, "Signal processing for swath bathymetry and concurrent seafloor acoustic imaging," in *Acoustic Signal Processing for Ocean Exploration*, edited by J. M. F. Moura and I. M. G. Lourtie (Kluwer Academic, Dordrecht, 1993), pp. 329–354.

## Comparing two 38-kHz scientific echosounders

J. Michael Jech, Kenneth G. Foote, Dezhong Chu,  
and Lawrence C. Hufnagle Jr.

Jech, J. M., Foote, K. G., Chu, D., and Hufnagle, L. C., Jr. 2005. Comparing two 38-kHz scientific echosounders. — ICES Journal of Marine Science, 62: 1168–1179.

The EK500 has been the state-of-the-art scientific echosounder for surveying marine fish stocks for over a decade; the EK60 is its successor. Ensuring comparability in performance is vital during the transition from the EK500 to the EK60. To quantify the respective performances, each echosounder was calibrated in tandem by the standard-target method using the same 38-kHz, 12° beam width, split-beam transducer, with alternating pinging by means of an external triggering-and-switching system. The principal measurements comprised split-beam-determined angle and target strength, on-axis sensitivity, and directionality in the plane normal to the acoustic axis, as measured with a 60-mm-diameter copper sphere. Ambient noise, including volumetric reverberation, was also measured. Principal comparisons included those of the time-series and histograms of split-beam-determined target strength; respective alongship and athwartship angles as determined by the split-beam system; and as expected, difference in the split-beam-determined and experimental target-strength values in the plane normal to the acoustic axis. The mean absolute difference in off-axis angle values was also compared. While the performance of the two echosounders is generally similar, systematic differences exist. For the particular calibration measurements, the time variability in measurements of on-axis target strength was of the order of 1 dB for the EK500 and 2 dB for the EK60. The target-strength distribution for measurements made with the EK500 was normal, with standard deviation 0.2–0.3 dB, whereas for the EK60, the target-strength distribution was distinctly skewed and the standard deviation varied over 0.3–0.5 dB. Differences were found between the split-beam and physical-angle measurements. They were noticeably larger in the case of the EK60. Differences in performance between the two echosounders suggest refinements to the new system that will help realize its full potential in scientific work.

Published by Elsevier Ltd on behalf of International Council for the Exploration of the Sea.

Keywords: calibration, echosounder, fisheries acoustics.

Received 14 September 2004; accepted 7 February 2005.

J. M. Jech: Northeast Fisheries Science Center (NOAA/NMFS), 166 Water Street, Woods Hole, MA 02543, USA. K. G. Foote and D. Chu: Woods Hole Oceanographic Institution, Woods Hole, MA 02543, USA. L. C. Hufnagle, Jr.: Northwest Fisheries Science Center (NOAA/NMFS), 2725 Montlake Blvd. E., Seattle, WA 98112, USA. Correspondence to J. M. Jech: tel: +1 508 495 2353; fax: +1 508 495 2258; e-mail: michael.jech@noaa.gov.

### Introduction

The SIMRAD EK500 scientific echosounder (Bodholt *et al.*, 1989) has defined the state-of-the-art since its introduction. It has been in worldwide use in the service of fisheries research for over a decade. (Any use of trade names does not imply endorsement by NOAA.) However, changes in the manufacture of solid-state electronics, specifically in the availability of components, rendered a number of essential components obsolete by 2000. At the same time, advances in data technology were sufficient to compel a fundamental redesign, resulting in the successor echosounder, the EK60 (Andersen, 2001).

Consistency in performance of the two systems is naturally a major concern to users, whether for water

column or seafloor measurements, as well as to fishery managers using data derived from echo-integrator surveys of fish and zooplankton stocks (MacLennan, 1990; Gunderson, 1993; Foote and Stanton, 2000). It is the goal of the present study to investigate the performance of the two echosounders and to verify or quantify differences.

The basis of the comparison is the standard-target method of calibration (Foote, 1983; Foote *et al.*, 1987) using optimal and other standard solid, elastic sphere targets (Foote, 1982; Foote and MacLennan, 1984). This method is well suited to measuring the overall system response both on and off the transducer axis. Specific parameters that can be derived from such measurements include the on-axis combined transmit-and-receive

sensitivity, product of the transmit- and receive-beam patterns, and the two-way directivity index, also called the equivalent beam width (Urick, 1983), equivalent beam angle (MacLennan, 1990), and integrated beam pattern (Medwin and Clay, 1998).

Two technical challenges have been met in the course of performing the comparison. Firstly, a new capability for determining the target position relative to the transducer axis has been exploited. This is available at a special facility, allowing a greater degree of control than was previously possible. Previous methods depended on using a fixed sphere-suspension system attached near the transducer and configured by an underwater diver, with angles controlled by trimming the vessel (Ona and Vestnes, 1985), making use of the split-beam functionality in moving the target through the beam (Kieser and Ona, 1988), and using extended outriggers (Reynisson, 1990, 1998). The *in situ* advantages of these methods are forfeited in return for much greater angular accuracy and precision. Secondly, conditions for making the comparative measurements have been rendered very similar by making the measurements in tandem via the alternate triggering of the two echosounders from ping to ping. Details are given below.

Comparisons based on the respective measurements are presented and discussed. While the results apply strictly to two particular 38-kHz units of the EK500 and EK60, they are believed to be indicative of these models.

## Material and methods

Acoustic-backscatter data were collected with a SIMRAD EK500 scientific echosounder and a SIMRAD EK60 Mark I scientific echosounder, each operating at 38 kHz, during 6–7 January 2003. The experiments were conducted in a sea well on Iselin Dock at the Woods Hole Oceanographic Institution (Doherty *et al.*, 2002). The echosounders shared the same 38-kHz split-beam transducer, SIMRAD model number ES38-12, by means of a multiplexing junction box (Figure 1). The beam width of this transducer was 12° as measured by the manufacturer between the half-power points.

The transducer was mounted facing sideways on a 6-m vertical shaft suspended at a water depth of approximately 3 m. The transducer-alongship axis was orientated in the vertical plane with positive angles up and with the athwartship angles oriented in the horizontal plane with positive angles to the right. The shaft was secured within a section of antenna tower and attached to a computer-controlled rotator. The accuracy of the rotator was better than  $\pm 0.1^\circ$ . A personal computer (PC) controlled the rotational parameters such as the beginning and end degree of rotation, rotation increment, speed of rotation, and the number of pings-per-rotation increment (Doherty *et al.*, 2002). For each rotation increment, the EK500 and EK60 were alternately triggered in tandem at a rate of two pings

per second, i.e. one ping per second for each echosounder. The trigger generator was connected to each echosounder and to a set of mechanical relays in the transducer junction box. The relays were coordinated to synchronize transmit and receive signals to and from the transducer for each echosounder. The EK500 and EK60 transmit data via Ethernet connections to another PC for analysis.

Operation of both echosounders was software-controlled through selection of parameter values. Operational parameters were: 1-ms pulse duration, wide receiver bandwidth, nominally 10% of the centre frequency, time-varied gain (TVG) of  $40 \log_{10}(r) + 2\alpha r$ , where  $r$  is the range, and  $\alpha = 10 \text{ dB km}^{-1}$ , the attenuation coefficient. These operational parameters were chosen as they are used for surveys conducted at the Northeast Fisheries Science Centre (Jech *et al.*, 2000).

Two general sets of measurements were performed: on-axis sensitivity, nominally within 1–2° of the transducer axis, and transducer beam directionality. A 60-mm-diameter copper calibration sphere (Foote, 1982) suspended with a monofilament line was used as the standard target. For on-axis measurements, the sphere was positioned on the geometric axis of the transducer by measuring the depth of the transducer and aligning the sphere by means of a laser mounted on the rotator perpendicular to the transducer face. The sphere was placed at a range of approximately 11.5 m from the transducer, well in the far field of the transducer, which is nominally 0.5 m (Gaunaud, 1985). At this range, a normal distance of 20 cm subtends an arc of about 1°. On-axis measurements consisted of 1000 pings per echosounder to evaluate the sensitivity and stability of echo amplitudes and angular locations derived by each instrument.

The transducer directivity was measured by rotating the transducer about its vertical axis spanning a set of athwartship angles, and raising and lowering the sphere over a set of alongship angles. Athwartship angles spanned 30°, from  $-15^\circ$  to  $+15^\circ$  in  $0.5^\circ$  increments (a "sweep"). Alongship angles spanned 18°, from  $-9^\circ$  to  $+9^\circ$  in  $1^\circ$  increments. One ping per echosounder was collected at each angle. A total of 21 sweeps was completed. The first sweep was performed at  $0^\circ$  alongships. Nine sweeps were then performed at successively greater positive alongship angles. The sweep at  $0^\circ$  was repeated, followed by nine sweeps at successively greater negative alongship angles. The final sweep was again performed at  $0^\circ$ . The three  $0^\circ$  alongship sweeps were done to verify the alignment of the sphere relative to the transducer.

The EK500 (Bodholt *et al.*, 1989; Demer *et al.*, 1999) and EK60 (Andersen, 2001; SIMRAD, 2001) have common, individual target-detection parameters and detect individual targets based on the amplitude and width of the echo. In one experiment involving 1000 ensonifications of the same target near or on the transducer axis by each echosounder, the number of single-target detections was 932 with the EK500 and 220 with the EK60 Mark I.

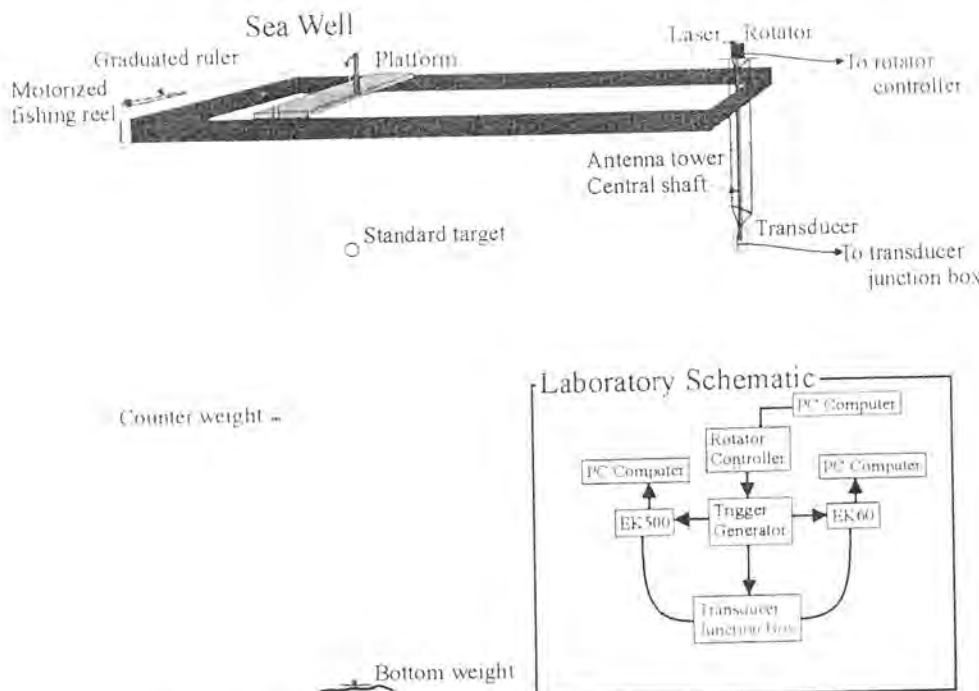


Figure 1. Schematic diagrams of the experimental set-up in the sea well and the EK500 and EK60 configuration. The transducer shaft was approximately 6 m long and the horizontally-orientated transducer was placed approximately 3 m below the water surface. The bottom weight was located approximately 20 m below the water surface.

Because of difficulties in configuring the respective post-processing systems with equivalent parameter settings, the raw echosounder data were exported to the Echoview post-processing software, version 3.00.80.04, developed by SonarData Pty Ltd. (GPO Box 1387 Hobart, Tasmania, Australia; [www.sonardata.com](http://www.sonardata.com)). Use of the single-target-detection algorithm in Echoview (split-beam method 1) resolved the discrepancies, providing a constant basis for comparing the two sets of data.

Single-target detection parameters were: -54-dB threshold, 6-dB maximum two-way beam-pattern compensation, and a maximum phase deviation of four phase steps. For reference, the EK500 has 64 phase steps and the EK60 has 128 phase steps per 180 electrical degrees. The angular locations of single targets are determined with the split-beam transducer according to electrical-phase differences between half-beam signals. Half-beam signals are formed by adding received signals from adjacent quadrants of the split-beam transducer (Ehrenberg, 1979; Foote *et al.*, 1986). Data exported from Echoview were the range, echo strength, target strength, and alongship and athwartship angles of the detected calibration target. In the manufacturer's terminology, the echo strength is sometimes referred to as the "uncompensated target strength", while the target strength is analogously called the "compensated echo strength".

Transducer beam patterns were determined by measurement in each of two ways: first the use of the split-beam-determined angles, and second, as determined by the external, sea-well instrumentation. Corresponding beam

patterns could thus be compared, i.e. beam patterns determined by the split-beam function of each echosounder with those determined by the experimental geometry, as well as between echosounders.

Both the EK500 and Echoview softwares assume a small-angle approximation to define the beam pattern. The effective one-way beam pattern is given in the logarithmic domain as

$$B(\alpha_{SB}, \beta_{SB}) = -3.0103 \left[ \left( \frac{2\alpha_{SB}}{BW_z} \right)^2 + \left( \frac{2\beta_{SB}}{BW_\beta} \right)^2 \right] - 0.18 \left( \frac{2\alpha_{SB}}{BW_z} \right)^2 \left( \frac{2\beta_{SB}}{BW_\beta} \right)^2 \quad (1)$$

where  $\alpha$  is the alongship angle,  $\beta$  is the athwartship angle, subscript "SB" denotes split-beam-determined angles,  $BW_z$  is the total angular beam width measured at the half-power points in the alongship direction, and  $BW_\beta$  is the total angular beam width measured at the half-power points in the athwartship direction. For the 38-kHz transducer,  $BW_z$  and  $BW_\beta$  are 12°. Equation (1) is used to compensate echo-strength measurements for angular location in the acoustic beam, since the echo strength is the sum of beam pattern and target strength.

An empirical compensation function was derived by fitting a second-order polynomial to the alongship and athwartship angles and echo-strength measurements. The form of the polynomial is:

$$B(\alpha, \beta) = G + c_0\alpha + c_1\alpha^2 + c_2\beta + c_3\beta^2, \quad (2)$$

where  $G$  is the overall echo-strength compensation value, and  $c_0$ ,  $c_1$ ,  $c_2$ , and  $c_3$  are the empirically determined coefficients.

Given the potential for discrepancies between the split-beam-determined angles and the angles based on the experimental geometry, the split-beam-determined angles could be adjusted *a posteriori* for an offset. The offset was computed using the slopes and intercepts from linear regressions of the split-beam-determined and geometry-based angles in both the alongship and athwartship directions. An empirically derived transducer directivity ( $B$ ) was computed using the angles adjusted for the offset and then compared with the small-angle-approximation compensation.

To measure consistency between the experimental-geometry-based and split-beam-determined directivity, an index was defined. This was the mean, absolute difference per each  $1^\circ$  off-axis interval. A similar index was computed to determine the consistency between the experimental-geometry-based and adjusted transducer directivities. The absolute values of the differences were computed to determine the magnitudes of the discrepancies.

The equivalent beam angle  $\psi$  or its logarithmic form  $\Psi = 10 \log_{10}(\psi)$  can be calculated from the measured far-field transmit- and receive-beam patterns,  $b_T$  and  $b_R$ , respectively (Urick, 1983), by integrating their product over the half space in front of the transducer:

$$\psi = \int_0^{2\pi} \int_0^\pi b_T(\theta, \phi) b_R(\theta, \phi) \sin \theta d\theta d\phi. \quad (3)$$

The beam patterns are evaluated here in the field direction  $(\theta, \phi)$ , which can be expressed in terms of rectangular coordinates. For the field point  $r = (x, y, z)$ , where the magnitude of  $r$  is the range, the unit vector  $\hat{x}$  is coincident with the alongship axis  $\hat{y}$  with the athwartship axis, and  $\hat{z}$  with the transducer axis. In these coordinates, the polar angle  $\theta = \arccos(z/r)$  and azimuth  $\phi = \arctan(y/x)$ . When measured by the split-beam function of the echosounder, however, the beam patterns are expressed in terms of the alongship angle  $\alpha = \arctan(x/z)$  and the athwartship angle  $\beta = \arctan(y/z)$ . The transformation between the spherical angles  $(\theta, \phi)$  and split-beam angles  $(\alpha, \beta)$  is (Foote, 1986):

$$\begin{aligned} \phi &= \tan^{-1} \left( \frac{\tan \beta}{\tan \alpha} \right). \\ \theta &= \tan^{-1} \sqrt{\tan^2 \alpha + \tan^2 \beta} \end{aligned} \quad (4)$$

which enables the split-beam angles to be converted to the spherical angles used in Equation 3.

## Results and discussion

Tidal stages for the measurements are given in Table 1. The copper-sphere, beam-pattern measurements were done during mid-flood tide, and the on-axis measurements were done near slack tide. The on-axis sensitivity measurements using the tungsten-carbide and aluminium-alloy spheres were conducted approximately mid-ebb tide. A vertical Conductivity-Temperature-Depth (CTD) profile conducted prior to each trial indicated that the seawater at the sea well was well mixed. The CTD was then placed at the depth of the transducer to collect time-series of temperature and salinity over the duration of each trial. The average temperature, salinity, and sound speed were  $2.88 \pm 0.02^\circ\text{C}$ ,  $31.60 \pm 0.25$  PSU, and  $1457.51 \pm 0.37 \text{ m s}^{-1}$ , respectively.

### On-axis angular measurements

Based on the geometry of the transducer mounting, the 60-mm-diameter copper calibration sphere was aligned on the geometric axis of the transducer. Observations of the alongship (vertical) and athwartship (horizontal) split-beam-determined angular locations of this target show that it was closely aligned with the alongship axis but not with the athwartship axis (Figure 2). Mean alongship angles were  $-0.08^\circ$  for the EK500 and  $-0.14^\circ$  for the EK60 (Table 2), with a total variation of about  $\pm 0.5^\circ$  for both echosounders. The mean athwartship angles were  $-0.62^\circ$  for the EK500 and  $-0.71^\circ$  for the EK60, with a total variation of about  $\pm 1.5^\circ$  for both echosounders. For the EK500, the mean alongship angle was well within the angular resolution of  $0.225^\circ$ , whereas the mean alongship angle for the EK60 was slightly greater than the angular resolution of  $0.1125^\circ$  (SIMRAD, 2001). The difference of about  $0.7^\circ$  between the mean EK500 and EK60 athwartship angles and the axis is greater than the angular resolutions of both echosounders, and is indicative of an offset in the

Table 1. Sphere type, time, experimental trial, and tidal stage. These measurements were conducted on 7 January 2003. Sphere types are: 60-mm-diameter copper (CU60), 60-mm-diameter aluminium alloy (AL60), and 38.1-mm-diameter tungsten carbide with 6% cobalt binder (WC38.1). Values in parentheses indicate the number of hours after the start of flood or ebb tide that the measurements were taken. The tides at Iselin Dock are semi-diurnal, but rectified at the sea well, with significant current only during the flood.

Sphere	Time (EST)	Trial	Tide stage
CU60	1040–1215	Beam pattern	Flood (+4 to +6)
CU60	1220–1240	On-axis	Ebb (+0)
WC38.1	1540–1600	On-axis	Ebb (+2)
AL60	1640–1650	On-axis	Ebb (+3)

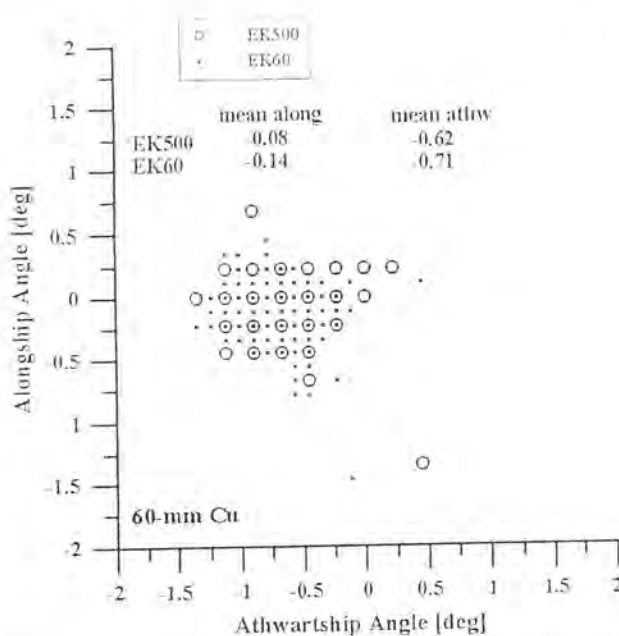


Figure 2. On-axis, split-beam-determined angular locations of a single target, the 60-mm-diameter copper sphere, from 1000 EK500 and EK60 tandem pings. The solid dots denote the EK60 single-target angular locations, and the open circles denote EK500 single-target angular locations.

experimental apparatus or the angular locations derived by the echosounders, or a mixture of both these factors.

To investigate the possibility that the angular offsets were sphere related, on-axis measurements were conducted with other sphere types. On-axis measurements with a 60-mm-diameter aluminium-alloy sphere showed a total variation in alongship and athwartship angles of about  $\pm 0.5^\circ$  and  $\pm 0.75^\circ$ , respectively (Figure 3). On-axis measurements with a 38.1-mm-diameter tungsten-carbide sphere with a 6% cobalt binder showed alongship and athwartship angle variation of approximately  $\pm 1^\circ$  and  $\pm 1.5^\circ$ , respectively (Figure 4). Mean alongship angles ranged from  $-0.18^\circ$  to  $0.18^\circ$  (Table 2) and are within or near the angular resolution of the echosounders. Mean athwartship angles ranged from  $-0.63^\circ$  to  $-0.69^\circ$ , which are also indicative of an athwartship offset.

#### On-axis target-strength measurements

The 60-mm-diameter copper sphere was placed on the geometric axis of the transducer,  $0^\circ$  alongship and  $0^\circ$  athwartship, and 1000 transmissions per echosounder were collected to evaluate the on-axis sensitivity and time-based stability of the echo-amplitude measurements. Echo strengths were compensated using Equation (1) to give split-beam-determined target strengths (TS) of the sphere. A 100-ping subset of the time-series was arbitrarily chosen to investigate consistency in the target-strength measurements

Table 2. Means and standard deviations of alongship angle, athwartship angle, and target strength (TS) from the on-axis measurements. The mean and standard deviation of target-strength values were calculated from Gaussian fits to the target-strength distributions. Sphere types and measurement parameters are given in Table 1.

Sphere	Alongship angle ( $^\circ$ )		Athwartship angle ( $^\circ$ )		TS (dB)	
	EK500	EK60	EK500	EK60	EK500	EK60
CU60	Mean	-0.08	-0.14	-0.62	-0.71	-33.6
	s.d.	0.17	0.14	0.23	0.22	0.2
AL60	Mean	0.08	0.18	-0.63	-0.68	-34.9
	s.d.	0.19	0.17	0.24	0.28	0.2
WC38.1	Mean	-0.17	-0.18	-0.69	-0.65	-42.4
	s.d.	0.28	0.35	0.41	0.50	0.3
						0.5

between the EK500 and EK60 (Figure 5). A general pattern of coherence does not appear to exist in target-strength measurements between the two echosounders over the 100 pings. The EK500 target strengths are more or less constant, with a jitter of about 0.3 dB. The EK60 target strengths show a basic decrease, with much larger jitter of about 1 dB.

Observations of split-beam target strength over the 1000-ping trial (Figure 6) from both echosounders showed both short-term variability and longer-term trends. The short-term variations, or jitter, spanned about 0.5 dB for the EK500 and 1 dB for the EK60, not inconsistent with the observations over the 100-ping interval. The total variations in target strength over the measurements were about 1 dB for the EK500 and 1.5 dB for the EK60.

Means of split-beam target strengths were  $-33.6$  dB for both EK500 and EK60, which were nearly equivalent for means derived from a Gaussian fit to the measurements (right panels, Figure 6). Gaussian fits to the EK500 and EK60 target-strength distribution resulted in a standard deviation of 0.2 dB for the EK500 and 0.3 dB for the EK60 data (Table 2). Both split-beam target-strength distributions were unimodal. However, EK500 distribution was narrower, with about 1.5 dB of total variability and greater than 70% of the target strengths within  $\pm 0.2$  dB of the mean, whereas the EK60 distribution was skewed towards target strengths greater than the mean, had approximately 3-dB total variability, and only 55% of the values were within  $\pm 0.2$  dB of the mean.

As with the copper sphere, EK500 split-beam target strengths were less variable than the EK60 split-beam-derived target strengths for the aluminium-alloy sphere (Figure 3) and tungsten-carbide sphere (Figure 4), and the target-strength distributions had similar skewness. Split-beam target strengths from the EK500 varied about 1 dB for the aluminium-alloy sphere and 1–1.5 dB for the tungsten-carbide sphere. Target strengths from the EK60 varied by approximately 1.5 dB for

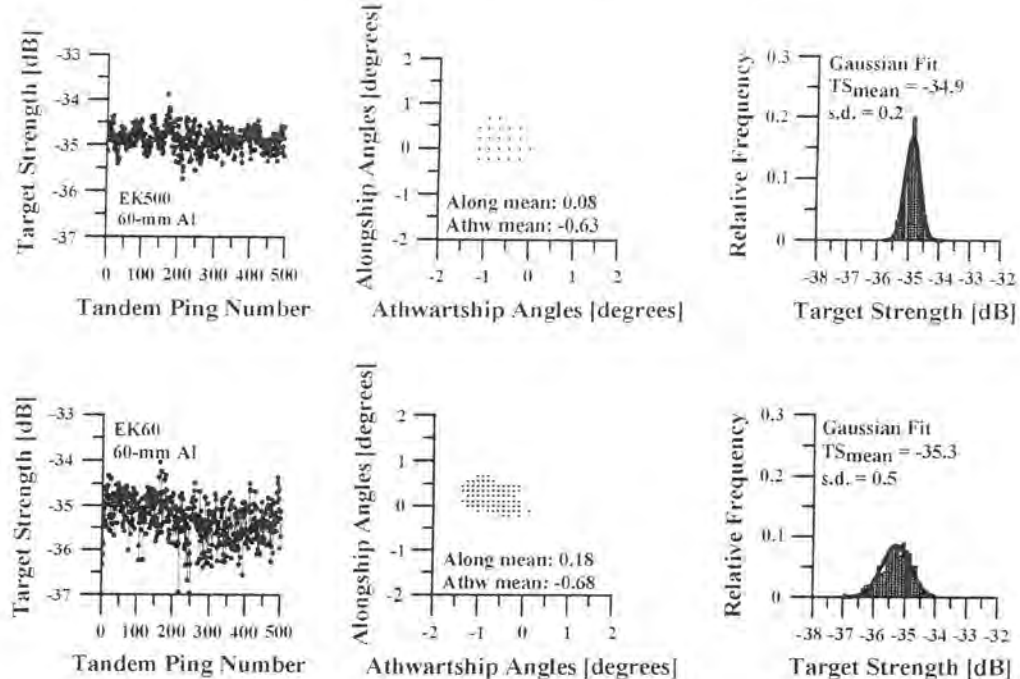


Figure 3. Time-series of split-beam-determined target strength, split-beam-determined angular locations, and histograms of split-beam-determined target strength for a 60-mm-diameter sphere made of an aluminium alloy. Five hundred tandem pings were collected with the EK500 (upper panels) and the EK60 (lower panels). The mean alongship and athwartship angles are given. Mean split-beam target strength (TS) and standard deviation (s.d.) are derived from a Gaussian fit to the data.

the aluminium-alloy sphere and more than 2 dB for the tungsten-carbide sphere.

#### Beam-pattern measurements

Regression analyses were performed to determine the linear relationships between split-beam-determined and the ex-

perimentally known angles for each of the echosounders (Figure 7). Slopes of the linear regressions were near 1 for the alongship angles (1.06 for the EK500 and 1.08 for the EK60) and athwartship angles (1.02 for the EK500 and 1.02 for the EK60). Intercepts for alongship angles were 0.11° for the EK500 and 0.06° for the EK60. As in the on-axis

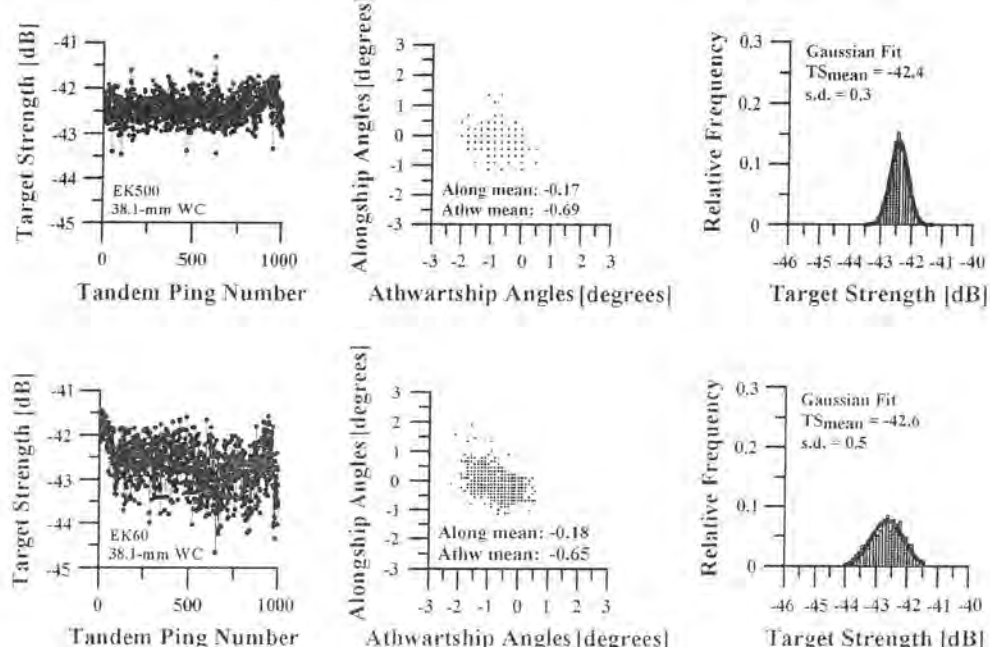


Figure 4. Time-series of split-beam-determined target strength, split-beam-determined angular locations, and histograms of split-beam-determined target strength for a 38.1-mm-diameter sphere made of tungsten carbide with 6% cobalt binder. One thousand tandem pings were collected with the EK500 (upper panels) and the EK60 (lower panels). The mean alongship and athwartship angles are given. Mean split-beam target strength (TS) and standard deviation (s.d.) are derived from a Gaussian fit to the data.

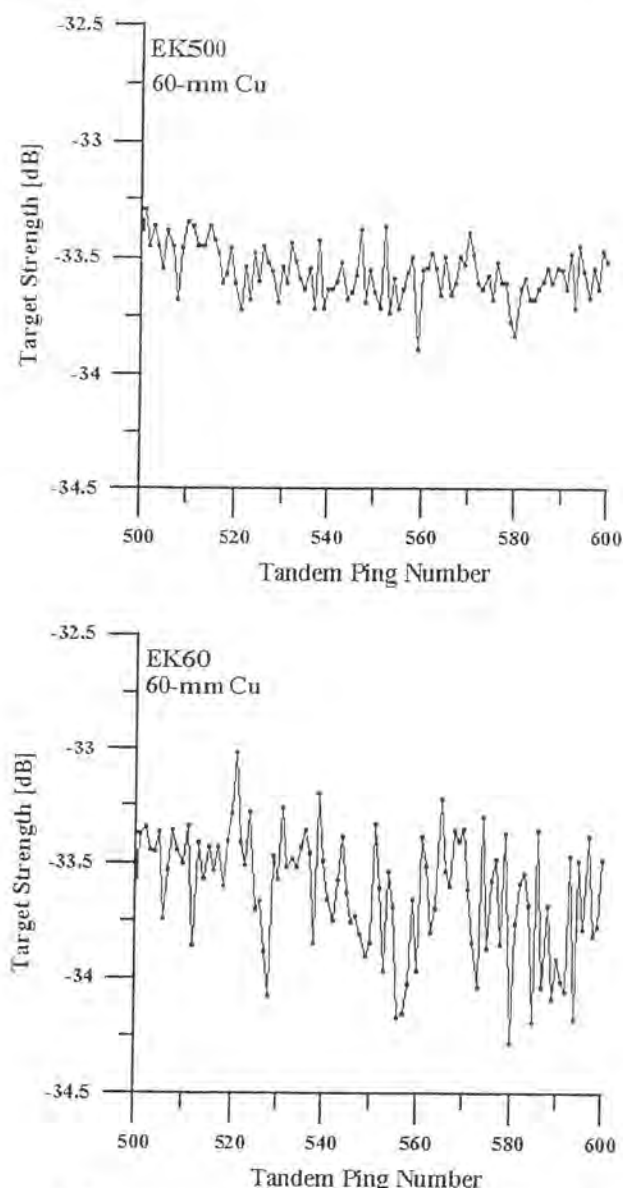


Figure 5. Time-series of split-beam-determined target strength for on-axis measurements of a 60-mm-diameter copper sphere from the EK500 (top panel) and EK60 (lower panel). The nominal ping rate was 1 ping  $s^{-1}$  for each echosounder, hence the reported time period is about 100 s. This time-series was extracted from the full time-series given in Figure 6 (pings 500–600).

measurements, alongship intercepts were within or near the angular resolution of each echosounder. Athwartship intercepts for athwartship angles were  $-0.86^\circ$  for the EK500 and  $-0.87^\circ$  for the EK60. Consistent with on-axis measurements, the magnitude of the intercepts indicates an athwartship-angle offset.

Beam-pattern measurements were conducted to assess the transducer directivity relative to that based on the experimental geometry and the SIMRAD-defined directivity. Transducer directivity was calculated using the SIMRAD beam pattern defined in Equation (1) and the alongship and athwartship angles based on the geometrical

Table 3. Beam widths (degrees) of the EK500 and EK60 observed beam patterns. G (decibels) is derived from Equation (2).

	EK500	EK60
Alongship beam width	11.4	11
Athwartship beam width	12.0	12
G (dB)	-33.6	-33

relationship of the transducer and 60-mm-diameter, copper calibration sphere. Similarly, the transducer directivities based on echo strengths and split-beam-determined angular locations of target detections were calculated. Difference between the directivities were computed by subtracting the split-beam-determined target strengths from the target strengths based on experimental geometry at each angular location:  $\Delta TS = TS - TS_{SB}$ .

In general, positive differences between geometry-based and split-beam determined target strengths occurred at negative athwartship angles, while negative differences occurred at positive athwartship angles (Figure 8).

#### Beam-pattern comparisons

The polynomial constant (G) in Equation (2) is the on-axis, echo-strength compensation value assuming  $0^\circ$  alongship and  $0^\circ$  athwartship angles. G sets the overall compensation level for echo-strength measurements. Differences between G and the calibrated on-axis sensitivity may affect the accuracy of split-beam-compensated target strengths. The value of G for the EK500 was within 0.05 dB of the theoretical target strength of the 60-mm-diameter copper calibration sphere ( $-33.6$  dB). However, G for the EK60 was 0.1 dB greater than the theoretical value.

The split-beam-determined angles were adjusted with the slope and intercepts derived from the linear regressions of the experimental-geometry-based and split-beam-determined alongship and athwartship angles (Table 3). The mean of the absolute differences between the geometry-based, split-beam-determined, and adjusted beam patterns was computed. Figure 9 displays the mean of the magnitudes of the differences between the geometry-based and split-beam-determined beam patterns and between the geometry-based and adjusted beam patterns for the EK500 and EK60, respectively. The mean difference was computed for each  $1^\circ$  interval.

The mean of the absolute differences between geometry-based and split-beam-determined, with or without offset adjustment, increased with angular distance off-axis (Figure 9). The mean of the absolute differences was greater for the geometry-based vs. split-beam-determined beam patterns than for the geometry-based vs. adjusted beam patterns. The intercept of the geometry-based vs. split-beam-determined beam patterns is a consequence of the athwartship angular offset. The difference between the

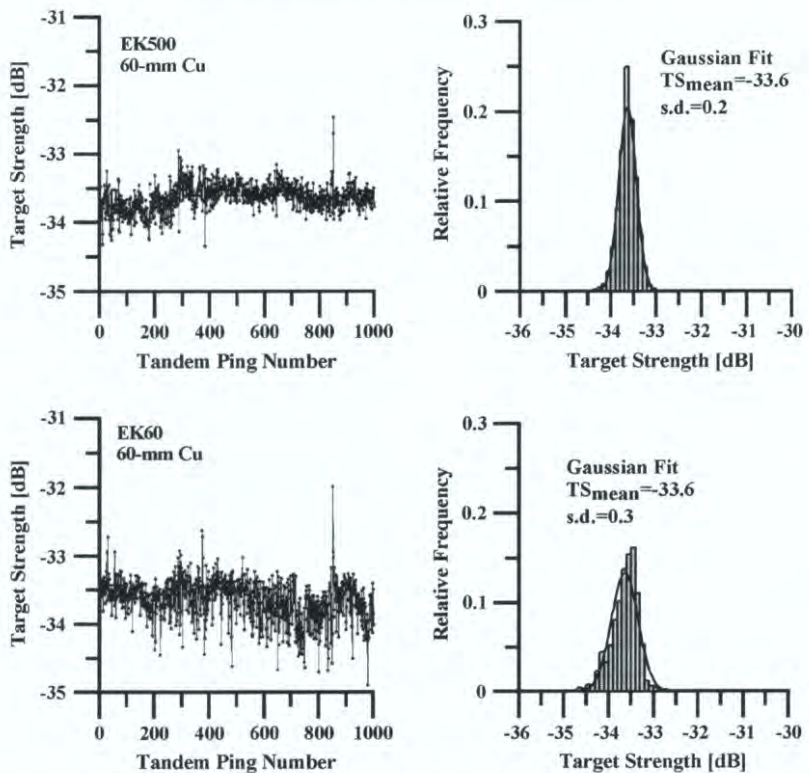


Figure 6. Time-series and histograms of split-beam-determined target strength for a 60-mm-diameter copper-sphere target on the acoustic axis. The ping rate was 1 ping  $s^{-1}$  per echosounder, and 1000 tandem pings represent approximately 17 min. Mean split-beam target strength (TS) and standard deviation (s.d.) are derived from a Gaussian fit to the data.

geometry-based and the split-beam-determined beam patterns ranged from 0.3 to 1.6 dB for both the EK60 and EK500. Adjusting the beam pattern for the athwartship and alongship offsets decreased the mean differences, as the differences between the geometry-based and the adjusted beam patterns ranged from near 0 to 0.3 dB.

An interesting result is that adjusting the EK60 beam pattern did not completely remove the error between the geometry-based and split-beam-determined beam patterns for off-axis angles less than  $1^\circ$ , whereas adjustments to the EK500 did nearly eliminate the error (Figure 9). This may be due in part to the value of G for the EK60 (Table 3), and potentially due to the skewed target-strength distribution from the EK60 (Figure 6). The TS distribution for the EK500 is unimodal and has a Gaussian shape, whereas the TS distribution for the EK60 is unimodal but skewed towards higher TS values. This skewed distribution may affect calculations of the empirical beam pattern and ultimately degrade the ability to compensate single-target, echo-strength measurements for location in the beam.

#### Beam width comparisons

Beam widths of the observed EK500 and EK60 beam patterns were compared with the manufacturer's stated

beam width of  $12^\circ$ . The beam width was measured as the total angular distance between the quarter-power points of the two-way beam pattern, which corresponds to the distance between the half-power points of the one-way beam pattern. Although beam widths were similar between the EK500 and EK60, athwartship beam widths for the EK60 and EK500 were closer to the specified  $12^\circ$  than were alongship beam widths (Table 2). Athwartship beam widths were within  $0.2^\circ$  of the manufacturer specification, whereas alongship beam widths differed by  $0.6^\circ$ .

#### Equivalent beam angle

Alongship and athwartship angles from beam-pattern measurements were converted to spherical coordinates, and the measured composite beam pattern  $b_T(\alpha, \beta)b_R(\alpha, \beta)$  was integrated. In reality, measurements encompassing the entire beam pattern are difficult to acquire. In the case of only measuring the central region of the target plane, the equivalent beam angle  $\Psi$  will be determined based on a threshold. The computed equivalent beam angle  $\Psi$  with a two-way threshold of  $-12$  dB was  $-15.2$  dB. This is consistent with the manufacturer-specified value of  $-15.5 \pm 1.0$  dB. For comparison, the equivalent beam angle computed with a threshold of  $-6$  dB was  $-17.6$  dB.

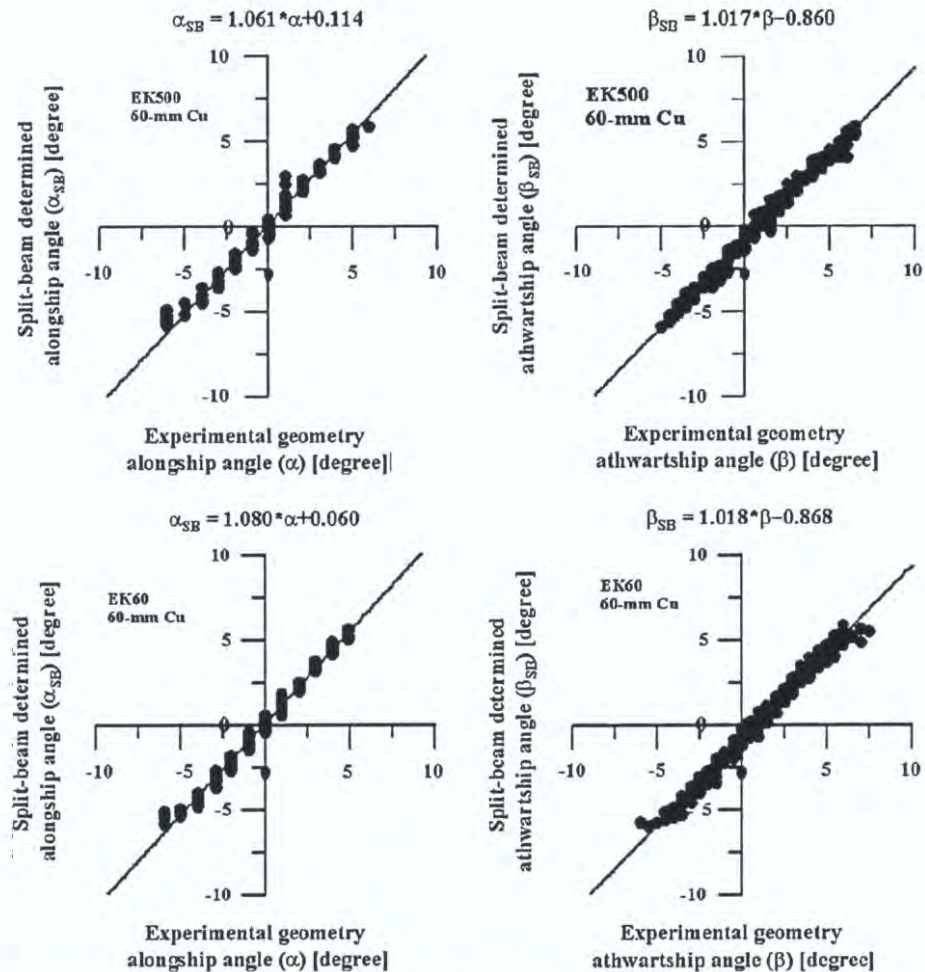


Figure 7. Split-beam-determined angular locations vs. those based on the known experimental geometry for a 60-mm-diameter copper-sphere target together with corresponding least-mean-squares linear regressions.

### Outstanding issues

The cause of the offset in the athwartship direction between the geometric axis and acoustic axis is uncertain at this time. This discrepancy could be due to inaccurate measurements of the geometry or inaccurate computation of the angular locations. Environmental conditions such as tidal currents or temperature and salinity discontinuities are not believed to be contributory because of the tidal mixing and the range of tidal states under which the trials were performed.

A relationship between the variability in angular locations and target strengths may exist, as the tungsten-carbide sphere had the greatest variability in target strength and split-beam-determined angles among the spheres. This relationship may be tidal-stage dependent, but it is difficult to discern owing to the lack of a systematic attempt to measure the tidal-current effects during the trials. Even

though the angular variability was different among spheres, mean alongship and athwartship angles were similar among trials, suggesting a potential alignment error with the apparatus or misalignment of the acoustic and geometric axes of the transducer. However, the angles are so small that the split-beam compensation should be fully adequate to eliminate such variability in target strength. The issue of apparatus alignment errors vs. split-beam, target-localization errors will be addressed in a future planned trial.

Greater variability in target strength derived from EK60 data relative to target strength derived from EK500 data, and the skewed target-strength distributions derived from EK60 data remain unresolved issues. On-axis time-series measurements on the 60-mm-diameter copper sphere show “ping-to-ping” variability of up to 2 dB in the target strengths from the EK60 echosounder, whereas ping-to-ping variability in target strengths from the EK500 was less than 1 dB. Additionally, target strengths derived from

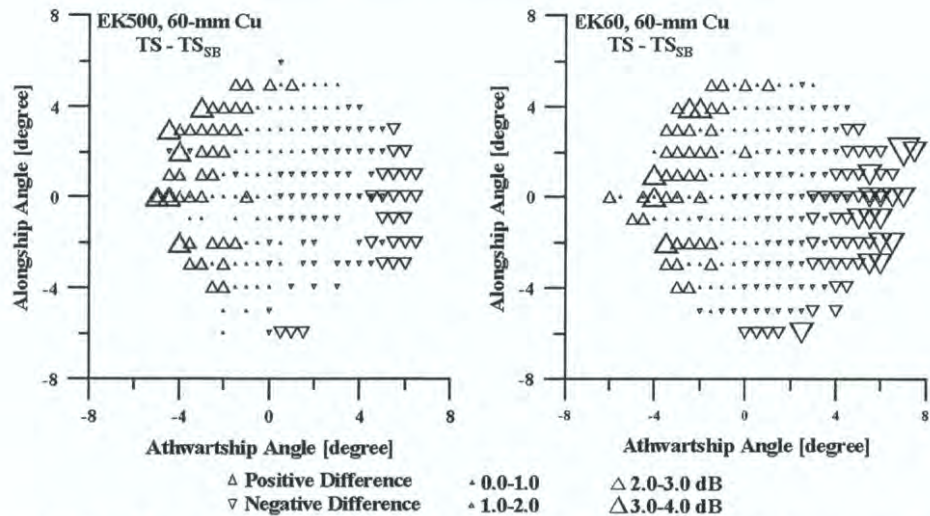


Figure 8. Differences in target strength from split-beam-determined angles ( $TS_{SB}$ ) and angles based on the experimental geometry (TS) of a 60-mm-diameter copper sphere when traversing the main lobe of the transducer beam pattern. Gaps in the measured beam pattern indicate that the calibration sphere was not detected as a single target for that angular location.

EK60 data were not normally distributed. Departures of target strength from the mean in the EK60 on-axis time-series tended to be less than the mean, which is reflected in the skewed target-strength distribution. On-axis time-series are fundamental measurements of echosounder performance and calibration, and are a basis for determining the accuracy and precision of acoustic estimates. Observations of increased variability and skewed distributions from the EK60 relative to an echosounder that has been a scientific standard for a decade and to tolerances that have been developed for scientific echosounder calibrations (e.g.

Simmonds *et al.*, 1984; Foote *et al.*, 1987; Simmonds, 1990) are disconcerting.

In addition to the ping-to-ping variability, an oscillatory trend in the on-axis time-series was observed in target strength derived from EK500 and EK60 data. The magnitude of the trend was more pronounced in the EK60 data, of the order of 0.5–0.75 dB, and cycled on the order of a few minutes. Longer-term measurements were not made, but it would be useful to investigate variability on the time scale of a survey. Variability in target-strength measurements is expected, but the variability is typically

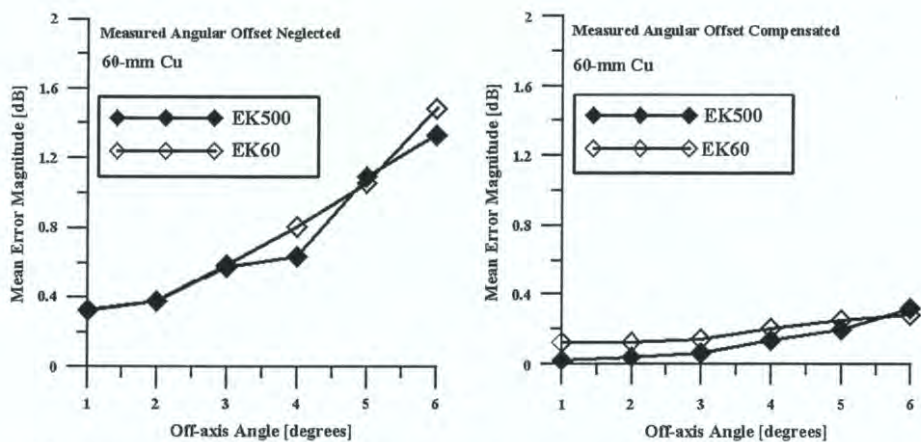


Figure 9. Mean of the absolute error between target strength based on the experimental geometry (TS) and split-beam-determined target strength ( $TS_{SB}$ ) of a 60-mm-diameter copper sphere corresponding to the data in Figure 8. Left panel: split-beam compensation as determined by the echosounder without use of the measured angular offset. Right panel: split-beam compensation with use of the measured angular offset according to the regression analysis in Figure 7.

random and normally distributed, as observed in target-strength distributions from the EK500. However, observed, skewed, target-strength distributions, and larger oscillatory trends in time-series data suggest biases in EK60 target-strength measurements.

The reason for these biases is unknown, but probably lies in the electronics or digital processing internal to the EK60. For the standard 1-ms-duration transmit pulse, the sampling rate of the EK60 is about half that of the EK500. This reduced sampling rate will lead to increased variability in EK60-measured target strengths (R. Kieser, pers. comm.). The consequences are clear, however: a bias will affect the distribution of characteristic target strengths and hence conversion of measurements of acoustic density to measures of biological density.

The longer-term stability in EK60 performance remains to be established. This may be determined directly by the measurement of lengthy time-series of standard-target echoes under good conditions, indirectly by comparing EK60 performance measures among calibration exercises, or by comparing data collected during surveys.

Analyses presented in this paper used a common single-target-detection algorithm, so comparisons do not characterize the implementation of the single-target-detection algorithms in the EK500 and EK60. Rather, comparisons underscore differences in the data- and signal-processing methods of the echosounders. Measurement and simulation efforts need to be conducted to determine the sources of these inconsistencies and to develop methods to rectify these concerns. Such efforts need to be collaborative endeavours among the scientific community, echosounder manufacturers, and third-party software developers, and discussions are ongoing.

### Acknowledgements

The authors thank T. R. Hammar for the construction of the transducer-mounting apparatus and general logistics, S. P. Liberatore for providing trigger signals to the rotator and switching unit, D. A. Demer for the design of the switching unit, R. Holley for construction of the switching unit, J. Condiotti for assistance with the EK60 echosounder, and R. Kieser for critical comments on the manuscript. The work was supported by National Science Foundation Grant No. OCE-0002664, the Northeast Fisheries Science Center (J. M. Jech) and the Northwest Fisheries Science Center (L. C. Hufnagle, Jr.). This is Woods Hole Oceanographic Institution contribution number 11220.

### References

Andersen, L. N. 2001. The new Simrad EK60 scientific echosounder system. *Journal of the Acoustical Society of America*, 109: 2336.

- Bodholt, H., Nes, H., and Solli, H. 1989. A new echosounder system. *Proceedings of the Institute of Acoustics*, 11(3): 123–130.
- Demer, D. A., Soule, M. A., and Hewitt, R. P. 1999. A multiple-frequency method for potentially improving the accuracy and precision of *in situ* target-strength measurements. *Journal of the Acoustical Society of America*, 105: 2359–2376.
- Doherty, K. W., Hammar, T. R., and Foote, K. G. 2002. Transducer mounting and rotating system for calibrating sonars in a sea well. *Oceans 2002 MTS/IEEE Conference Proceedings*, pp. 1407–1410.
- Ehrenberg, J. E. 1979. A comparative analysis of *in situ* methods for directly measuring the acoustic target strength of individual fish. *IEEE Journal of Oceanic Engineering*, OE-4(4): 141–152.
- Foote, K. G. 1982. Optimizing copper spheres for precision calibration of hydroacoustic equipment. *Journal of the Acoustical Society of America*, 71: 742–747.
- Foote, K. G. 1983. Maintaining precision calibrations with optimal spheres. *Journal of the Acoustical Society of America*, 73: 1054–1063.
- Foote, K. G. 1986. Digital representation of split-beam-transducer beam patterns. *ICES C.M.* 1986/B: 2. 7 pp.
- Foote, K. G., Aglen, A., and Nakken, O. 1986. Measurement of fish target strength with a split-beam echosounder. *Journal of the Acoustical Society of America*, 80: 612–621.
- Foote, K. G., Knudsen, H. P., Vestnes, G., MacLennan, D. N., and Simmonds, E. J. 1987. Calibration of acoustic instruments for fish-density estimation: a practical guide. *ICES Cooperative Research Report*, 44.
- Foote, K. G., and MacLennan, D. N. 1984. Comparison of copper and tungsten carbide spheres. *Journal of the Acoustical Society of America*, 75: 612–616.
- Foote, K. G., and Stanton, T. K. 2000. Acoustical methods. In *ICES Zooplankton Methodology Manual*, pp. 223–258. Ed. by R. Harris, P. Wiebe, J. Lenz, H. R. Skjoldal, and M. Huntley. Academic Press, San Diego (ch. 6).
- Gaunaard, G. C. 1985. Sonar cross-section of bodies partially insonified by finite sound beams. *Oceanic Engineering*, OE-10: 213–230.
- Gunderson, D. R. 1993. *Surveys of Fisheries Resources*. Wiley, New York. 248 pp.
- Jech, J. M., Michaels, W., Overholtz, W., Gabriel, W., Azarovitz, T., Ma, D., Dwyer, K., and Yetter, R. 2000. Fisheries acoustic surveys in the Gulf of Maine and on Georges Bank at the Northeast Fisheries Science Center. In *Proceedings of the Sixth International Conference on Remote Sensing for Marine and Coastal Environments*. 1–3 May, Charleston, South Carolina, USA. Veridian ERIM International, Ann Arbor, Michigan, USA.
- Kieser, R., and Ona, E. 1988. Comparative analysis of split-beam data. *ICES C.M.* 1988/B: 44. 9 pp. + 7 Figures.
- MacLennan, D. N. 1990. Acoustical measurement of fish abundance. *Journal of the Acoustical Society of America*, 87: 1–15.
- Medwin, H., and Clay, C. S. 1998. *Fundamentals of Acoustical Oceanography*. Academic Press, New York. 712 pp.
- Ona, E., and Vestnes, G. 1985. Direct measurements of equivalent beam angle on hull-mounted transducers. *ICES C.M.* 1985/B: 43. 6 pp. + 5 figs.
- Reynisson, P. 1990. A geometric method for measuring the directivity of hull-mounted transducers. *Rapports et Procès-Verbaux des Réunions du Conseil International pour l'Exploration de la Mer*, 189: 176–182.
- Reynisson, P. 1998. Monitoring of equivalent beam angles of hull-mounted acoustic survey transducers in the period 1983–1995. *ICES Journal of Marine Science*, 55: 1125–1132.
- Simmonds, E. J. 1990. Very accurate calibration of a vertical echosounder: a five-year assessment of performance and accuracy. *Rapport et Procès-Verbaux des Réunions du Conseil International pour l'Exploration de la Mer*, 189: 183–191.

- immonds, E. J., Petrie, I. B., Armstrong, F., and Copland, P. J. 1984. High-precision calibration of a vertical sounder system for use in fish-stock estimation. *Proceedings of the Institute of Acoustics*, 6(5): 129–138.
- SIMRAD. 2001. Simrad EK60 Scientific Echosounder Instruction Manual — Base Version. Simrad AS, Horton, NO. 246 pp.
- Urick, R. J. 1983. *Principles of Underwater Sound*, 3rd edn. McGraw-Hill, New York. 423 pp.